University of Alberta

Advanced Control of the Twin Screw Extruder

by

Mohammad Hasan Iqbal

A thesis submitted to the Faculty of Graduate Studies and Research in partial fulfillment of the requirements for the degree of

Doctor of Philosophy

in

Process Control

Department of Chemical and Materials Engineering

Fall 2010
Edmonton, Alberta

Examining Committee

Sirish L. Shah, Chemical and Materials Engineering

Uttandaraman Sundararaj, Chemical and Materials Engineering

Amos Ben-Zvi, Chemical and Materials Engineering

Pierre Mertiny, Mechanical Engineering

Sohrab Rohani, Chemical and Biochemical Engineering, University of Western Ontario

Abstract

This research deals with the modeling and control of a plasticating twin screw extruder (TSE) that will be used to obtain consistent product quality. The TSE is a widely used process technology for compounding raw polymers. Compounding creates a polymer with improved properties that satisfy the demand of modern plastic applications. Modeling and control of a TSE is challenging because of its high nonlinearity, inherent time delay, and multiple interactive dynamic behavior. A complete methodology is proposed in this thesis to design an advanced control scheme for a TSE. This methodology was used to develop a model predictive control scheme for a laboratory scale plasticating TSE and to implement the control scheme in real-time. The TSE has a processing length of 925 mm and a length to screw diameter ratio (L/D) of 37. High density polyethylenes with different melt indices were used as processing materials.

Manipulated variables and disturbance variables were selected based on knowledge of the process. Controlled variables were selected using a selection method that includes a steady state correlation between process output variables and product quality variables, and dynamic considerations. Two process output variables, melt temperature (T_m) at the die and melt pressure (P_m) at the die, were selected as controlled variables.

A new modeling approach was proposed to develop grey box models based on excitation in the extruder screw speed (N), one of the manipulated variables. The extruder was excited using a predesigned random binary sequence (RBS) type excitation in N and nonlinear models relating T_m and P_m to N were developed using this approach. System identification techniques were used to obtain model parameters.

The obtained models have an autoregressive moving average with exogenous (ARMAX) input structure and the models explain the physics of the extrusion process successfully.

The TSE was also excited using a predesigned RBS in the feed rate (F) as a manipulated variable. Models relating T_m and P_m to F were developed using a classical system identification technique; both models have ARMAX structures. The model between P_m and F was found to give excellent prediction for data obtained from a stair type excitation, indicating that the obtained models provide a good representation of the dynamics of the twin screw extruder.

Analysis of the TSE open loop process indicated two manipulated variables, N and F, and two controlled variables, T_m and P_m. Thus, a model predictive controller (MPC) was designed using the developed models for this 2×2 system and implemented in real-time. The performance of the MPC was studied by checking its set-point tracking ability. The robustness of the MPC was also examined by imposing external disturbances.

Finally, a multimodel operating regime was used to model T_m and N. The operating regime was divided based on the screw speed, N. Local models were developed using system identification techniques. The global model was developed by combining local models using fuzzy logic methodology. Simulated results showed excellent response of T_m for a wide operating range. A similar approach was used to design a global nonlinear proportional-integral controller (n-PI) and a nonlinear MPC (n-MPC). Both the controllers showed good set-points tracking ability over the operating range. The multiple model-based MPC showed smooth transitions from one operating regime to another operating regime.

Acknowledgements

I express heartfelt thanks to my supervisors Dr. Sirish L. Shah and Dr. Uttandaraman Sundararaj for their unique supervision and excellent guidance throughout my PhD thesis work. Their timely advice and inspiration enabled me to complete my research successfully and on time. Working with them was a learning experience that I thoroughly enjoyed.

I thank Mr. Steven Jackson at Coperion for his valuable suggestions for modifying the twin screw extruder. I also thank Mr. Dirk Hair and Mr. Darcy Pacholok at AT Plastics Inc. for allowing me to use their melt indexer. I thank Nova Chemicals for providing high density polymers.

I thank NSERC and Alberta Ingenuity Fund for providing financial support and the NSERC-Matrikon-Suncor-iCORE Industrial Research Chair program for additional financial support.

I had a great opportunity to work with the process control group and the polymer processing group in the CME department. I thank my friends and colleagues, especially Dr. M. A. A. Shoukat Choudhury, Dr. Iman Izadi, Dr. Dave Shook, Mr. Anuj Narang, Mr. Sandeep Kondaveeti, Mr. Arjun Shenoy, and Mr. Saneej Chitralekha from the process control group, for valuable discussions and feedback. I thank people from the polymer processing group, especially Dr. Bin Lin for rheological analysis, and Dr. Mohammed Al-Saleh and Dr. Huaping Lee for important discussions. I thank Dr. J. Praksh from Anne University, India, for his valuable discussions and suggestions for the real-time implementation of control schemes and the multimodel approach.

I am grateful to the instrumentation shop and machine shop people in this department, particularly Mr. Les Dean, Mr. Walter Boddez, and Mr. Bob Smith for their support in modifying the extruder. I particularly thank to Mr. Les Dean for his continuous support in instrumentation, data acquisition set-up, and process

automation.

I am grateful to my parents for their inspiration and love throughout my life. Heartfelt thanks go to my sister Mrs. Nahida Sultana for her encouragement. My deepest thanks to my wife Mrs. Mehtaz Sharmin for her encouragement, mental support, inspiration, and cooperation. Special thanks go to my son Mohid Muntasir Iqbal who was born during my PhD program. I am grateful to my son and my wife for the sacrifices they made so that I could complete my research work successfully.

Finally, my greatest thanks go to Almighty Allah for all of His blessings.

Contents

List of Figures

List of Tables

List of Symbols

ARMAX	Autoregressive Moving Average with eXogenous input
HDPE	High density polyethylene
RBS	Random binary sequence
D_{ext}	External diameter of the screw
C_l	Distance between screw axes
B	Screw pitch
$\dot{E}$	energy per unit volume
F	Feed rate
H	Screw channel depth
M	Number of operating regime
N	Screw speed
n-PI	Non-linear proportional-integral controller
n-MPC	Non-linear model predictive controller
P_m	Pressure of polymer melt
S	Number of screw flights
T_m	Temperature of polymer melt
$Y(s)$	Process output in Laplace domain
$U(s)$	Process input in Laplace domain
$G(q, \theta)$	Process transfer function
$H(q, \theta)$	Noise transfer function
Q	Weighting matrix for output
R	Weighting matrix for change in input
a_i	Coefficients of A polynomial
b_i	Coefficients of B polynomial
c_i	Coefficients of C polynomial
c_p	Heat capacity
d_i	Coefficients of D polynomial
f_i	Coefficients of F polynomial
f	Frequency in Hz
k	Sampling instant

$\dot{m}$	Mass flow rate
n	Power law index
na	Order of A polynomial
nb	Order of B polynomial
nc	Order of C polynomial
nd	Order of D polynomial
nf	Order of F polynomial
nk	Time delay
s	Laplace domain variable
$y(t)$	Process output in time domain
$e(t)$	Process noise in time domain
q	Backshift operator
r	Reference point
t_s	Sampling time
α	Weight for exponentially moving average filter
β	Parameter vector
γ	Parameter vector
δ	Parameter vector
θ	Parameter vector
$\dot{\gamma}$	Shear rate
η	Viscosity
ω	Frequency in rad/time
τ	Time constant
ε	Process noise

Chapter 1

Introduction

1.1 Introduction

Polymers are used with increasing frequency in many industrial fields such as food, electronics, and automobiles manufacture and repair. In 1995, plastics production in the world was about 100 million tons (Kiparissides 1996). Plastics are typically polymers of high molecular weight, and may contain other substances to improve performance and/or reduce cost. In the United States from 1976 to 1994, the growth of plastics production increased five-fold (Rodriguez 1996). The use of plastics in Asia has also been increasing in the last few decades, and increasing demand of plastics is expected to continue for new and expanded applications; examples are the use of polyethylene to make plastic bags and the incorporation polypropylene in automobile manufacture. Thus, it is necessary to develop technologies that improve polymer properties and increase polymer production. Originally, polymer properties were controlled by selection of appropriate monomers. The diverse use of today's plastics require more stringent quality specifications, which are difficult to achieve with individual base polymers (Potente *et al.* 2001a). Thus, polymers are usually blended or compounded with other polymers, fibers, or composites. Polymer compounding is more economical and expedient than synthesis of new polymers to meet the requirements of specific applications. In most cases, the products we see in the market today are made of a blend of polymers.

Polymer extrusion is a major compounding process used in the plastics industry for the continuous production tubing, pipe, film, sheet, coated wire, and other polymer products (Rauwendaal 2004, Fisher 1976). About 60% of all polymers pass through extruders before the final product is made (Levy and Carley 1989). In the polymer extrusion process, suitable raw material is pushed across a metal die to produce a melt in a desired shape (Tadmor and Gogos 1979). Several unit operations can be performed in a single machine, including mixing, heating, kneading, shearing, reaction, and shaping.

1.2 Polymer Blends

The concept of polymer blending is not new. As the cost of developing and industrializing new polymers increased sharply, the value of polymer blending began to attract ever-increasing attention. For the past few decades, more than 4,000 patents on polymer blends have been published every year (Utracki 1990). Recently, the number of patents has risen to nearly 10,000 per year. Also, increased uses for compounds that comprise high molecular weight polymers with low molecular organic and inorganic substances has accelerated the development of new polymer materials.

Material performance is one of the most important factors in the design of new polymer blends. The performance of a polymer blend depends on two main factors: blend components and the blending process. The components of a polymer blend are the individual polymer(s) and different additives or agents. Interactions among components under certain processing conditions result in a particular morphology of a polymer blend. This morphology varies under different processing conditions, even with identical components. That is, the process is strongly correlated to the properties and morphology of the polymer blend (Utracki 1990, Tadmor and Gogos 1979, Imagawa and Qui 1995, Pesneau *et al.* 2002, Huang *et al.* 2003, Fortelny *et al.* 2003, Premphet and Paecharoenchai 2002). Thus, to obtain a polymer blend with desired properties, the selection of components and processing method is extremely important.

Three methods are widely used in industry to prepare polymer blends: melt mixing, solution mixing, and dry mixing. Melt mixing is the dominant method used in extruders to make polymer blends in industry (Tadmor and Gogos 1979). A number of researchers have attempted to correlate the properties of polymer blends with their morphologies (Bai *et al.* 2004, Lee *et al.* 1998, Thongruang *et al.* 2002, Luo and Daniel 2003, Yeo *et al.* 2001). Improvements in new polymers include mechanical properties such as toughness, tensile strength, temperature resistance, stiffness, and elongation at breaks; functional properties such as permeability, conductivity, and antistatic, flame retard, and antibacterial properties (Lee 1992, Zhang and Chen 2004, Sohn *et al.* 2003).

1.3 Extruders

The earliest industrial extruder was a hand operated plunger and die combination invented by Joseph Bramah in 1797 and used for continuous manufacturing of lead pipe (Janssen 1977). The first twin screw extruder (TSE) was developed by Follows and Bates in 1873 (Janssen 1977). The first screw extruder designed specifically for

thermoplastic materials was invented in Germany by Paul Troester in 1935 (Tadmor and Klein 1970). Three types of extruders: screw, drum or disk, and reciprocating are used for material processing.

Screw extrusion is essentially a screw of special form rotating in a heated cylindrical barrel and material is pushed forward by the screw rotation. The screw extruder converts solid polymer into melt and continuously pumps the very high viscosity melt through a die at high pressure (Tadmor and Klein 1970). At least 95% of thermoplastics products are produced by using screw extruders (Levy and Carley 1989). Although there are a variety of different types of screw extruders, the main division is between the single screw extruder (SSE) and the twin screw extruder (TSE).

A single screw extruder consists of one screw rotating in a closely fitting barrel. Materials are transported due to their friction with the channel walls. If the polymer materials slip at the barrel wall, the material will rotate with the screw without being pushed forward. Moreover, the effect of extrusion is null if the material adheres to the screw. The pressure buildup by the SSE is poor because of the backflow of material.

1.4 The Twin Screw Extruder

The first objective of twin screw technology was to overcome the problems faced by the SSE. The presence of two screws makes it possible to force materials to move forward in the machine, making the propulsion of materials less dependent on friction. The TSE has several advantages over the SSE:

- Better feeding and more positive conveyance characteristics allow the machine to process "hard-to-feed" materials (powders, slippery materials, etc.);
- Better mixing and a large heat transfer surface area allow good control of the stock temperature;
- Residence time distribution is short and narrow;
- There is a good control over residence times and stock temperatures for the profile extrusion of thermally sensitive materials; and
- Interchangeable screw and barrel sections can be arranged to serve distinct and precise processing requirements.

1.4.1 Process Description of a TSE

Figure 1.1 shows a schematic of a generic TSE. Screw shafts are coupled with the motor to rotate the screw. The barrel has electrical heating and water cooling systems. Usually, the feed is charged in to the extruder at room temperature through the hopper. More than one feed can be charged from different feeders using a feed controller to maintain a certain feed composition. Feed is transported from the hopper to the end of the barrel, i.e., die by the drag force because of the friction and by the screw rotation. The twin screw essentially acts as a positive displacement pump. Solid feed gets melted as it travels along the heated barrel because of the applied heat, viscous dissipation and friction.

The feed material is almost solid at the conveying zone. Because of the screw rotation and friction, material is transported from the conveying zone to the melting zone where feed is partially melted and a number of processes such as mixing and reaction happen (Chen *et al.* 2004). The pumping or melt conveying zone is next to the melting zone; here the feed is essentially considered a complete melt. The pressure of the melt in this zone is increased by the screw rotation to extrude the melt polymer across the die.

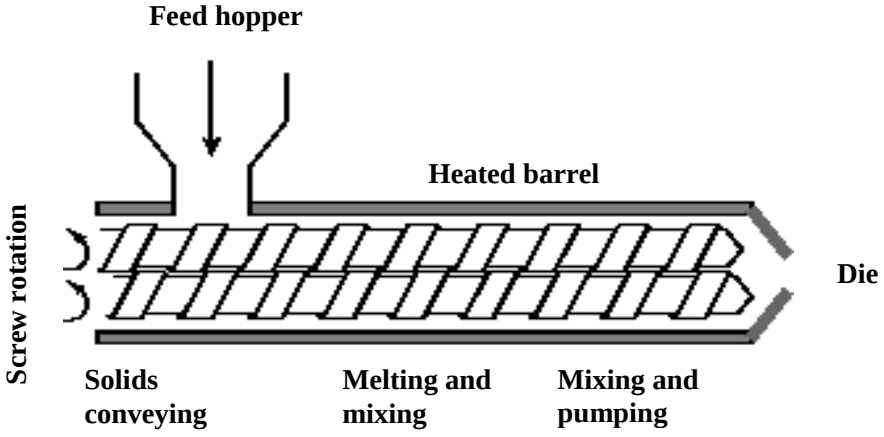

Figure 1.1: Schematic diagram of a generic TSE.
(www.polymerprocessing.com/operations/tscrew/ts1.gif).

1.4.2 Classification of TSEs

As its name indicates, a TSE contains two parallel screws that rotate inside a heated barrel. However, according to the direction of rotation and engagement of the screw, a TSE can be classified as follows:

- **Direction of rotation:** When the two screws have the same direction of rotation, the extrusion machine is known as a co-rotating extruder. In a

counter-rotating extruder, the screws rotate in opposite directions.

- **Interpenetration:** Based on the degree of penetration of the two screws into each other, a TSE is classified as an intermeshing or nonintermeshing twin screw extruder. Intermeshing screws imply that C-shaped chambers are present which positively convey the process material to the die end of the extruder.

1.4.3 Principle Elements of a TSE

A TSE consists of a drive section and a processing section. The drive section usually consists of a gear and a motor. The processing section comprises the screws enveloped by a barrel. The screw section and the barrel section are described below:

- **Screw section:** The screw section is made by combining different elements of a screw module. Each screw module provides a distinct conveying, mixing, shearing, or pressure buildup action. This makes it possible to compose the geometrical configuration to fit the application. There are three types of screws: a screw element for direct flow (positive helix angle), a screw element for reverse flow (negative helix angle), and a kneading block. Kneading blocks are combinations of any desired number of kneading disks of different widths and offset angles. In addition, special mixing elements are used to increase the degree of mixing. Figure 1.2(a) shows different types of screw modules.

- **Barrel section:** The barrel section is a fixed outer jacket in which the screws rotate. Like the screw section, the barrel unit is assembled in a modular way. This modularity allows great flexibility. The barrel section can be made of different barrel modules depending on the particular function (food, venting, etc.). The geometrical shape of the barrel can be either rectangular or cylindrical. Figure 1.2(b) shows a photograph of rectangular modular barrel elements.

1.4.4 Geometry of a TSE

The screw geometry of a TSE was studied by Booy (1978) and Potente *et al.* (1994). The following four parameters are sufficient to completely describe the geometry of a TSE.

- External diameter of the screw (D_{ext});

- Distance between screw axes (C_l);

- Screw pitch (B); and

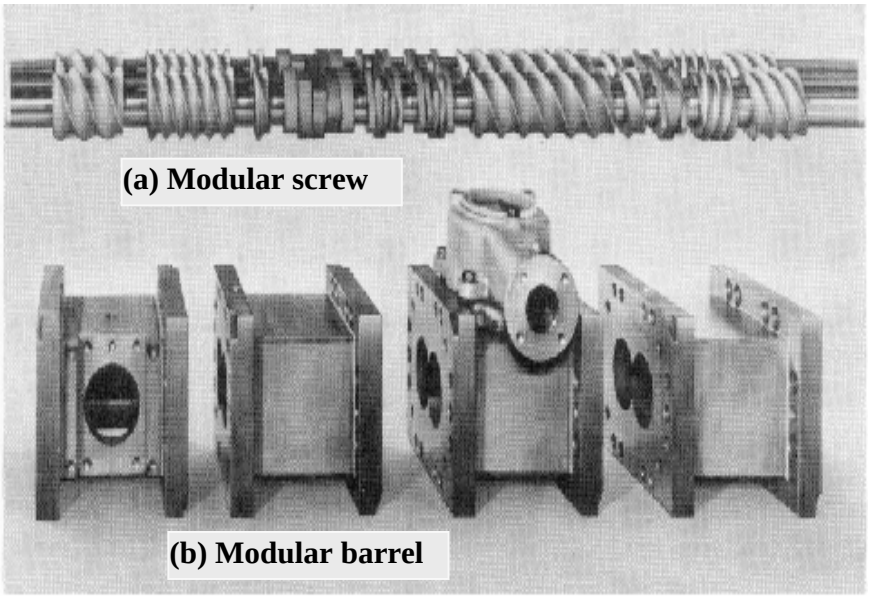

Figure 1.2: Principle elements of the processing section of a TSE (Tadmor and Gogos 1979).

- Number of screw flights (S).

Table 1.1 shows the geometric relationships of a TSE.

Table 1.1: Geometric relationships in a tightly intermeshing TSE.

Geometrical parameter	**Description**	**Relation**
Channel width (W)	Distance between two successive flights of a screw	W=$\frac{BCos\phi}{S} - e$
Helix or pitch angle (ϕ)	Angle of a screw flight	$\phi = arctan\frac{B}{\pi D_{ext}}$
Tip width (e)	Width of flight tip	e=$\alpha R_{ext} sin\phi$
Intermeshing angle (ψ)	Angle of the zone of interpenetration	$\psi = arccos\frac{C_l}{D_{ext}}$
Flight angle (α)	Flight angle with the normal of the screw surface	$\alpha = \frac{\pi}{S} - 2\psi$

1.5 Introduction to Advanced Control Schemes

In the 1960s, advanced control was used to describe any algorithm or strategy other than the classical proportional-integral-derivative (PID) controller. At that

time, NASA used real-time programming and remote-control using models. Over the last 50 years, significant research has been done on advanced control, the underlying theory, implementation, and the benefits that its applications will bring. The advent of modern computers and digitalization made the execution of algorithms easier than was possible using analog technology. Now a days, advanced control is synonymous with the implementation of computer based technologies. Advanced control techniques include a number of methods from model-based predictive controllers to intelligent sensors to neuro-fuzzy control and expert systems. Model predictive control, feedforward control, multivariable control, and optimal control strategies are practical alternatives. These methods have been used in chemical and petrochemical industries (Linko and Linko 1998). Advanced control can improve product yield, reduce energy consumption, increase capacity, improve product quality and consistency, reduce product giveaway, increase responsiveness, improve process safety, and reduce environmental emissions. Advanced process control techniques using digital computers have significant potential to improve the operation of extruders (Wang *et al.* 2008).

Advanced control is a multi-disciplinary technique. It describes an exercise that draws elements from a number of disciplines ranging from control engineering, signal processing, statistics, decision theory, artificial intelligence, and hardware and software engineering. Advanced control requires an engineering appreciation of the problem, an understanding of the process, and judicious use of control technologies. Dynamic relationships between variables are used to predict how variables will behave in the future. Based on this prediction, necessary action can be taken immediately to maintain variables within their limits before a deviation occurs. Thus, such schemes are mainly model based. Advanced control strategies have been successfully used in unstable processes such as aerospace, robotics, radar tracking, and vehicle guidance systems. Advanced controllers are also used in processing plants in order to increase efficiency or reduce costs. However, processing plants are relatively stable processes. Thus, advanced control strategies for processing plants are different than that of unstable systems.

1.6 Control of Twin Screw Extrusion Processes

Molecular and morphological properties of a polymer product strongly influence its physical, chemical, rheological, and mechanical properties as well as properties of the final product. These properties are affected by the processing conditions. Polymer industries aim to produce polymers or polymer blends that meet specifications such as impact strength and melt index. However, on-line measurement of end use properties is very difficult. Parameters that are measured relatively easily and that

correlate with end use properties are usually reported in the specifications. For example, melt index (MI) or intrinsic viscosity is reported instead of molecular weight. The MI has an inverse power law relationship with the weight average molecular weight of the product. The MI of a polymer melt is usually measured according to ASTM D 1238 . In most cases the MI is measured off-line and infrequently. Therefore, in most plants, a polymer process is controlled without a real-time quality indicator for several hours. Lack of on-line measurement is a major challenge to advanced and automatic control in an extrusion process.

In addition, an extrusion process has an inherently significant transportation delay. For example, a temperature sensor located at the die takes considerable time to sense any effect due to any change in feed rate. Moreover, a change in one process variable causes changes in several other variables, depending on the particular conditions used at that time (Tadmor *et al.* 1974a). Thus, the process is highly interactive and has significant time delay. However, it is very important to have a stable extrusion process to establish consistent product quality. Any fluctuation in operating variables can cause variations in the quality of the final product. Thus, a closed loop with an advanced control strategy is imperative to overcome this problem.

1.7 Scope of the Research

Although the TSE is very common in compounding technology, its smooth operation is hard to achieve. A number of researchers (Kulshreshtha *et al.* 1991a, Kulshreshtha *et al.* 1995, Hofer and Tan 1993) have highlighted the following challenges in controlling product quality in TSEs:

- interactions among mass, momentum, and energy transfer, and little understanding of these interactions;
- inherent time delay of the process;
- multiple inputs and multiple outputs process;
- highly nonlinear processes;
- lack of real-time measurement of quality variables; and
- disturbances.

Extrusion is a complex process. Control of the twin screw extrusion process is an active area of research. Characteristics of extrusion processes reveal a need for advanced control schemes for consistent product quality. Researchers have developed

some advanced control strategies for twin screw food extruders, but advanced control for the plasticating twin screw extruder is very limited and much research is needed in this area of polymer processing.

1.8 Objectives

The objective of this project was to design and implement advanced control schemes that provide consistent operation of a plasticating twin screw extruder. The objective was accomplished by performing the following steps:

- The most sensitive product quality parameters were identified and related to available and measurable process variables to select candidate variables as indicators. These relations were obtained using statistical methods and were validated with experimental data.
- Variables that gave better prediction of product quality parameters were selected as controlled variables.
- Dynamic models were developed using controlled variables and available manipulated variables.
- Advanced control schemes were designed based on the obtained models and closed loop simulations.
- Control schemes were implemented in real-time and controller performance was evaluated.

1.9 Structure of the Thesis

A brief literature review on modeling and control of twin screw extrusion processes is given in chapter 2. Research and development of twin screw extrusion process control are explained with emphasis on the plasticating TSE. Based on the literature review, challenges and perspectives leading to research objectives are identified.

The experimental setup is explained in chapter 3. Work performed to automate an existing TSE is described, where data from the extruder's programmable logic controller is sent to the computer and then to the extruder in real-time. Modification and mounting of new sensors to obtain more process output variables is explained.

In chapter 4, a systematic approach is detailed for developing a dynamic grey box model to predict the behavior of output variables due to changes in screw speed in a plasticating TSE. This approach comprises the selection of controlled

variables among a number of process variables and the development of grey box models relating the selected controlled variables and the screw speed.

Black box models relating the selected controlled variables and the feed rate are explained in chapter 5. Different excitation methods were used and the effects of excitation on model predictions are described. Frequency domain analyses were performed with the obtained models.

In chapter 6, closed loop control of a laboratory scale plasticating TSE is detailed. A multiple-input multiple-output model predictive controller (MPC) was designed for this closed loop control. This controller regulates polymer melt temperature and melt pressure by manipulating screw speed and feed rate. The control scheme was implemented in real-time. Both servo and regulatory performances of the MPC are discussed in chapter 6.

Multimodel approaches are used to model and control a TSE. The operating range is divided based on the screw speed and local models are developed. Development of a global model by combining local models is described in chapter 7. A similar approach is used to design nonlinear proportional-integral controller and nonlinear MPC. Design of nonlinear controllers and simulated closed loop responses are presented in chapter 7.

The necessary steps for closed loop control are outlined in chapters 3 to 6. The major findings of this work are summarized in chapter 8, and recommendations for future work are presented.

Chapter 2

Literature Review

2.1 Introduction

Significant research has been done in many areas of extrusion process such as study of flow behavior inside a twin screw extruder (TSE), modeling of extrusion processes, and control of product quality parameters. Modeling and control (especially advanced control strategies) of TSEs are reviewed in this chapter with a focus on plasticating twin screw extrusion processes. A TSE control system ensures consistent product quality despite disturbances and process upsets. In section 2.2, an extrusion process is described from a control point of view and depicted in an open loop block diagram (Figure 2.1). The diagram provides information about controlled variables, manipulated variables, disturbance variables, and product quality parameters. The state of the art in modeling using manipulated and controlled variables is explained. A detailed review of available literature on modeling TSEs is presented. A review on control strategies developed and/or implemented in real-time is discussed with an emphasis on modeling and control of TSEs used for polymer processing.

2.2 Process Analysis

The extrusion process is characterized by strong interactions between mass, energy, and momentum transfer. Such interactions are coupled with physiochemical transformations which predominantly determine the properties of the final products. An extrusion process is essentially a multiple-input multiple-output (MIMO) system. Conventional control strategies are not effective in controlling MIMO systems.

Identification or selection of manipulated variables, disturbance variables, and controlled variables is required for the proper design of control systems. Figure 2.1 depicts an open loop block diagram of a typical plasticating TSE with manipulated variables, disturbance variables, process output variables, and product quality

variables.

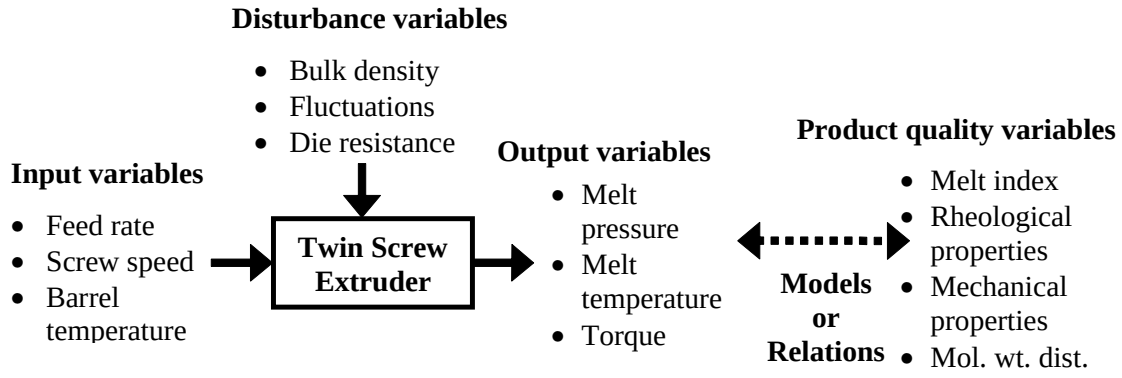

Figure 2.1: Open loop diagram of a plasticating TSE.

2.2.1 Manipulated Variables

For a plasticating extruder, the available input variables are screw speed, barrel temperature, and feed rate. If there is more than one raw material, then composition is another input variable. Input variables can be used as manipulated variables (MVs) as well as to control the extrusion process. Seborg *et al.* (2004) discussed the criteria for selecting MVs. For instance, due to the slow speed of correction, barrel temperature is the least suitable MV. In addition, heating and cooling have different dynamics in many cases. Costin *et al.* (1982a) mentioned some innovative MVs such as take up speed, restrictor valve, and plunger, but these MVs are not commonly used in industry. In food extrusion processes, moisture content is used as a MV along with other previously mentioned MVs.

2.2.2 Disturbance Variables

If systems were not affected by disturbances, there would be no need for control. Disturbances are inevitable in any process. One must know what type of disturbances are associated with a particular system before designing a control scheme to regulate the process. Three major disturbances associated with extrusion processes are discussed below.

Fluctuations

A steady flow rate, constant pressure, constant temperature, and uniform extrudate composition are required for a good quality extrusion. Thus, stability of these variables determines the quality of the extrudate. However, these fluctuations are interrelated. Pressure fluctuation will induce flow rate fluctuation; temperature

fluctuation will cause viscosity fluctuation, which eventually will induce pressure fluctuation as well as flow rate fluctuation. The type and source of these fluctuations, commonly referred to as surging, were summarized by Tadmor and Kelin (1970):

- *High frequency fluctuation:* This fluctuation happens at the same frequency as the rotational speed of the screw. Such a fluctuation is easily detected in pressure data. It is caused by the periodic changes in the feed rate due to the passage of the flights at the hopper opening. This kind of fluctuation usually occurs when an extruder operates at a very low back pressure, for example extremely cooled screws and screws with an inadequate compression ratio. High frequency fluctuations are picked up by a pressure transmitter if it is mounted close to the tip of the screw. In this case, the fluctuations are due to the periodic passing of the screw flights and have nothing to do with instability.

- *Intermediate frequency fluctuation:* This kind of fluctuation occurs at fairly constant frequency (1-15 cycles/min) and is one of the main reasons of poor quality product. The origin of this fluctuation can be related to the melting mechanism of polymer in the extruder. The solid bed formed by the unmelted polymer pellets breaks up at a certain point in the melting zone and the steady state melting process goes into an unstable process. This process makes blocks of solid polymer which continue to melt for a period, after which they float down the channel and slowly melt by conduction. This breaking up process is a function of the type of polymer, the pellet size, and the screw geometry. However, steady state operating conditions have little effect on this process. This variation in the length of the melting region causes a surging effect in the extruder. Thus, intermediate frequency fluctuations originate in the melting zone. One of the ways that might help to overcome this problem is to move the originating point as far from the delivery end of the extruder as possible. High back pressures and high heat levels on the rear zones are also helpful to overcome this surging effect.

- *Low frequency fluctuation:* This kind of fluctuation has a period of the order of magnitude of an hour. It is caused by external reasons such as variation in cooling water pressure, heater cycling, variation in plant voltage, etc.

Sometimes high frequency fluctuations due to the rotation of the screw are superimposed on lower frequency fluctuations, making the amplitude of the fluctuations even higher.

Bulk density

This disturbance happens at the feed end due to variations in feed bulk density and the nature of the feed itself. The feed end disturbances can lead to poor product quality and need to be controlled. Thus, feed related input variables, for example, feed rate, can be used as MVs to reduce the effects of this variable.

Die resistance

This disturbance occurs due to sudden changes in die resistance. Changes in die resistance are due to partial or complete blockage of the die. In TSEs, die end disturbances are often dramatic in nature, sometimes leading to sudden shut-down. In most cases, die end disturbances occur during start-up or after sudden changes in operating conditions.

Screw wear, heat loss from the extruder, and changes in the value of the heat transfer coefficient between barrel wall and melt are typically responsible for a slow drift in extrusion processes. These disturbance variables are important to the quality of the final product. Fluctuations are the predominant disturbances associated with the extrusion process (Iqbal *et al.* 2010a). Any kind of fluctuation makes the flow rate unstable and the quality of the extrudate poor.

2.2.3 Controlled Variables

In most cases, process output variables are used as controlled variables (CVs) in an extrusion process due to difficulties in using product quality variables as primary controlled variables. The usual measured process output variables of a plasticating TSE are polymer melt pressure and polymer melt temperature. Torque and energy, which are calculated from available process information, are also process output variables. For example, an increase in a polymer melt temperature decreases viscosities and an increase in a polymer melt pressure increases viscosities. Torque required to rotate a screw shaft decreases with an increase in a temperature and increases with an increase in a pressure.

These output variables can be used as controlled variables as well to design a closed loop control scheme. The selection of process output variables as controlled variables also serves to take care of stability considerations. It is worthwhile to mention that although process output variables have a strong correlation with actual product quality, the final controlled variables are the product qualities. Selection of the process output variables to be used as controlled variables needs to be based on their influence on the quality parameters most characteristic of the product. For example, torque may be the most pertinent controlled variable for one product and melt pressure at the die for another.

2.2.4 Product Quality Variables

The ultimate goal of any control system in a plasticating TSE is to control the product quality variables (PQVs) such as melt index, rheological properties, molecular weight distribution, and mechanical properties within a specified range. However, these parameters are often not measured on-line due to cost, operational effort, and maintenance, and it is possible to evaluate these parameters only after a delayed laboratory analysis. Control of PQVs requires good understanding of the process and prediction of PQVs from available process variables. A number of techniques can be used to predict PQVs from available process variables (Sharmin *et al.* 2006, Wang *et al.* 2001a, Zhang *et al.* 1997, McAuley *et al.* 1990, McAfee *et al.* 2003). In the studies cited, relations between product quality variables and process variables are developed using statistical techniques or first principles. For example, melt index has a logarithmic relationship with a temperature. Such relations allow us to predict or infer the values of PQVs from the process data. The obtained relations are known as the inferential model or soft-sensor. This is an active area of research but is beyond the scope of this work.

2.3 Process Model

The model of a process should encapsulate dynamic information. However, some analysis and design techniques require only steady-state information. In general, models use simplified properties of the system, and retain only information relevant to the problem statement or objective. Therefore, the use of models reduces the need for real experiments and facilitates the achievement of many different purposes at reduced cost, risk, and time. From a control point of view, a model must contain information that enables the prediction of the consequences that will result from changes in the process operating conditions. Within this context, a model can be formulated on the basis of physiochemical or mechanistic knowledge of the process, it can be obtained from process data or it can be derived from a combination of knowledge and measurement. It can also be in the form of qualitative descriptions of process behavior. Figure 2.2 shows a classification of model forms. The model type to be employed depends on the task or objective.

The main purpose of a control system is to ensure consistent product quality despite disturbances and process upsets. A control scheme needs to be based on an understanding of the process to be controlled. A good mathematical model for the process is therefore extremely important and a prerequisite for the design of control systems for extrusion processes (Haley and Mulvaney 2000b).

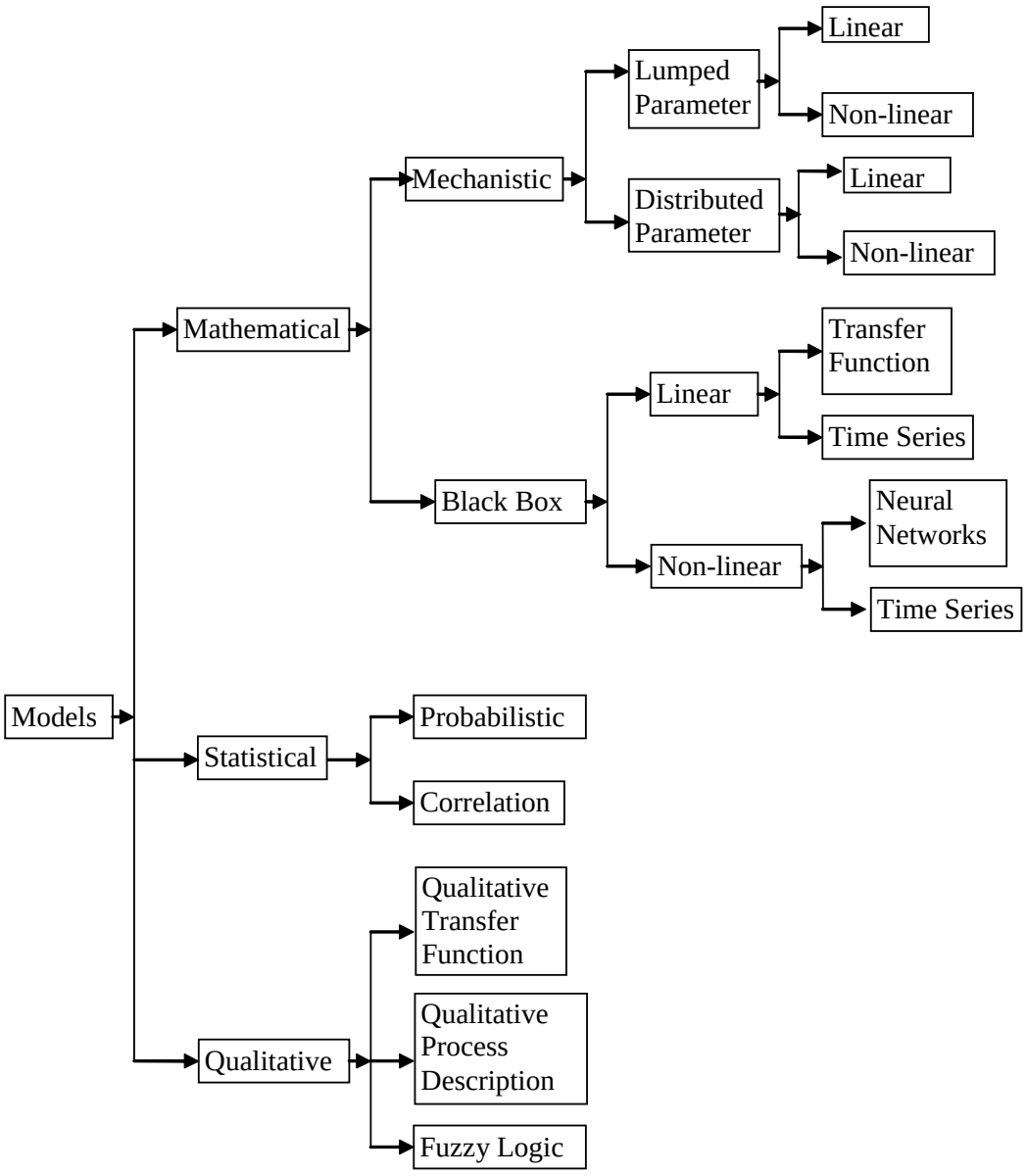

Figure 2.2: Classification of models for process monitoring and control.

2.3.1 First Principles or Mechanistic Models

First principles or mechanistic models are developed from basic principles of physics and chemistry such as conservation of mass, momentum and energy. If a process and its characteristics are well defined, a model can be developed using first principles. The structure of the final model may be represented by a lumped parameter or a distributed parameter depending on the process. Lumped parameter models are described by ordinary differential equations (ODEs) while distributed parameter systems are represented by partial differential equations (PDEs). For example, a change in liquid height in a tank with time can be presented by an ODE, and a change in temperature in a tank with time and at different locations can be represented by PDEs.

A distributed parameter model is more complex than a lumped parameter model, and hence harder to develop. In addition, solving PDEs is less straightforward than solving ODEs. However, a distributed model can be approximated by a series of ODEs given simplifying assumptions. Both lumped and distributed parameter models can be further classified into linear or nonlinear descriptions. Usually nonlinear differential equations are linearized to enable tractable analyses. Many researchers have tried to develop first principle models for TSEs in steady state or dynamic conditions.

Steady State Models

Potente and other groups developed steady state models for plasticating TSEs (Poulesquen and Vergnes 2004a, Poulesquen *et al.* 2004b, Vergnes and Berzin 2004, Carneiro *et al.* 2002, Potente *et al.* 2001a, Vergnes *et al.* 2001, Carneiro *et al.* 2000, Delmare and Vergnes 1996, Wang and White 1989, Booy 1978, Booy 1980, Booy 1981, Denson and Hwang 1980, Mohamed and Ofoli 1990). The melting mechanism of a polymer in the melt section of a TSE was modeled and compared with experimental values (Potente *et al.* 2001a, Potente *et al.* 2001b, Potente *et al.* 1996). Variables such as volume, maximum width and maximum depth of a screw channel, and free cross-sectional area were evaluated from machine geometry according to Potente *et al.* (1994). Moreover, models for power consumption and temperature (Potente *et al.* 2004) development were obtained and a simulation software, SIGMA (Potente *et al.* 2001b), was developed to simulate the pressure profile, temperature profile, etc. In another research group, White and coworkers (Wang and White 1989, Wang *et al.* 1989, Szydlowski and White 1988, Szydlowski *et al.* 1987, White and Chen 1994, White *et al.* 1987, White and Szydlowski 1987, Hong and White 1998, Szydlowski and White 1987, Bawiskar and White 1997, Bawiskar and White 1998) did extensive work on plasticating TSEs to construct a mechanistic model

for steady state flow behavior. Vergnes *et al.* (1998) developed a global model to simulate pressure, mean temperature, residence time, and shear rate of a molten polymer in a co-rotating TSE. Rios *et al.* (1998) simulated the mixing behavior in a co-rotating TSE to increase the quality of mixing. In other studies, mechanistic models were developed for steady state reactive extrusion processes (Poulesquen *et al.* 2004, Gimenez *et al.* 2001, De Loor *et al.* 1996).

Extensive research has also been done by a number of researchers to develop a first principles model for a twin screw food extrusion process (Della Valle *et al.* 1993, Vergnes *et al.* 1992, Barrès *et al.* 1991, Kulshreshtha *et al.* 1991b, Della Valle *et al.* 1987, Yacu 1985). Tayeb *et al.* (1988*b*) obtained a steady state model for a twin screw food extruder to compute isothermal flow through the reverse screw element of a twin screw extrusion cooker. In this study, some of the model parameters were obtained from screw and barrel geometry according to Booy (1978). In each study, a drift from experimental values was observed because of a number of restrictive assumptions and some classical assumptions.

Steady state models can be used to predict performance corresponding to a given set of operating conditions and are very useful in designing TSE performance monitoring, etc. But if the set of operating conditions changes to different values, then the process moves to a new steady state that is not possible to predict by the steady state model. Steady state models also can not predict the path followed by the extruder during the transition, or the rate at which the change occurs. For example, it is not possible for steady state models to predict the response of the process and the influence of various fluctuations on extruder performance. Therefore, a dynamic extrusion model is very important in the design of a control system (Akdogan and Rumsey 1996).

Dynamic Models

The main objective of dynamic modeling is to understand how physical transport phenomena, operating conditions, etc., affect the polymer quality of the final product. A number of research groups have attempted to model the process behavior of plasticating single screw extrusion processes but work on plasticating twin screw extrusion processes is limited. Dynamic models of TSEs have been investigated theoretically over the last few decades. Table 2.1 summarizes some major published articles on dynamic mechanistic models of twin screw extrusion processes. In most cases, models are developed to predict melt pressure, melt temperature, residence time distribution, and filling factor. Conservation of mass, momentum balance, and energy balance are used to develop the models. Power law and geometric relationships are also used to develop the models. Mechanistic models are developed based on both classical and conservative assumptions.

Kim and White (2000a, 2000b) developed models to predict output flow rate and length of the fill in front of the die and kneading block in cases of isothermal and non-isothermal transient start up. The study was done using Newtonian fluids which are hardly used as processing materials in commercial TSEs. Kulshreshtha and Zaror (1992) developed dynamic models to predict shaft power and the melt pressure at the die for a twin screw food extruder. In another study, Li (2001) developed a one-dimensional model to predict pressure, temperature, fill factor, residence time distribution, and shaft power from available operating conditions such as feed rate, screw speed, feed temperature/moisture, barrel temperature, etc., for cooking extrusion processes. This model was similar to Kulshreshtha and Zaror (1992) model, but Li developed a faster solution algorithm. Lack of simulated results presented in the article makes the accuracy of the predictions questionable. A literature survey on mechanistic models shows that much more research on twin screw extrusion process modeling has been performed for food extruders than for plasticating extruders.

Despite the availability of mechanistic models for extrusion processes, it is a challenge to use such models as a basis for automatic control systems. In fact, no mechanistic models were used to design and implement control schemes by the researchers, probably for the following reasons:

- Mechanistic models need good understanding and knowledge of physical, chemical, rheological, and thermodynamic properties of the polymer melt and its interactions within the extruder. In many cases, these properties and their transport behaviors are either unknown or not well defined for the extreme process conditions that exist within an extruder during operation.

- Such models do not consider stochastic disturbances derived from nonhomogeneous feed stock components, transient surging behavior, vibration at different frequencies (Costin *et al.* 1982a), and sensor noises, which are inherent in extrusion processes and very important considerations in the design of control schemes.

- Mathematical models are developed based on a number of assumptions; hence, simulation gives biased values. Thus, there are always difference between predicted and experimental values.

- Mechanistic models contain parameters that are time consuming and sometimes hardly possible to measure.

Table 2.1: Summary of literature on first principles modeling of twin screw extrusion processes.

References	**Summary**	**Comments**
Tadmor *et al.* (1974a)	Models were developed for the transient solid bed profile, temperature profile, and pressure profile of a plasticating extruder due to the changes in the screw speed, feed rate, and barrel temperature.	Only qualitative explanations were given without model validation.
Tayeb *et al.* (1988*a*)	Models were developed to predict temperature in the conveying section, isothermal evolution of pressure in the melt pumping and reverse screw elements, and residence time distribution in a plasticating TSE.	Considerable mismatch was observed between model predicted pressure and experimental pressure.
Kim and White (2002, 2001)	Models were developed for transient output composition variation due to input disturbances from feeders and surging due to superposed disturbances from feeders.	Models predictions were not validated or compared with experimental values.
Kulshreshtha and Zaror (1992)	Mathematical models were developed for die pressure and shaft power to predict dynamic behavior of die pressure and shaft power of a twin screw food extruder due to step change in feed rate, feed moisture content and screw speed.	Predicted values showed significant deviation from experimental values.
Li (2001)	Models were developed to predict pressure, temperature, fill factor, residence time distribution, and shaft power from feed rate, screw speed, feed temperature/moisture, barrel temperature, etc., for cooking extrusion processes.	Lack of simulated results presented in the article questions the goodness of prediction.
Choulak *et al.* (2004)	Models were developed to predict transient and stationary behavior for pressure, temperature, filling ratio and molar conversion profile as well as residence time distribution under different operating conditions for a reactive extrusion process.	No model predicted output was validated with experimental data except pressure. Considerable mismatch between model prediction and experimental values was observed.

2.3.2 Black Box or Empirical Models

Extrusion is a complex process and use of first principle models is severely limited especially in real-time control applications. Another way to model dynamic extrusion processes is an empirical or black box modeling approach. Dynamic black box models offer an understanding of the extrusion process during transition from one steady state to another steady state. These models are valuable tools for analyzing the performance of an existing control system (Seborg *et al.* 2004) and designing model-based control schemes (Kulshreshtha and Zaror 1992, Haley and Mulvaney 2000a). These are also promising tools for product development and quality improvement. Thus, recent research has focused on obtaining black box models and designing control systems based on these models.

Transfer Function Models

A transfer function expresses algebraically a dynamic relation between selected input and output values of a process. Transfer function models are developed from observations of input-output behavior of a process. Consider the process depicted in Figure 2.3 with process input, output, and disturbance.

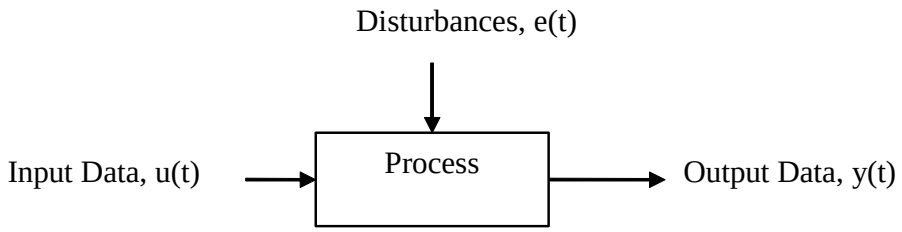

Figure 2.3: Process input, output, and noise.

The transfer function between input and output data can be written according to equation 2.1,

$$G(s) = \frac{Y(s)}{U(s)} = \frac{b_m s^m + b_{m-1} s^{m-1} + \cdots + b_0}{a_n s^n + a_{n-1} s^{n-1} + \cdots + a_0}. \tag{2.1}$$

where *Y(s)* and *U(s)* are Laplace transfer functions of y(t) and u(t), respectively. A Laplace domain transfer function is assumed from the response of an output variable due to the excitation of an input variable. Then, the values of the parameters of the transfer function are obtained from the response. For example, consider an output variable that follows a first order trajectory due to the step change in an input variable. Two parameters, time constant and process gain, are required to model this response. There are a number of techniques available to obtain transfer function models from responses (Seborg *et al.* 2004).

Transfer function modeling has been done extensively for plasticating single screw extruders by a number of researchers (Hassan and Parnaby 1981, Costin *et al.* 1982b, Chan *et al.* 1986, Yang and Lee 1988, Previdi *et al.* 2006). However, transfer function modeling of plasticating twin screw extrusion processes is very limited. A summary of the published work on transfer function modeling of twin screw extruders is presented in Table 2.2. A review of transfer function modeling reveals the following:

- Step type excitation is the most common perturbation method to develop transfer function models of twin screw extruders.
- Transfer function modeling has been done mostly for twin screw food extruder.

To develop black box models for a process or a system, sufficient excitation is imposed to capture the underlying process behavior. Thus, it is necessary to use well designed excitation methods to model complex extrusion processes. Parnaby *et al.* (1975) explained the step, impulse, and random binary sequence type excitation to identify extrusion processes. It has been observed experimentally that following a step change in screw speed, there is a rapid pressure change followed by a slower temperature change. However, subsequent step changes in the screw speed require further modification to the temperature so that the pressure continues to alter due to the changes in viscosity of the polymer flowing through the die. This behavior is difficult to model using a single step change in screw speed.

Step and impulse type excitations are classical approaches to evaluate a transfer function from the resulting transient response. However, step tests only excite low frequency components of the process. Obtaining models that adequately describe the process requires excitation of the process across all the important frequencies. Thus, developed models using step excitation can not predict the responses at high frequencies. In addition, in practice, sufficient random changes in raw material properties occur continuously to distort and make nonstationary the transient responses. Therefore, while a step change is useful in building up a basic understanding of the process, it provides inaccurate transfer functions. Incorrect modeling of dynamics can result in derived controller parameters that provide unstable closed loop behavior.

Well designed random binary sequence (RBS) and pseudo random binary sequence (PRBS) are good methods to excite (Hofer and Tan 1993, Schonauer and Moreira 1995) the desired frequency components of an extrusion process. Usually, RBS or PRBS design is based on the step responses of a process. Relay-feedback, another excitation method, is usually used in closed loop systems.

Table 2.2: Summary of literature on transfer function modeling of twin screw extrusion processes.

References	**Process**	**Excitation method**	**Summary**
Moreira *et al.* (1990)	Food extrusion process	Step changes in feed rate, screw speed, and moisture content were performed.	Dynamic responses of the die pressure due to the step changes in screw speed, moisture content, and feed rate were modeled by first order, first order plus lead-lag, and second order transfer functions, respectively.
Lu *et al.* (1993)	Food extrusion process	Step changes in moisture content, screw speed, barrel temperature, and feed rate were imposed.	Responses of product temperature were modeled by overdamped second order models for step changes of all the variables. Responses in the die pressure and motor torque were modeled by second order transfer functions with non-minimum phase zero due to changes in screw speed, feed rate, and barrel temperature. Overshoot responses were found for die pressure and motor torque due to step changes in feed moisture.
Cayot *et al.* (1995)	Food extrusion process	Step changes in feed rate, moisture content, and screw speed were imposed.	Process stability, stationarity, and linearity were studied. No response was modeled.
Akdogan and Rumsey (1996)	Food extrusion process	Step changes in feed rate and screw speed were made.	Dynamic responses of die pressure and motor torque were modeled. Responses to a feed rate change were modeled by a first order transfer function model and responses to a screw speed change were modeled by inverse response for both the outputs.
Nabar and Narayan (2006)	Food extrusion process	Step changes were made in starch feed rate, moisture content, screw speed, and poly hydroxy amino ether (PHAE) feed rate.	Responses of the die pressure due to changes in input variables were modeled by first order plus time delay transfer functions.

Time Series Models

Time series analysis deals with experimental data measured at different time instants for statistical modeling and prediction (Shumway and Stoffer 2005). An intrinsic feature of time series analysis is the nature of the dependence between adjacent observations of a time series (Box *et al.* 1994). Time domain and frequency domain are used in time series analysis. The time domain approach focuses on modeling future values of a time series as a parametric function of current and past values. The frequency domain approach assumes the primary characteristics of interest in time series analysis relate to periodic or systematic variations. However, models developed using the time domain approach are generally used to design control schemes.

The signals obtained from the sensors in extrusion processes are very noisy. For example, disturbances caused by pressure surges can be almost as large as those caused by a step of six rpm in screw speed (Costin *et al.* 1982b). When the process disturbances are such a large part of the overall process behavior, they need to be modeled so that an effective control strategy to eliminate these disturbances can be implemented. It is possible to model both process and noise using time series modeling. The noise model can then he used to predict the next value of the disturbance allowing for improved control.

Processes regulated by digital controllers are often modeled in discrete time domain. It is possible to rearrange Figure 2.3 in a discrete time domain according to Figure 2.4, where two additional blocks $G(q,\theta)$ and $H(q,\theta)$ have been introduced. Now, the output can be written according to equation 2.2.

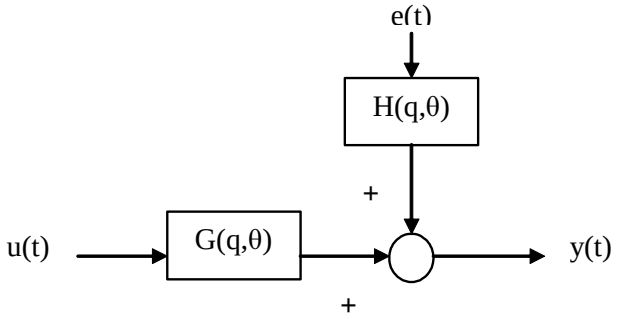

Figure 2.4: Process input, output and noise in discrete domain.

$$
\begin{aligned}
y(t) &= G(q,\theta)u(t) + H(q,\theta)e(t) \\
Or, y(t) &= \frac{B(q)}{F(q)}u(t) + \frac{C(q)}{D(q)}e(t)
\end{aligned} \tag{2.2}
$$

where the parameter vector θ contains the coefficients b_i, c_i, d_i and f_i of the transfer function. This time series model is known as the Box-Jenkins model. Here,

$$G(q,\theta) = \frac{B(q)}{F(q)} = \frac{b_1 q^{-nk} + b_2 q^{-nk-1} + \cdots + b_{nb} q^{-nk-nb+1}}{1 + f_1 q^{-1} + \cdots + f_{nf} q^{-nf}} \tag{2.3}$$

and

$$H(q,\theta) = \frac{C(q)}{D(q)} = \frac{1 + c_1 q^{-1} + \cdots + c_{nc} q^{-nc}}{1 + d_1 q^{-1} + \cdots + d_{nd} q^{-nd}} \tag{2.4}$$

Equation 2.2 is described by five structural parameters: nb, nc, nd, nf, and nk(delay). The q-transform exhibits a time shift property. For example, $q^{-1}y(k) = y(k-1)$. This property makes the q-transform an extremely valuable tool for the study of discrete time systems. In equation 2.2, polynomials D and F describe the present value of output in terms of past values of output. The discrete time model with these polynomials has an autoregressive nature. The polynomial B shows the present output in terms of present and past values of input. A model with this polynomial is referred to as having external or exogenous components. The polynomial C describes the present output in terms of present and past values of process disturbances. Models with this polynomial are considered to have moving average characteristics. Equation 2.2 is named according to the structure of the polynomials.

- When $F(q) = D(q) = A(q)$, then equation 2.2 is known as autoregressive moving average with extra input (ARMAX),

$$A(q)y(t) = B(q)u(t) + C(q)e(t) \tag{2.5}$$

- If $F(q) = D(q) = A(q)$ and $C(q) = 1$, then equation 2.2 is called autoregressive with extra input (ARX),

$$A(q)y(t) = B(q)u(t) + e(t). \tag{2.6}$$

- Incase of $C(q) = D(q) = 1$, the model is known as an output error (OE) model and the structure is

$$y(t) = \frac{B(q)}{F(q)}u(t) + e(t) \tag{2.7}$$

Limited work has been done to develop time series models for twin screw extrusion processes. Published articles on time series modeling of twin screw extruders are summarized in Table 2.3.

The following comments are based on a literature review of time series modeling:

- Twin screw food extrusion processes have been studied for the last couple of decades, but work on plasticating twin screw extrusion processes is very limited.

Table 2.3: Summary of literature on time series modeling of twin screw extrusion processes.

References	**Process**	**Excitation method**	**Summary**
Hofer and Tan (1993)	Food extrusion process	PRBS in cooling rate and heating rate.	Responses of extrudate temperature were modeled by a third order ARX structure and responses of specific mechanical energy were modeled by a second order ARMAX structure.
Haley and Mulvaney (2000a)	Food extrusion	Relay-feedback excitation in screw speed.	Dynamic responses of the motor load due to changes in screw speed were captured by a first order ARMAX model.
Schonauer and Moreira (1995)	Food extrusion process	PRBS in feed rate, water rate and screw speed.	Moisture content and color B responses were modeled by second order ARX structures. However, a second order ARMAX structure provided white residuals and independence of inputs and residuals.
Iqbal *et al.* (2007)	Plastic extrusion process	RBS in screw speed.	Melt temperature was modeled by a first order Box-Jenkins structure.

- The plasticating extruder usually operates at high temperatures compare to the food extruder. Since plastic has complex rheology, models of food extrusion processes are not adequate to understand the behavior of the plasticating extruder.

2.3.3 Neural Network Models

Recent developments in control technology have focused on user friendliness and on techniques in which exact mathematical modeling of the process is not required. With the advancement of modern computers, fuzzy control, neural networks and various hybrid systems are being used in real plants (Willis *et al.* 1992, Chiu 1997). Fuzzy control can deal well with nonlinear and task-oriented problems which has led to the wide availability of hybrid PID-fuzzy controllers. Linko and coworkers developed neural network and fuzzy logic control systems for food extrusion processes (Linko *et al.* 1997, Linko and Linko 1998, Eerikinen *et al.* 1994). Chiu and coworkers (Chiu and Pong 1999, Chiu and Pong 2001) applied a fuzzy control strategies to predict viscosity in a single screw extrusion molding process, and a fuzzy gain-scheduled

PID controller was developed to control the melt viscosity during extrusion process.

Artificial intelligence can predict the behavior of a nonlinear system. However, such an approach is computationally demanding and has limited application in plasticating twin screw extruders in real-time. In addition, a control scheme without a process model does not explain the process intuitively.

2.3.4 Grey Box Models

In recent years, significant advances have been made in incorporating a greater level of intelligence and process knowledge in system identification techniques. The obtained model is known as a hybrid model or a grey box model. Grey box modeling approach develops models on prior knowledge of the system and uses appropriate linear/nonlinear empirical techniques to refine the predictions (te Braake *et al.* 1998).

McAfee and coworkers (McAfee and Thompson 2007, McAfee 2007) developed grey box models for a plasticating single screw extruder. Gaussian type excitations were imposed on screw speed and barrel temperature. Nonlinear models were developed to predict responses of melt viscosity and melt pressure. In another study, Tan *et al.* (2004) developed grey box models to predict dynamic responses of polymer melt temperature and melt pressure due to changes in screw speed and barrel temperature for a plasticating single screw extruder. Only simulated results were presented and the models were not validated with experimental data. Garge *et al.* (2007) developed a hybrid transfer function model for a co-rotating TSE to quantify the effect of operating conditions on the melting process. Moreover, obtained model parameters were used to predict tensile strength of the final product. The results showed significant differences between predicted and experimental values. No attempt was made to control the quality of the final product.

Recently, Iqbal and coworkers developed a grey box model to predict polymer melt temperature (Iqbal *et al.* 2008, Iqbal *et al.* 2010a) and polymer melt pressure (Iqbal *et al.* 2010a) from screw speed. Nonlinear relations between melt temperature and melt pressure with screw speed were formulated based on first principles. However, the model parameters were estimated using a system identification technique. A predesigned RBS excitation was imposed on the screw speed to excite the process. Second and third order models with ARMAX structures were obtained to capture the dynamics of melt temperature and melt pressure, respectively due to changes in screw speed. Based on the melt temperature, a PID controller was designed using direct synthesis method (Iqbal *et al.* 2008). Simulated results showed good performance in set-point tracking and disturbance rejection.

Development of grey box models to predict responses of plasticating twin screw extruders are limited but such models are able to incorporate process knowledge and

are expected to capture process dynamics more accurately than empirical models. Thus, control schemes based on the grey box models are more likely to give better control over the processes than control schemes based on empirical models.

2.4 Control of TSEs

Polymers undergo very complex thermo-mechanical transformations inducing strong changes in the physical properties of the material during the extrusion process. Extrudate quality is essentially characterized by a precisely regulated output volumetric flow, which can be achieved by finely regulating the melt temperature and the melt pressure at the die at the output of the extruder (Previdi *et al.* 2006). Table 2.4 summarizes the current literature on control schemes of twin screw extrusion processes.

Previdi *et al.* (2006) developed a multiloop feedback controller for a plasticating single screw extruder. Melt temperature and melt pressure at the die were controlled by manipulating a screw-engine inverter command voltage and heater power commands. First order plus time delay transfer function models between the controlled variables and manipulated variables were developed according to Previdi and Lovera (2003). Two proportional-integral-derivative (PID) controllers were designed with a standard model-based indirect approach. Experimental results showed satisfactory regulatory performance of the PID controllers. No set-point tracking by the controllers was studied. In some studies, other final quality related problems, e.g., viscosity, have been studied and control schemes have been designed to regulate product qualities (Broadhead *et al.* 1996, Scali *et al.* 1997, Wellstead *et al.* 1998, Chen *et al.* 2003).

Kamal and coworkers studied the dynamics of a single screw injection molding machine (Kalyon *et al.* 1980). Transfer function and time series models were developed between hydraulic pressure and nozzle pressure (Fara *et al.* 1980, Kamal *et al.* 1984, Kamal *et al.* 1987). Using the models a discrete proportional, a proportional-integral (PI), and a PID controller were designed. Only simulated results were reported.

As model predictive controllers (MPCs) have been used successfully in processing industries, research has been focused to develop an MPC as an advanced controller for extrusion processes. Wang and coworkers modeled and designed control schemes for twin screw food extrusion processes (Wang and Cluett 1996, Wang and Cluett 1997, Wang *et al.* 2001a, Wang and Gawthrop 2001b, Wang 2001c, Wang 2004a, Wang *et al.* 2004b, Gawthrop and Wang 2004, Gawthrop and Wang 2005). In a recent work, Wang *et al.* (2008) designed a continuous time MPC for a twin screw food extruder. The MPC was designed for two controlled variables: mo-

tor torque and specific mechanical energy, and two manipulated variables: screw speed and liquid pump speed, according to the methodology developed by Wang and Young (2006). Transfer function models between the controlled variables and the manipulated variables were used to design the MPC. The obtained MPC was implemented in real-time to control the two-input two-output process. Results from real-time implementation showed good set-point tracking and disturbance rejection.

The following notes have been summarized from a literature review of control schemes for extrusion processes:

- The empirical or black box model has good potential for controlling twin screw extruders.
- Significant research has been done on the control of twin screw food extrusion processes and single screw plasticating extrusion processes.
- Control schemes for plasticating twin screw extrusion processes have not been reported to our knowledge.
- Implementation of control schemes in real-time is limited.

2.5 Challenges and Motivation

Many papers have been published on the application of process control to extrusion processes. Many commercial products are extruded and plastics are constantly finding new applications. With more exacting product specifications, it is crucial to minimize fluctuations in the operating conditions of the extruder. In fact, the extruder must be operated under precisely controlled conditions for persistent product quality and to avoid degradation of certain polymers. It is imperative to understand dynamic behaviors of a process to design control schemes.

Development of dynamic mechanistic models has been performed extensively for plasticating single screw extrusion processes and twin screw food extrusion processes. Very limited work has been done for plasticating twin screw extrusion processes. In most cases, only mechanistic models are used to predict the behavior of the extrusion processes. No attempt has been made to design and implement control schemes in real-time using mechanistic models.

Empirical models can be used effectively in designing control schemes for an extrusion process and thus are the focus of recent work. Methods of excitation are important in empirical modeling. Step change, random binary sequence, and pseudo random binary sequence are the most common excitation methods for open loop systems. Step type excitation is commonly used in extrusion processes, but excites only the lower frequency components. A properly designed RBS or PRBS

Table 2.4: Summary of literature on control schemes of extrusion processes.

References	**Process**	**Control scheme**	**Control objective**
Kochhar and Parnaby (1977)	Plasticating single screw extruder	Feedforward controller	Melt pressure and melt temperature at the die were controlled by manipulating screw speed.
Moreira *et al.* (1990)	Twin screw food extruder	Feedforward-feedback controller	Disturbance on die pressure due to variations in feed rate and moisture content was reduced.
Wagner and Montague (1994)	Plasticating single screw extruder	PI controller	Extrudate viscosity was controlled by manipulating screw speed.
Tan and Hofer (1995)	Twin screw food extruder	MPC	Extrudate temperature was regulated.
Elsey *et al.* (1997)	Twin screw food extruder	PI controller and MPC	Product gelatinization was controlled by manipulating screw speed.
Haley and Mulvaney (2000b)	Twin screw food extruder	MPC	Specific mechanical energy was regulated by manipulating screw speed. Only simulated results are presented.
Wang and Tan (2000)	Twin screw food extruder	Dual-target predictive controller	Die pressure and die temperature were controlled by manipulating screw speed, feed rate, and moisture addition rate.
Chiu and Lin (1998)	Single screw plasticating extruder	Constrained minimum variance controller	Viscosity of the polymer melt was controlled by manipulating screw speed.
Previdi *et al.* (2006)	Single screw plasticating extruder	Multiloop feedback controller	Melt pressure and melt temperature at the die were regulated by manipulating heater power and screw engine inverter voltage.
Wang *et al.* (2008)	Twin screw food extruder	Continuous time MPC	Motor torque and specific mechanical energy were controlled by manipulating screw speed and liquid pump speed.

can excite the full range frequency components. Thus, models developed using data obtained from RBS or PRBS excitation capture more information about a process. Few researchers have used RBS or PRBS excitation methods in modeling twin screw food or single screw plasticating extrusion processes. To the best of our knowledge, no work has been published on the dynamic modeling and control of a twin screw plasticating extruder where RBS or PRBS has been used as an excitation method.

In recent years the grey box modeling approach has been used to develop models for extrusion processes. Grey box models explain processes more intuitively than empirical models. A literature survey showed that grey box models have been used for the prediction of extruder behavior only. No attempt has been made to design control schemes using such models.

According to the literature, there have been many attempts to construct dynamic models for extrusion processes. However, very few researchers have tested their models or control schemes by attempting to regulate an actual extruder. Feedback, feedforward, minimum variance, adaptive, and predictive control schemes have been reported in the literature. In most cases, control schemes have been designed for plasticating single screw extruders or twin screw food extruders as single-input single-output process. Extrusion is inherently a multiple-input multiple-output process. In addition, process variables interact among themselves. So, model-based control schemes might be a better choice to control extrusion process. Thus, multiple-input multiple-output (MIMO) model-based predictive controller should control an extrusion process better than conventional control schemes. Such a control scheme was reported recently for a twin screw food extruder (Wang *et al.* 2008). Much work is needed to develop MPC for twin screw plasticating extruders as MIMO systems.

Chapter 3

Process Data Access and Automation

3.1 Introduction

One of the important requirements in modeling a process is to validate the model with real plant data. Thus, it is necessary to establish an infrastructure for data gathering. An important prerequisite for model building and validation is the availability of process data. In addition, this infrastructure can be exploited with some extensions for process automation. Process automation involves using computer technology and software engineering to help processes operate more efficiently and safely. In process automation, process data is acquired by a computer and computer controlled commands are sent to the process. This automation comprises both hardware and software development.

The twin screw extruder used in this study is described at the beginning of this chapter. Necessary work performed to gather process output variables is also discussed. To implement a computer control scheme, it is important to establish process automation as well. This process automation is detailed in this chapter.

3.2 Extruder

This work has been performed on a ZSK-25 World Lab co-rotating twin screw extruder with intermeshing screws. The screw profile is designed so that the crest of one screw wipes the flank and root of the other screw resulting in a self-wiping action.

The extruder has interchangeable screw and barrel sections that can be arranged to serve distinct and precise processing requirements to provide optimum laboratory and processing flexibility. The ZSK-25 extruder consists of a drive section and a processing section mounted on a common base cabinet; a schematic is shown in Figure 3.1.

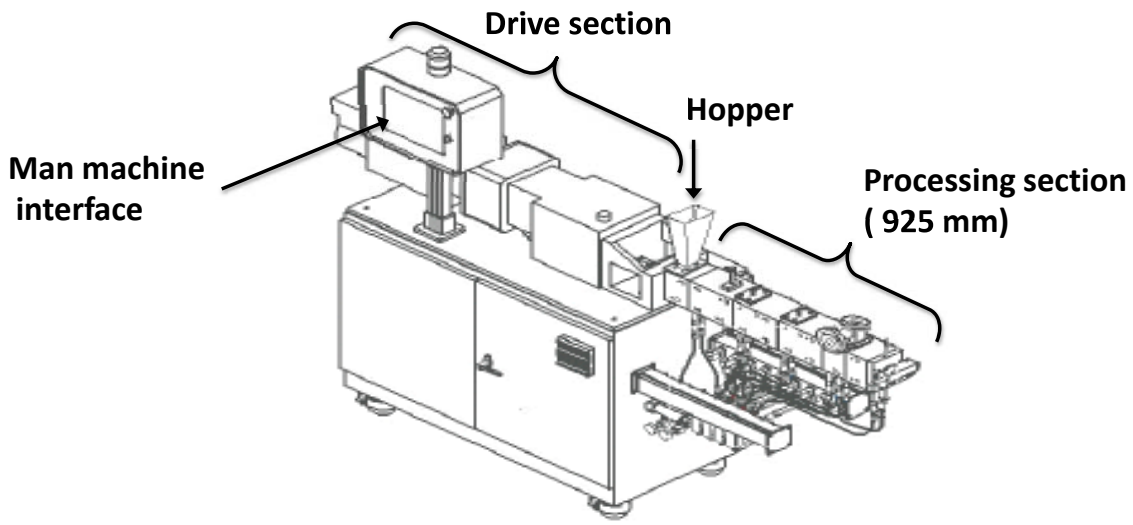

Figure 3.1: Schematic diagram of a ZSK-25 extruder.

3.2.1 Drive Section

The extruder drive section consists of a reduction and distribution gear with integrated oil lubrication, a motor, and a torque limiting coupling with a coupling disengagement sensor.

Motor: An AC motor with its matching AC vector drive is designed to provide a 10:1 constant torque over its base speed range. The motor and drive system selected provides full starting torque and excellent speed regulation.

Torque limiting coupling: The torque limiter is a spring loaded ball-detent device which is set to disengage the motor shaft from the gearbox input shaft when the motor torque exceeds 115% of the rated gearbox input torque.

Extruder gear box: The extruder gearbox is a multi stage split torque gear unit common to co-rotating TSEs; it consists of a reduction and a distribution section. On the output side a lantern connects the extruder barrel section to the gearbox housing. The gearbox housing is cast construction (grey cast iron). The gearbox gears are heavy duty, constructed of case hardened alloy steel. The tooth flanks are ground. Thrust bearings are employed to take up the thrust generated by

the extruder screws. All bearings are anti-friction type. Radial seals on the input and output shafts prevent oil leakage. The gear intermeshes and the bearings of the gearbox are splash lubricated. Internal circulating oil lubrication is incorporated for the thrust bearings and for the bearings situated higher than the general oil level in the gearbox. The ZSK-25 gearbox with a 3.22 ratio for up to 600 rpm screw speed is normally cooled by air convection. The gearbox with a 2.5 ratio for screw speed up to 1200 rpm has water cooling connections provided which are piped to the extruder water cooling manifold.

3.2.2 Processing Section

The modular construction principle of the screws and barrel makes it possible to build up successive conveying, plastification, homogenization, venting, and pressurization zones to suit the particular process application. Table 3.1 shows measurements of a processing section of a ZSK-25 TSE. The intermeshing co-rotating twin screws are designed with a sealing profile. The processing section consists of a barrel section and a screw section.

Table 3.1: Data for the processing section.

Number of barrels	9
Length of processing section	925 mm
Speed of screw shafts	1200 rpm
Length of screw element set	925 mm
Shaft centerline spacing	21.1 mm
Diameter of screw	25 mm
Admissible torque on screw shaft	82 N-m/shaft
Depth of flight	4.15 mm
Processing volume (per meter)	0.32 L/m

Barrel section: The barrel section consists of individual replaceable barrels. Depending on the process, solids feed connections, liquid feed connections, vent connections, or side connections for side feeders can be provided. Most barrels are drilled longitudinally for heating or cooling with water and have two piping connections. The closed barrels have temperature wells and, if required, openings for measuring the pressure or temperature of the product. Figure 3.2 shows a photograph of the barrel section of a ZSK-25 extruder. Individual barrel sections are assembled to obtain the desired process length. Different barrel designs are available to allow multiple feeding of ingredients, injection of liquids, and venting of moisture or removal of other volatiles along the process section.

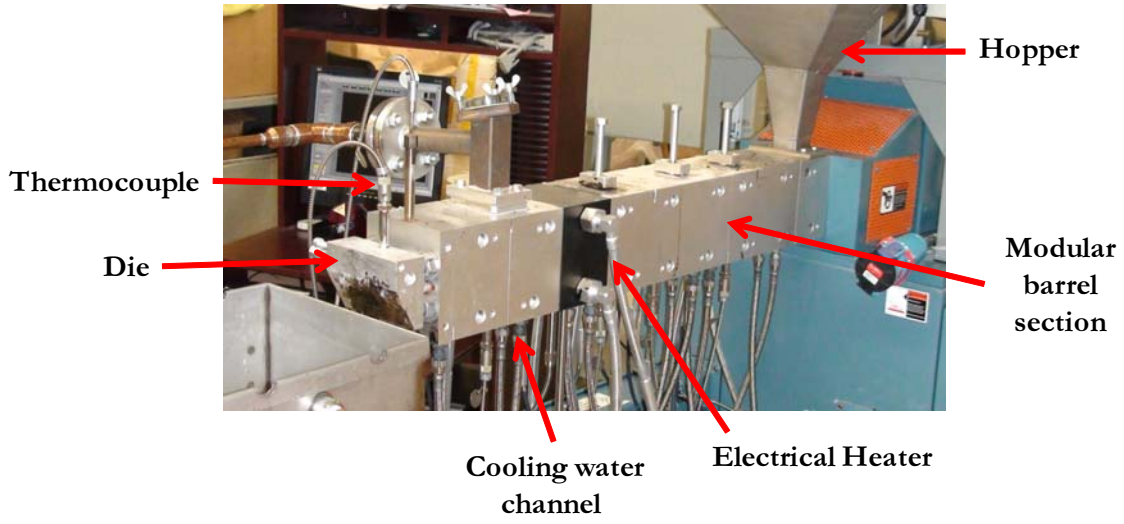

Figure 3.2: Photograph of the barrel section of a ZSK-25 extruder.

The ZSK-25 World Lab Extruder is supplied with electric barrel heaters and a cooling manifold with a solenoid valve for each barrel for cooling water (see Figure 3.2). The temperature control scheme provides for controlled heating and cooling of the extruder. The temperature controller is a dual output heat/cool type with adaptive auto-tuning suitable for an extrusion process. The heating output controls the electric heater and the cooling output controls the cooling water solenoid valve for a particular zone via time-proportioned algorithms. The barrel is divided into five temperature zones and the temperature of each zone is controlled separately. Table 3.2 shows power consumptions by different zones.

Table 3.2: Data for electrical heating of a ZSK-25 extruder.

Zone	**Barrel**	**Power**
1	2 and 3	3.2 kW
2	4 and 5	3.2 kW
3	6 and 7	3.2 kW
4	8 and 9	3.2 kW
5	Die	0.8 KW

When the temperature controller for a particular zone (1 or more barrels) calls for heating, the heater "on" time is increased with demand. When the temperature controller for a particular zone calls for cooling, the barrel cooling solenoid valve is time-proportioned to open and close to pulse water to the barrel. The water flashes to steam and heat is removed from the barrel. This pulsing action provides space in the cooling bores of the barrel to allow for the expansion of the water as the change of state to steam occurs. The steam produced is condensed back to water in the

return tubing or immediately as it enters the water return header.

The temperature of each zone is controlled by a local proportional-integral-derivative (PID) controller. However, barrel temperature at zone 4 is not controlled properly. At higher screw speeds, temperature at zone 4 fluctuates. Temperatures of polymer melt increases at higher screw speeds because of higher shear rates. If temperature difference between polymer melt temperature and zone 4 temperature is more than 6^oC, then this fluctuation occurs which indicates poor temperature control at this zone. Thus, a higher screw speed (> 200 rpm) is not recommended to use for this TSE. It is also not recommended to use too high barrel temperature to process a polymer since a high barrel temperature might degrade a polymer.

Screw section: The screw section can be made up from a wide selection of different types of screw bushings, kneading blocks and special mixing elements, all of which slide onto splined shafts. Each individual screw element provides a distinct conveying, shear, or pressure buildup action which can be controlled. Figure 3.3 shows the schematic diagram of a screw of a ZSK-25 co-rotating twin screw extruder. A part of the arrangement of the barrel section is also shown in Figure 3.3.

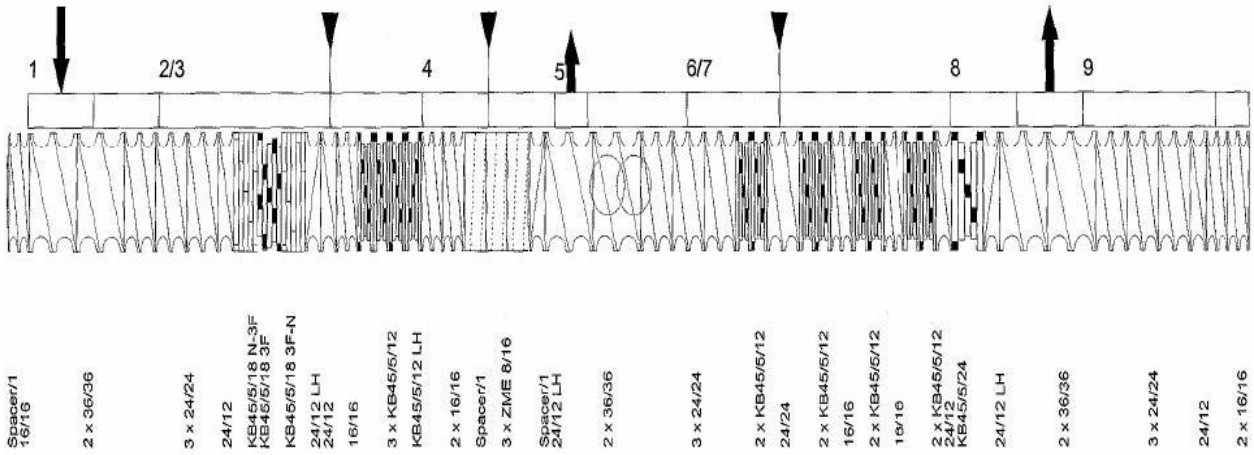

Figure 3.3: Schematic diagram of a screw of a ZSK-25 extruder.

Figure 3.3 shows the notations of the different screw arrangements for ZSK-25 screw that are explained in Table 3.3.

The extruder has a touch screen man machine interface to set the barrel temperature at five zones and a lever to set the screw speed. The ZSK-25 TSE has one Dynisco pressure transmitter at the die to measure melt pressure at the die. The melt pressure and the torque along with the five zone temperatures can be observed in the the man machine interface.

Table 3.3: Explanation of ZSK-25 screw notations.

Screw type	**Notation**	**Explanation**	**Application**
Forward conveying screw	36x36	Conveying element 36 mm long with 36 mm pitch	Pushes materials forward.
Reverse conveying screw	24x12 LH	Left hand screw 12 mm long with 24 mm pitch	Pushes materials backward.
Kneading block	KB45/5/12	Two flights kneading block contains 5 disks with 45^o stagger angle between adjacent disks; the block has a length of 12 mm	Increases degree of mixing.
Kneading block	KB45/5/18N-3F	Kneading block contains 5 disks with 45^o stagger angle between adjacent disks; the block has a length of 18 mm. This block also contains a transition from a two flight disk to a three flight disk	Increases degree of mixing.

3.3 Feeder

Loss-in-weight feeders (LWFs) are used in this study to feed polymers in the ZSK-25 extruder. A loss-in-weight feeding system includes a supply hopper or tank, a metering feeder or pump, a supporting scale system, and a microprocessor controller. The system electronically balances tare weight so the controller senses only the weight of the material in the supply hopper. Advantages of using a LWF are:

- It handles floodable, hot, and difficult materials.
- It is unaffected by dust and materials accumulation.
- It works well at low feed rates.
- There are no errors from belt tensioning and tracking, since the entire system is weighed.
- It uses only one process input for reduced error in operation.
- There is no transportation lag, the entire weight is sensed at all times.
- The feed accuracy can always be checked during normal operation without a need for sampling.

The feeders are controlled by a KSL/KLCD multiple feed controller manufactured by K-Tron America. The KSL/KLCD provides the capability to interface with a maximum of 8 feeders within 1 line.

3.4 Modification of Barrel Section

Two process output variables, melt pressure at the die and torque, were available at the beginning of this project. This number of process output variables was not adequate. It was necessary to measure more process output variables related to the extrusion process to correlate with the final product quality. Thus, some pressure and temperature measuring devices had to be mounted. However, it is important to have a fully filled region to get a stable pressure reading of the product. Such a region is available at the left hand screw element, the kneading block, or the die. Thus, the kneading block, 625 mm away from the feeder end, was selected as a potential location for the new measuring devices.

The existing barrel section did not have any option to mount new measuring devices. Thus, it was necessary to design and prepare a new barrel section with these facilities. Figure 3.4 shows a photograph of the modified barrel section. An old barrel section was replaced with the modified barrel section. The modified barrel section can also be seen in Figure 3.2.

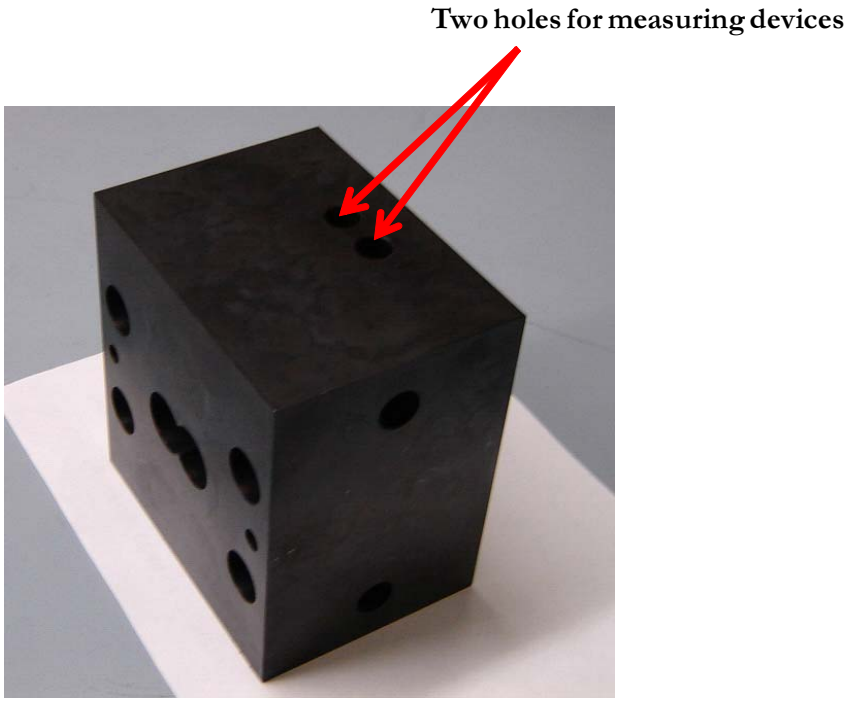

Figure 3.4: Modified barrel section.

The modified barrel section has two holes, location A and location B, at the

same cross section. The centers of these holes are 625 mm from the feeder end with this arrangement. A pressure transmitter with built-in thermocouple in location A was mounted to measure both melt pressure and temperature at the same location. In location B, one pressure transmitter was mounted to get melt pressure at that location. All the transmitters are manufactured by Dynisco. Mounting both pressure transmitters at the same cross section will show the effect of direction of screw rotation on pressure. In addition, one more thermocouple was mounted at the die to measure melt temperature in the die section. These measuring devices give 4 more process output variables.

3.5 Data Access

The ZSK-25 extruder has a man machine interface to observe data. There was no option for data collection and dissemination at the beginning of this project. However, it is important to have data access for modeling, validation, control, and monitoring of extruder operation, the objectives of this study.

3.5.1 OPC Data Communications

Object linking and embedding for process control is the standard for plant floor communications between data servers and client applications. It is a standard developed by the OPC Foundation for process data communication between systems. Each standard has its application depending on the function required. There are many regulatory control vendors and advanced control vendors of systems used in plants. These systems make use of plant data through OPC communication. OPC allows the end user to have the freedom to choose a mix of systems without system inter-connectivity issues. The OPC Foundation has published a number of standards; the following three are the standards used mainly in industries:

- Real-time Data Access-OPC DA;
- Alarm and Event-OPC AE; and
- Historical Data Access-OPC HDA.

3.5.2 Process Data Access

The extruder has a programmable logic controller (PLC). It is possible to acquire data from the PLC using OPC DA. An OPC server and an OPC client are necessary to establish a complete OPC DA setup. A PC with an RSLinx OPC server is connected to the extruder's PLC using RS232 cable. RSLinx is an OPC-compliant

data server supporting the OPC DA. LabVIEW 7.1 acts as the OPC client. Figure 3.5 shows the details of the data acquisition setup between the PC and the extruder. This acquisition setup obtains all the data available from the PLC: barrel temperatures at five different zones, melt temperature at the die, melt temperature at location A, melt pressure at the die, melt pressures at locations A and B, motor torque and screw speed.

The K-Tron feed controller has a Modbus RTU protocol. Modbus RTU is an open, serial (RS-232 or RS-485) protocol derived from the client/server architecture. It is a widely accepted protocol due to its ease of use and reliability. A Modbus RTU Master Driver was installed in the PC to communicate with the feed controller using RS232 cable. Again, LabVIEW 7.1 was used as a client to communicate with this protocol. Figure 3.5 shows details of the communication between the PC and the feed controller.

Data for all process variables could be acquired as fast as every 0.1 sec and logged in spreadsheets for further use. Figure 3.5 shows that data were collected from two different sources, the extruder's PLC, and from the K-Tron feed controller. However, all data were synchronized and logged in the spreadsheet with the same time stamp.

3.6 Process Automation

It is necessary to establish two-way communication between computer and process to implement computer controlled schemes, i.e., process automation. In advanced control strategy, control algorithms are executed in the computer and the resulting output is sent to the process. In this study, the control algorithm was executed in the MATLAB script of LabVIEW. LabVIEW sends the necessary input arguments to MATLAB. MATLAB executes the control algorithm and sends the controller outputs to LabVIEW. Finally, these controller outputs are sent from the PC to the extruder's motor drive and feed controller.

Figure 3.5 shows the communications established between the feed controller and the PC. That is, any command from the PC can be sent to the feed controller and the feed controller will take the necessary action to control the feed rate. However, no such communication was established for PC-PLC communication, rather only data acquisition from the extruder's PLC was performed. The PLC has complicated interlocking programs that make it difficult to send control commands from the computer to control process input variables, e.g., screw speed, through the PLC. Moreover, understanding and rewriting the PLC program for sending control commands is not a trivial task. Thus, screw speed was controlled bypassing the PLC. Output (screw speed) of a control algorithm was sent directly from the PC to the motor drive using

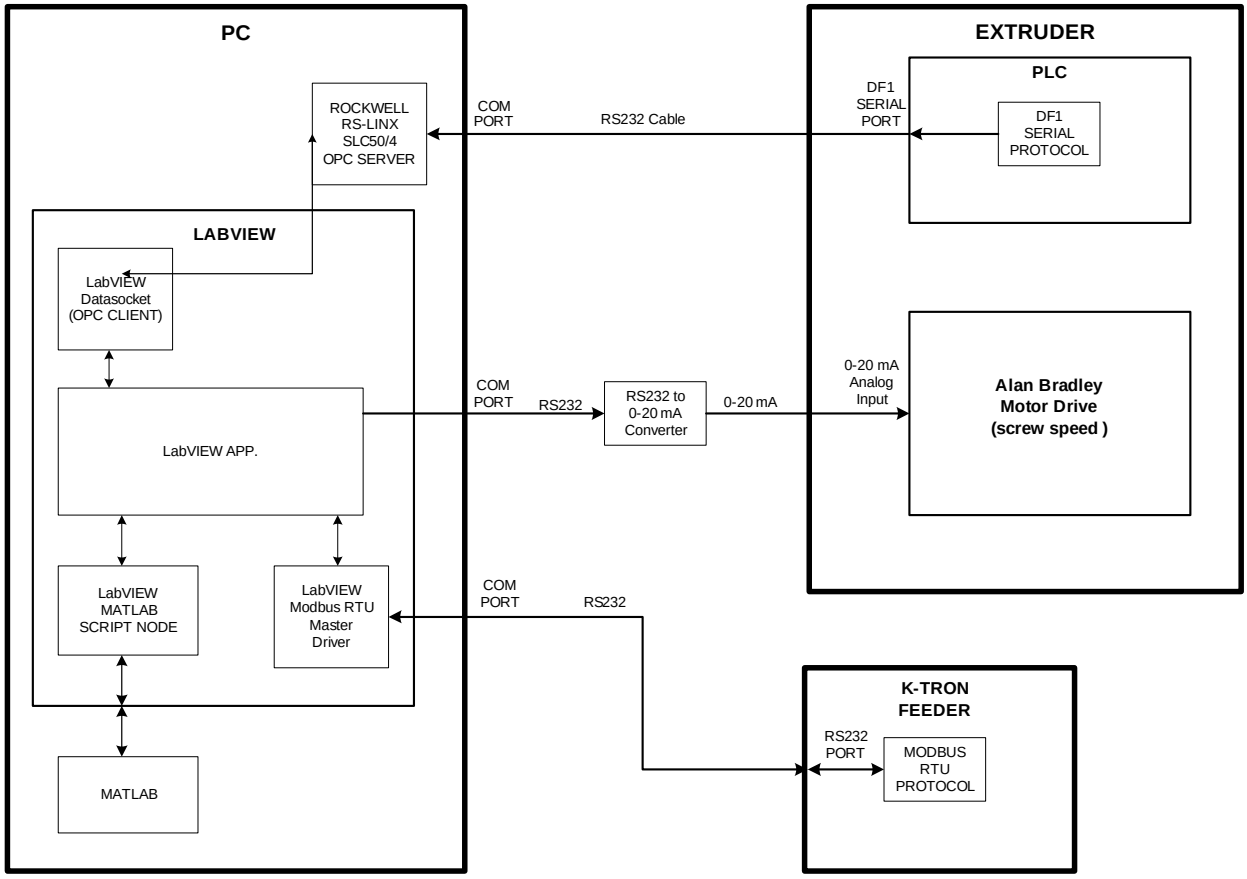

Figure 3.5: System diagram for data access and control.

an RS232 cable. In this route, a digital to analog converter was used to send analog input to the motor drive (see Figure 3.5). It is worthwhile to mention that the PC to motor drive communication was one-way.

A graphical user interface (GUI) was developed in LabVIEW to acquire data in the PC. Data were acquired from the extruder's PLC using this interface. Figure 3.6 shows the PC-extruder data acquisition interface. This interface shows melt pressures at three locations (die, location A and location B), melt temperatures at two locations (die and location A), torque, screw speed, and barrel temperatures at five zones. This GUI shows all the process variables in a table format and in plots to check process abnormality. Data acquisition frequency can be changed from this interface.

Another GUI was developed to acquire data from the feeder's PLC. Figure 3.7 shows PC-feeder data acquisition interface. This interface was also used for closed loop control. Bumpless transfer from manual to auto mode was done using this GUI. PC-feeder interface pulled necessary data from PC-extruder interface to execute any control algorithm. Outputs from algorithms, manipulated variables, were sent to the final control elements from this interface.

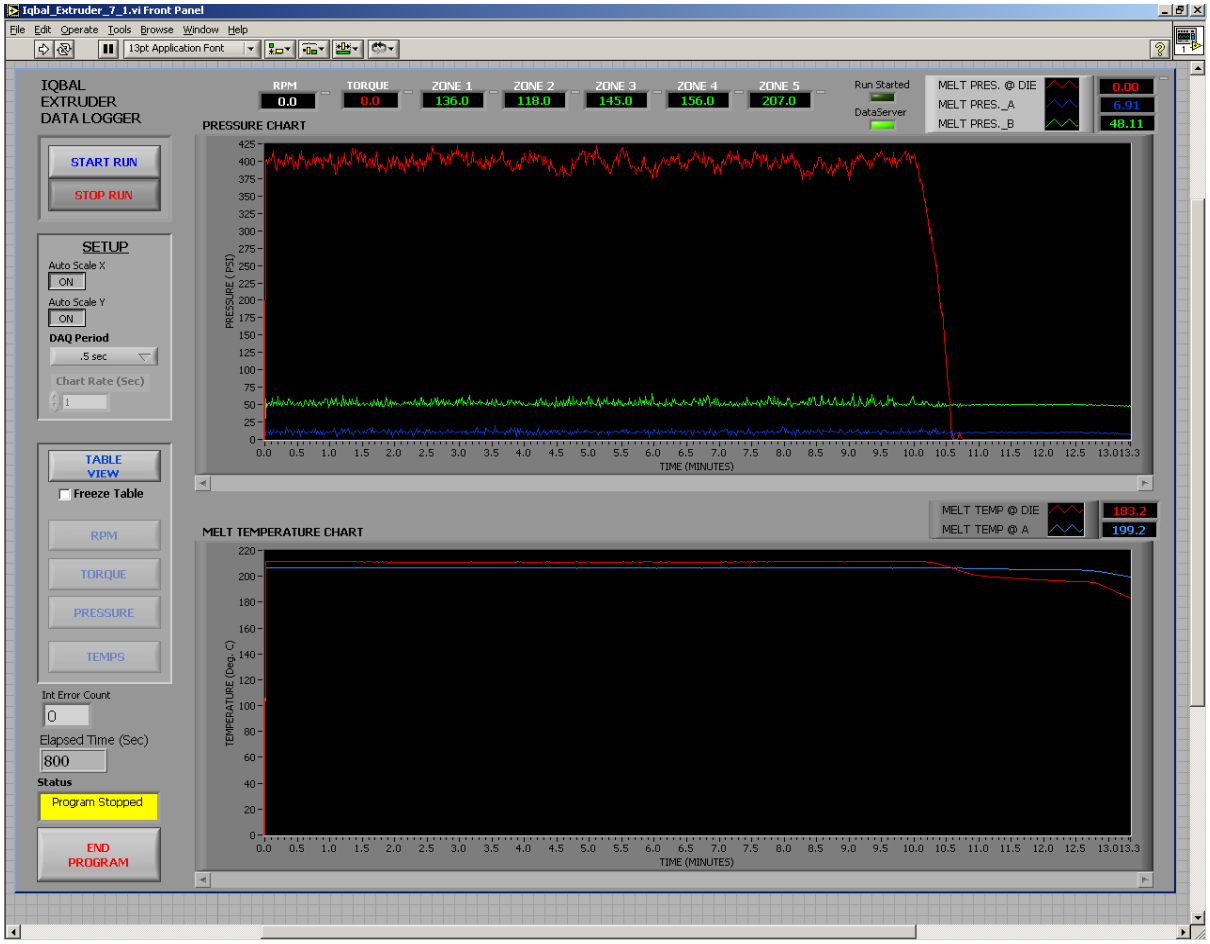

Figure 3.6: PC-extruder data acquisition interface.

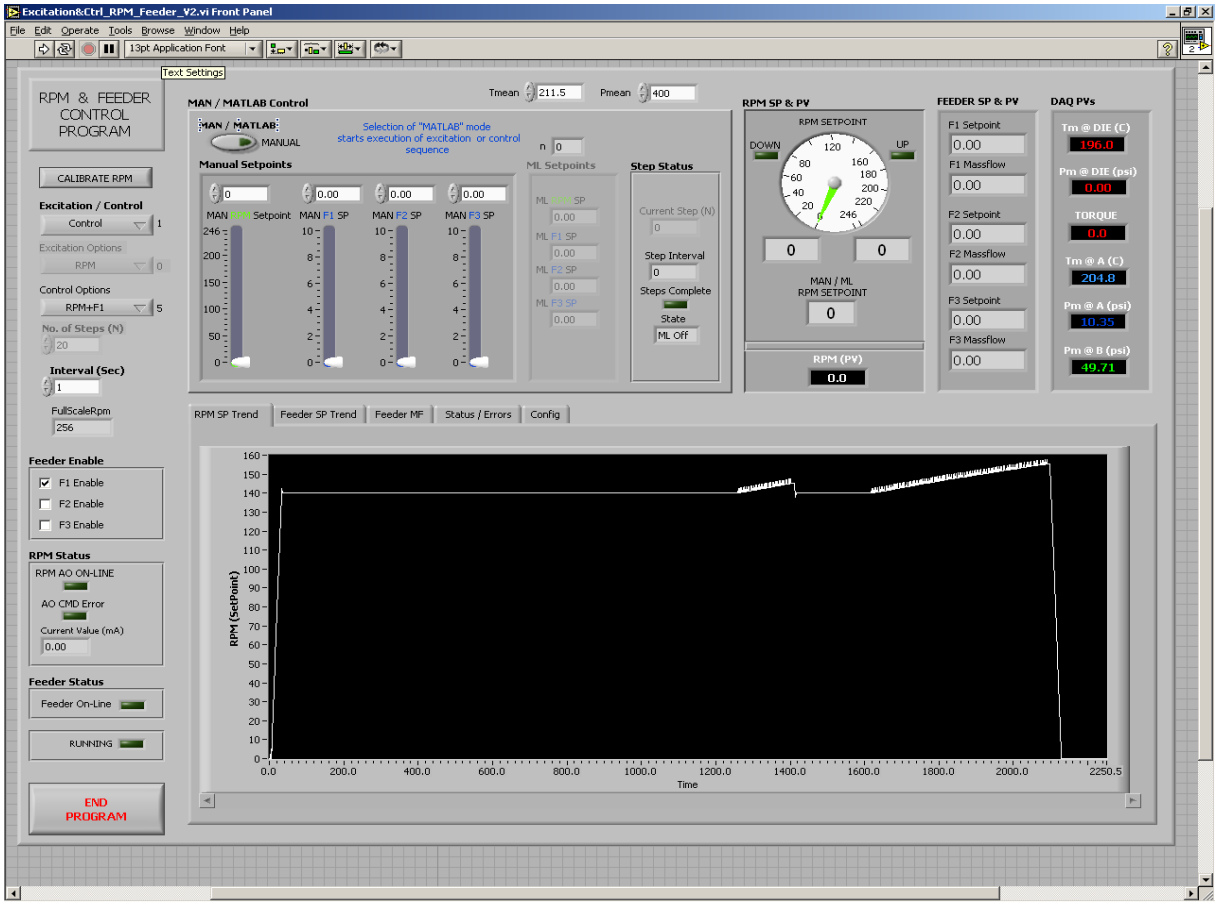

Figure 3.7: PC-feeder data acquisition interface.

Chapter 4

Grey Box Modeling

4.1 Introduction

Grey box modeling incorporates both a fundamental knowledge of the process and access to the process data. Incorporation of a greater level of intelligence about the system and process knowledge in system identification technique has showed significant advancement in modeling techniques. It is imperative to incorporate product quality attributes in the modeling techniques as well for extrusion processes. The objective of any control system in a plasticating TSE is the control of product properties. Product properties are often not measured online; hence, product qualities cannot be controlled directly in most cases. A number of researchers have developed grey box models for plasticating extrusion processes (McAfee and Thompson 2007, McAfee 2007, Garge *et al.* 2007), but none of the modeling techniques have been used to control the processes.

In this chapter, a systematic approach is detailed for developing dynamic grey box models to predict the behavior of output variables due to changes in input variable-screw speed (N) for a co-rotating TSE. Controlled variables were selected based on steady state and dynamic analyses, then developed dynamic grey box models relating the controlled variables to N. The selection procedure, based on product quality parameters, is described in this chapter. Models developed using this approach were used to design advanced control schemes.

4.2 Theory

It is imperative to understand the underlying behavior of process variables using fundamental knowledge of the twin screw extrusion process. Incorporation of such mechanistic knowledge makes the model more robust. The effect of a change in

Portions of this chapter: was published in Mohammad H. Iqbal, Uttandaraman Sundararaj, Sirish L. Shah, *Ind. Eng. Chem. Res.*, 49, 648-657, (2010) and was presented in the 58^{th} *Conference of Canadian Society for Chemical Engineers*, (2008).

screw speed on different process output variables, e.g., melt temperature and melt pressure, can be modeled based on first principles knowledge of the extrusion process.

4.2.1 Effect of Screw Speed on Melt Temperature

In a TSE, the shear rate for any screw speed can be defined according to equation 4.1:

$$\dot{\gamma} = \frac{\pi D_{ext} N}{H} \tag{4.1}$$

where $\dot{\gamma}$ is the shear rate, D_{ext} is the diameter of the screw, and H is the screw channel depth. In an extrusion process, polymer melts experience high shear rates and thus are in the shear thinning regime where the viscosity follows a power law relationship with shear rate according to equation 4.2:

$$\eta = k\dot{\gamma}^{n-1} \tag{4.2}$$

where η is the viscosity, k is the consistency index, and n is the power law index. The required power ($\dot{E}$) per unit volume to rotate the screw at a certain speed can be expressed as:

$$\dot{E} = \eta\dot{\gamma}^2 \tag{4.3}$$

Polymer melt temperature increases mainly due to energy dissipation provided there is no energy loss in the system. Thus, the power heats the polymer melt and is proportional to the change in melt temperature (T_m):

$$\dot{E} = \dot{m}c_p\Delta T_m \tag{4.4}$$

where $\dot{m}$ is the mass flow rate and c_p is the heat capacity of the polymer melt. By combining equations 4.1, 4.2, 4.3 and 4.4, the following relation between T_m and N is obtained:

$$\Delta T_m \propto N^{n+1} \tag{4.5}$$

Equation 4.5 indicates a nonlinear relation between T_m and N. However, a linear relation can be obtained using a variable transformation such as $u_1 = N^{n+1}$.

4.2.2 Effect of Screw Speed on Melt Pressure

A change in N affects both the throughput and the viscosity. Melt pressure (P_m) has a linear relation with throughput and viscosity. Thus, the effect of a change in N on P_m is likely to be a product of the dual effects of throughput and viscosity. However, the effect of throughput is instantaneous for a TSE. Because a TSE is starve-fed, the throughput returns to its original value immediately. That is, the effect of filling in the extruder changes when N is changed but a new steady state is

achieved fairly quickly. So, the behavior of P_m due to a change in N is assumed to be mainly due to a change in viscosity. This relation can be written as:

$$P_m \propto \eta \tag{4.6}$$

By combining equations 4.1, 4.2, and 4.6, the following relation between P_m and N is obtained:

$$P_m \propto N^{n-1} \tag{4.7}$$

Like the relation between T_m and N, equation 4.7 shows the nonlinear relationship in P_m due to a change in N. Screw speed can be transferred as $u_2 = N^{n-1}$ to obtain a linear relationship with P_m.

Equations 4.5 and 4.7 show that the models for T_m and P_m are lumped parameter models. However, model parameters can be estimated using experimental data. Use of experimental data to estimate model parameters eliminates the potential shortcomings of models developed based solely on first principles. For example, the effect of throughput due to a change in N was not considered in developing equations 4.5 and 4.7 to keep the models as simple as possible. However, it is possible to capture the effect of the throughput by estimating model parameters using the experimental data.

4.3 System Identification

From a modeling point of view, a system is an object in which variables of different kinds interact and produce observable signals. Typically, these observable signals are called outputs. Different external stimuli affect the system. The signals, which can be manipulated, are called inputs. System identification means the development of a model of a dynamic system from measured input-output data. Essentially, it is an experimental approach for modeling dynamic systems. The term system is a wide and broad concept, which plays an important role in modern science. Knowledge of the model is important for many industrial processes as it is required for design and simulation of the plant. System identification develops a model of a system without any prior knowledge of the physical process. It allows us to model a high order process to obtain a lower order one with a very good fit using only the input and output data of the system, provided the input data has sufficient excitation. Even when the significant process parameters cannot be calculated, or the process is too complicated to be expressed analytically, system identification can be applied successfully.

Ljung *et al.* (2006) explained the basics steps in the system identification procedure to develop a model from data:

- Experiment with data collection using pre-designed experimental procedures.
- Preprocess data to remove noise, outliers, etc., from measured data.
- Select a set of candidate models.
- Estimate model parameters using the data.
- Validate the model preferably with a different set of data.

Model flexibility allows use of the same model to describe the dynamics of the plant under various situations and operating conditions. That is, the model should be able to cover the true system. However, the existence of disturbances that cannot be controlled by the user makes it difficult to achieve the parameters of the true system.

The type of model structure and its order should be selected based on the factors outlined below:

- A good fit between model predicted outputs and experimental data is desirable. This model fit indicates how close model predictions are to the measured states.
- Statistical tests on model prediction errors should be performed. If a model captures the process dynamics quite well, prediction errors should be white noise.
- The model with the smallest number of independent parameters is chosen (parsimony principle).
- The model with the smallest value of final prediction error is selected.
- The model with the smallest value of Akaike's Information Criterion is selected.

The model fit is calculated according to equation 4.8

$$Modelfit = 100 \times [1 - \frac{norm(y_{measured} - y_{predicted})}{norm(y_{measured} - y_{average})}] \tag{4.8}$$

where y is the process output.

4.4 Experimental Section

4.4.1 Process Variables

This work was performed on the ZSK-25 twin screw extruder. Figure 4.1 shows the location of one thermocouple and one pressure transmitter at the end of the

processing section (i.e., at the die) to measure the temperature and pressure, respectively, of the polymer melt. In addition, two more pressure transmitters, one with an integrated thermocouple, were mounted 625 mm away (locations A and B) from the feeder end to measure the temperature and pressures of the polymer melt. All the temperature and pressure sensors were manufactured by Dynisco (Akron, Ohio, USA). Five output variables, three melt pressures, and two melt temperatures are measured using these sensors. Torque is another process output variable. All together there are six output variables available to correlate with the product quality variables (PQVs), and these output variables can be used also as controlled variables.

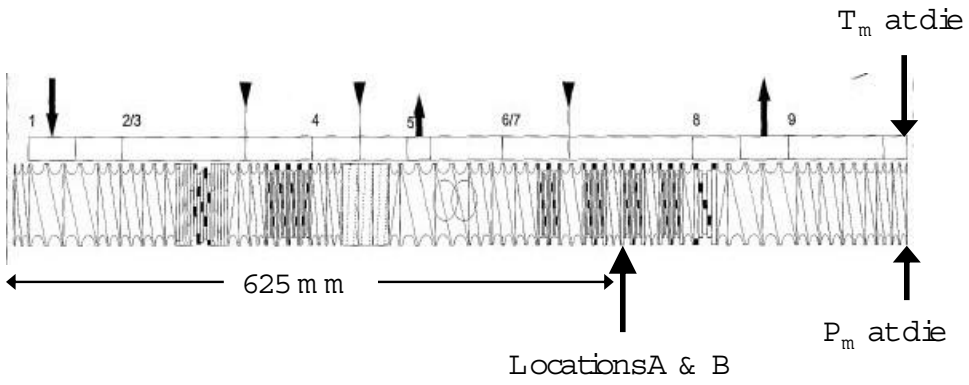

Figure 4.1: Schematic of a ZSK-25 TSE with sensors.

4.4.2 Materials

Two high density polyethylenes (HDPEs) generously donated by Nova Chemicals (Calgary, Alberta, Canada) were used in this study. The commercial names of these polymers are SCLAIR 2907 and SCLAIR 19G but are named HDPE1 and HDPE2, respectively, in this study. According to the manufacturer, the melt index of HDPE1 is 4.9 g/10 min and that of HDPE2 is 1.2 g/10 min. Both the polymers have a

melting point of 135^{o}C.

4.5 Experimental Procedures

4.5.1 Steady State Operation

For the correlation analyses between the six process output variables and PQVs, the steady state operation of the TSE was performed for blends of the two HDPEs. A barrel temperature of 200^{o}C, a screw speed of 150 rpm, and a feed rate of 5 kg/h were used as nominal operating conditions. Three compositions of HPDE1 (30%, 50%, and 70%) were blended with HDPE2 in the TSE. The TSE was allowed to run for sufficient time to achieve all the operating conditions at their nominal values before collecting samples of extrudate. Samples were collected in pellet form in a container for 50 sec. A total of 20 containers of samples were collected to measure the PQVs. Process data were acquired every 0.1 sec. Two different types of PQVs were studied for the correlation analysis: melt index and rheological properties.

4.5.2 Melt Index

The melt index (MI) of extrudate samples was measured according to the ASTM D1238 procedure. A temperature of 190^{o}C and a weight of 2.16 kg were used. The melt indexer used in this analysis was manufactured by Tinius Olsen, Horsham, PA, USA and generously made available by AT Plastics Inc., Edmonton, Alberta, Canada.

4.5.3 Rheological Characterization

At identical operating conditions, rheological properties will vary with the blend concentration of the samples (Hussein *et al.* 2005). Thus, two samples from each composition of the HDPE1 blend were considered for rheological characterization. For rheological analysis, 25 mm circular discs with a thickness of 2 mm were prepared at 200^{o}C using a Carver press (Wabash, IN). A Rheometrics RMS800 rheometer with parallel plate geometry was used for dynamic rheological characterization. Frequency sweeps were performed from 0.1 to 100 rad/s with 10% strain at 200^{o}C. Nitrogen was used to avoid any possible degradation of materials during the experiment. A similar procedure was followed to determine the power law index for HDPE1.

4.5.4 Input Excitation

The classical excitation method for an open loop process is to subject the process to a step change in each of the manipulated variables and subsequently measure the responses of the output variables. Both positive and the negative step tests in screw speed were performed to get an estimate of the time constants for melt pressure and melt temperature at die. Nominal operating conditions for barrel temperature and feed rate were 210^{o}C and 6 kg/h, respectively. Only HDPE1 was used as the processing material for the dynamic analysis. The screw speed was excited between 120 rpm to 160 rpm to get better signal to noise ratio in the process output variables. Responses in process output variables due to a smaller change in screw speed might be confounded with fluctuations. Starting from the central set point of the screw speed (140 rpm), a magnitude of 10 rpm was used in each step in the positive direction up to 160 rpm and sufficient time was given to settle the response of the process variables between two successive steps. Similar magnitude of step and the same procedure were used in the negative direction down to 120 rpm. Time constants (τ_p) of 50 sec and 10 sec were estimated for melt temperature at die and melt pressure at die, respectively, from the step test in screw speed.

Step response tests mainly excite low frequency components of the process; hence, dynamic models developed from these experiments do not fit the process well at higher frequencies. Therefore, a random binary sequence (RBS) type excitation was designed for the screw speed with minimum and maximum screw speed rates of 120 rpm and 160 rpm to obtain a set of meaningful data. Such an excitation is completely random. The estimated time constant from the step test data showed that the response of P_m is quite fast compared to that of T_m. To capture the dynamics of P_m properly, a RBS signal was designed based on the response of P_m. Thus, τ_p obtained from the response of P_m was used to design the RBS for N.

A sampling interval (t_s) of 1 sec was selected according to $\frac{\tau_p}{20} \leq t_s \leq \frac{\tau_p}{10}$. The Nyquist frequency (f_N) is then one half of the sampling frequency (f_s). A value of zero was used for a lower bound of input frequency (ω_L) to get a good estimate of the gain. The normalized upper bound of the input frequencies was calculated according to equation 4.9,

$$\omega_U = K\frac{\omega_{CF}}{\omega_N} \tag{4.9}$$

where K is any value between 2 and 3, ω_{CF} is the corner frequency of the process ($\frac{1}{\tau_p}$) in rad/time, and ω_N is the Nyquist frequency ($2\pi f_N$) in rad/time. From the range of input frequencies obtained from equation 4.9, a value of 0.08 was selected as an upper bound of input frequency for the experimental design. A total of 120 RBS samples of N were generated between 120 rpm and 140 rpm within the bound of input frequencies. Figure 4.2 shows the designed RBS excitation in screw speed.

The mean and standard deviation of this excitation were 141 rpm and 20 rpm, respectively. Each sample of N was excited for 1 min so, in Figure 4.2, when the RBS sequence shows the first five samples are at 120 rpm, the TSE was run at 120 rpm for the first five minutes. This excitation covered both low frequency and high frequency spectra. The process data were acquired every 0.1 sec (10 Hz).

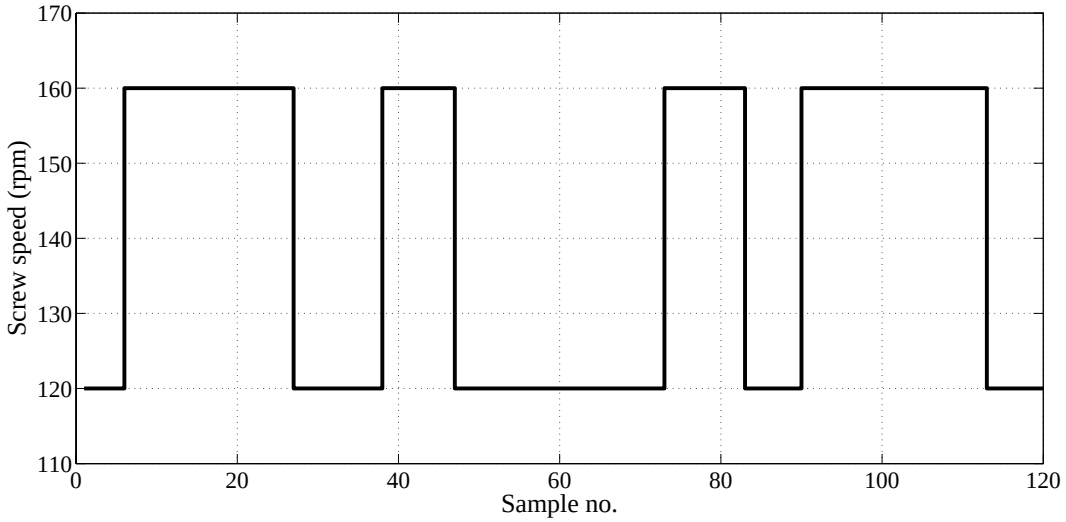

Figure 4.2: Random binary sequence excitation in screw speed.

4.5.5 Data Preprocessing

In most cases, measurement of process variables is corrupted with different types of process noise or disturbances resulting from a number of sources mentioned previously. In addition, measured data might have outliers, which can have a significant effect on the process modeling. Essentially, data preprocessing is the key to obtain a desirable final application. The effects of noise can be reduced by signal conditioning or filtering. There are a number of techniques available in the literature for filtering. In this analysis, an exponentially weighted moving average (EWMA) filter was used to reduce the noise level from the measured data. The analog version of this filter can be represented by a first order differential equation,

$$\tau_f \frac{dy_f(t)}{dt} + y_f(t) = y_r(t) \tag{4.10}$$

where y_r is the raw data (measured), y_f is the filtered data, and τ_f is the time constant of the filter. τ_f is chosen to be much smaller than the dominant time constant (τ_{do}) of the process to avoid introducing any dynamics from the filter into the process. Usually, $\tau_f < 0.1\tau_{do}$ is used to meet with this requirement (Seborg *et al.* 2004). Equation 4.10 can be approximated by a first order backward difference

equation at the k^{th} step and the final filter equation in the discrete time domain can be written as follows:

$$y_f(k) = \alpha y_r(k) + (1-\alpha) y_f(k-1) \tag{4.11}$$

where $\alpha = \frac{t_s}{\tau_f + t_s}$, and t_s is the sampling time. Equation 4.11 is the form of an EWMA filter. Equation 4.11 shows that if $\alpha = 1$, there is no filtering, and if $\alpha \to 0$, data is heavily filtered and the measurement is ignored.

4.6 Results and Discussions

4.6.1 Steady State Analysis

Analysis of Melt Index

Figure 4.3 shows the log-log plot of the melt index of 20 samples with six process output variables. HDPE1 compositions of 30%, 50%, and 70% were represented by open triangles, circles, and squares, respectively. No considerable variation in MI measurement was observed for any HDPE1 composition. The MI of the polymer blend increased with an increase in HDPE1 composition, as HDPE1 has a higher MI than that of HDPE2. However, in general, with an increase in MI, the values of the six process output variables decrease. MI has an inverse relationship with viscosity. Thus, an increase in MI leads to a decrease polymer viscosity. Polymers of lower viscosity provide less viscous heat dissipation and less frictional heat generation; hence, melt temperatures also decrease with increases in MI. Pressure is proportional to viscosity, therefore, an increase in MI is accompanied by a decrease in melt pressure. These behaviors are reflected in Figure 4.3.

Figure 4.3 shows a significant variation in melt pressures, especially in P_m at A and in P_m at B. This is reasonable since these two pressure transmitters are mounted in the zone of kneading blocks and on top of the screw flights. The periodic passing of the screw flights over the transmitters introduces significant noise in the data. In addition, continuous mixing and breaking down of the solid polymer bed into the melt in the kneading blocks increases the noise level. It is observed that the variabilities of P_m at A and P_m at B increase with an increase in HDPE1 composition. HDPE1 has lower viscosity than that of HDPE2; hence, the viscous heat dissipation of HDPE1 is lower than that of HDPE2. Thus, for blends with higher HDPE1 composition, more solid polymer comes to the kneading block zone. The extra solid material melts in this zone and increases the noise level. On the other hand, the higher viscosity of HDPE2 generates more heat via viscous heat dissipation. Therefore, less solid polymer reaches this zone and thus there is less noise. Neither of these two output variables showed a correlation with MI. Torque

data did not give good correlation with MI either. The 50% HDPE1 concentration blend showed lower torque than the 30% and 70% HDPE1 blends. However, the P_m at the die showed little variation and correlated well with the MI. Both melt temperatures showed good correlation with the MI. However, the T_m at location A has considerable variation, especially at 70% HDPE1.

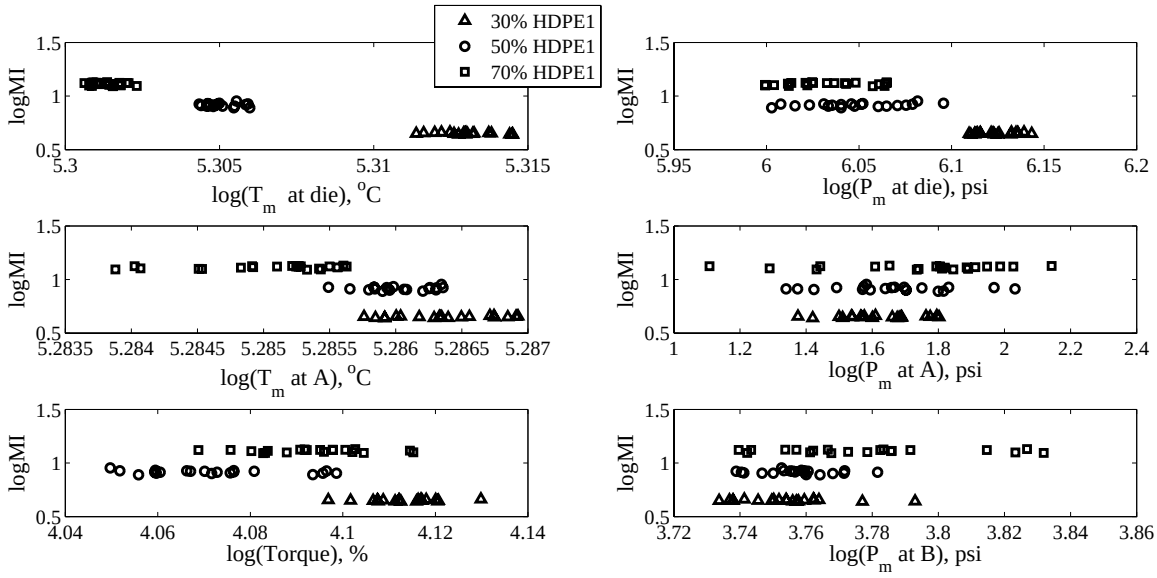

Figure 4.3: Logarithmic plots of melt index vs. output variables.

Rheological Analysis

Dynamic rheological data were obtained using frequency sweeps performed on two samples from each blend. Using this data, a power law model was developed for each sample invoking the Cox-Merz rule that states that the viscosity versus steady shear rate curve is identical to the dynamic viscosity versus dynamic frequency curve. A power law index of pure HDPE1 was determined to be 0.8. The shear rate of the TSE at steady state was calculated to be about 48 sec^{-1} according to equation 4.1. Steady shear viscosity at this shear rate was calculated using the obtained power law model and the average viscosities were (1270±7) Pa-s and (1155±7) Pa-s for 50% HDPE1 and 70% HDPE1, respectively. The standard deviations in the viscosities were very small for 50% HDPE1 and 70% HDPE1. However, slightly higher standard deviations in viscosity were observed among 30% HDPE1 samples. Thus, two more samples were used for the rheological test to calculate the average viscosity. The obtained average viscosity was (1570±35) Pa-s for the 30% HDPE1 blend. It was observed that the variability in viscosity between samples decreased with an increase in HDPE1 concentration. This essentially indicates that mixing becomes more uniform as the proportion of HDPE1 in the blend increases.

Figure 4.4 shows a logarithmic plot of viscosity versus the six process output variables. It was found that values of P_m at A, P_m at B, and torque did not show any trend with changes in viscosity. Note that plots of viscosity vs. melt temperature in Figure 4.4 showed that changes in melt temperature and viscosity were due to changes in HDPE1 composition only. The plots did not indicate any change in viscosity with changes in temperature, a relation usually modeled by the Arrhenius equation. Two samples with 50% and 70% HDPE1 and four samples with 30% HDPE1 were used in this plot to observe the trend of the viscosity change with the process output variables. Viscosity of HDPEs in general does not have a strong dependence on temperature. An increase in HDPE1 in the blend decreased the viscosity; hence, the melt temperature also decreased. Both the melt temperatures showed good correlations with the viscosity. However, T_m at A showed more variation than that of T_m at the die.

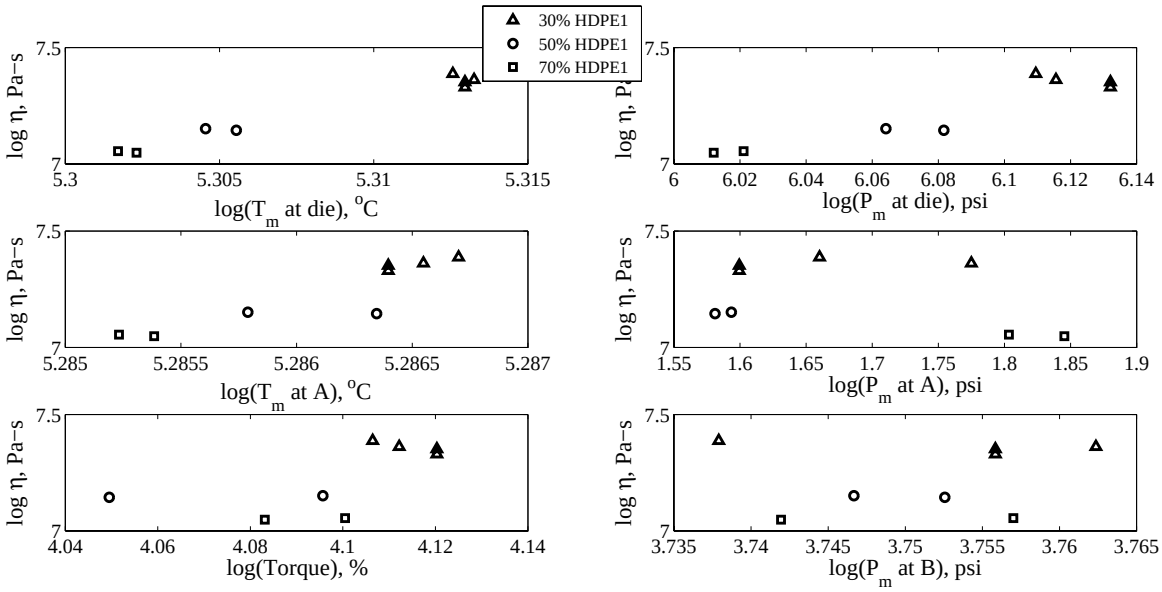

Figure 4.4: Logarithmic plots of viscosity vs. output variables.

From a correlation analysis between product quality variables and process output variables at steady state, P_m at the die, T_m at A, and T_m at the die were selected as potential controlled variables. However, the dynamic behaviors of these variables were also considered for the final selection of controlled variables. Eventually, the dynamic model will be used to design a model-based control scheme, thus it is necessary to check the dynamic behaviors of the variables.

4.6.2 Dynamic Analysis

Figure 4.5 shows the time trend of the six output variables due to the predesigned RBS excitation in N. It was observed that T_m at the die increased with an

increase in N and T_m at the die decreased with a decrease in N. However, a slow drift was noticed, which made this variable non-stationary. This drift could be due to loss of heat from the extruder during operation. However, this drift is so slow that it was neglected. T_m at A was also found to change with N but not as the same magnitude as T_m at the die. Thus, T_m at the die was selected as the controlled variable among the two melt temperatures. Significant variations in pressure and torque data were observed due to noise. Therefore, P_m at A, P_m at B, and torque were not considered for further analysis.

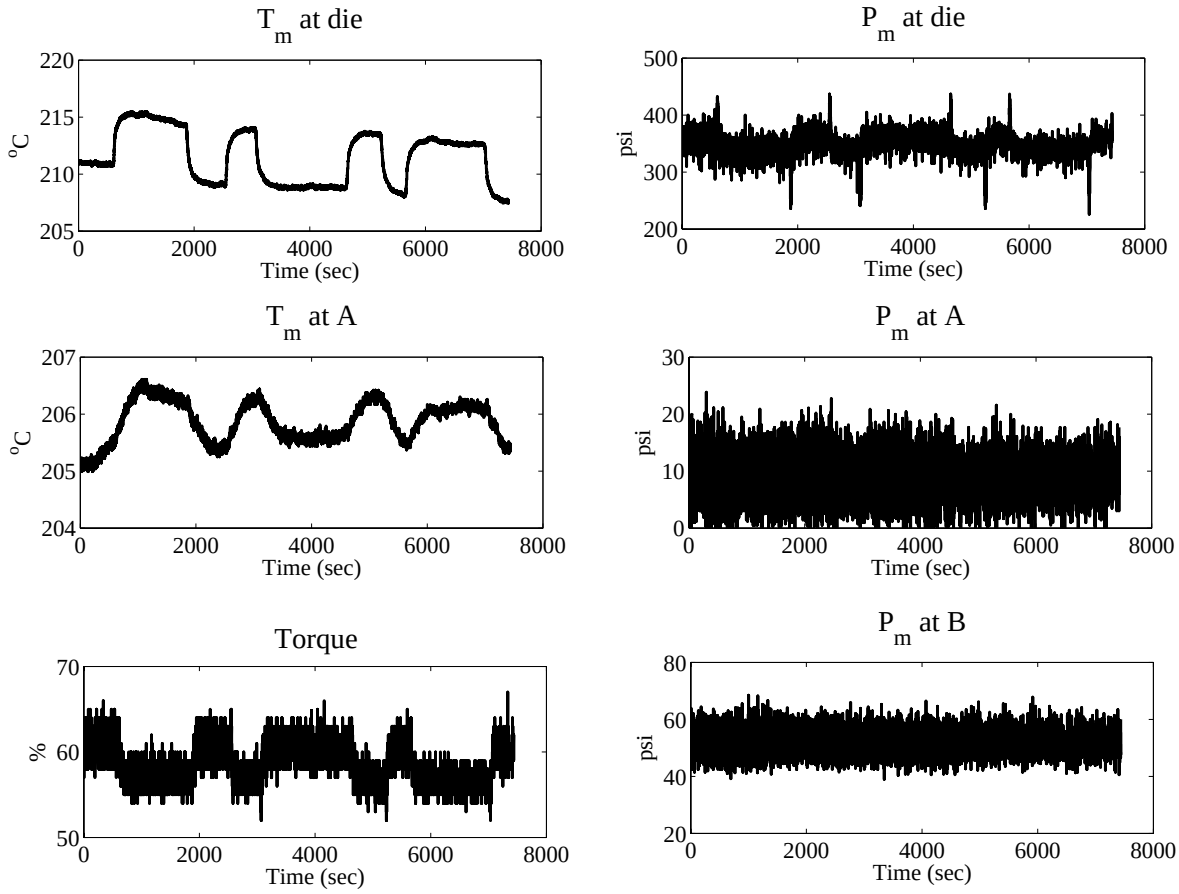

Figure 4.5: Time plots of the output variables.

P_m data were filtered because of noise prior to developing a model using these data. The mean residence time was calculated to be 98 sec for the TSE with the given screw configurations and the steady state operating conditions. This residence time was considered to be the dominant time constant. Thus, $\tau_f = 8$ sec was used to avoid introducing filter dynamics into the process, which gives 0.012 as a preliminary estimation of α. However, some fine tuning of this filter parameter was performed based on the level of noise in the measured data. Different values of α were used to filter the data and the level of noise in the data was used to select the final value of

α. The obtained final discrete filter is presented in equation 4.12,

$$y_f(k) = 0.03y_r(k) + 0.97y_f(k-1) \tag{4.12}$$

P_m at the die was filtered using the EWMA filter to remove noise. The filtered P_m at the die (Figure 4.6) was found to change inversely with changes in N. This is quite reasonable since an increase in screw speed increases shear rate; hence, viscosity decreases and, thus, P_m decreases. Therefore, P_m at the die was also selected as controlled variable. Peaks with significant magnitude were observed in this variable. No filtering was performed on data for T_m at the die data.

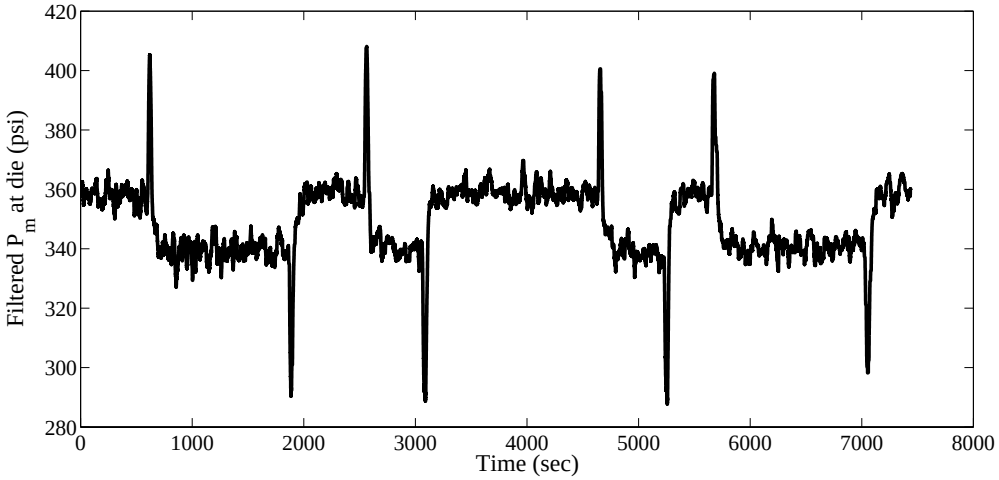

Figure 4.6: Time plot of the filtered P_m at the die.

Based on both the steady state and the dynamic analyses, T_m and P_m at the die were selected as controlled variables. Development of dynamic grey box models between these two process output variables and N is detailed in the following sections of this chapter.

To develop a dynamic model relating melt temperature and screw speed, a nonlinear transformation of N was performed according to equation 4.5. However, to make the data stationary, the linear trend from the data was removed, i.e., the data were detrended. As the complete response to thermal changes due to any input excitation is much slower compared to other process variables, the use of high-frequency data hinders modeling of the low and mid-frequency dynamics of the process. Thus, data were downsampled to every 1 sec. Such a sampling rate was used to design the RBS excitation in N. A nonlinear transformation of N was also performed according to equation 4.7 to develop a model between filtered P_m and N. Linear trends from the dataset was removed. Like the T_m dataset, data for P_m at the die were also downsampled to every 1 sec.

4.6.3 Impulse Response

To get an estimate of the possible time delay and the order of the process, an impulse response between detrended T_m at the die and N was estimated and is presented in the Figure 4.7(a). The impulse response estimate shows that the first peak outside the 99% confidence interval appears at the seventh lag, which indicates that the time delay between the input and the output is 7 samples. However, the physics of the process indicates that there should not be any significant time delay. Whenever any change in N is implemented, this change happens simultaneously over the entire screw shaft. The thermocouple at the die also senses this change immediately. Moreover, a gradual increase in the co-efficient of impulse response was observed from the second lag. This supports the claim that there might not be any time delay in this process except for the minimum one lag delay due to discretization of the process with a zero-order hold (ZOH) device. Thus, there is only one sample time delay between T_m and N. The shape of the impulse response coefficients indicated that the model order is at least second order.

The impulse response estimate for the filtered and detrended P_m at the die was also checked and is depicted in Figure 4.7(b). It was observed that the first statically nonzero peak, i.e., the peak outside the 99% confidence interval, appeared at the second lag. So, the possible time delay between P_m at the die and N is 1 sample. However, this is the inherent time delay due to discretization using the ZOH device. The arrangement of the impulse response coefficient indicated an inverse response of P_m due to the change in N and that the model order was second order or higher.

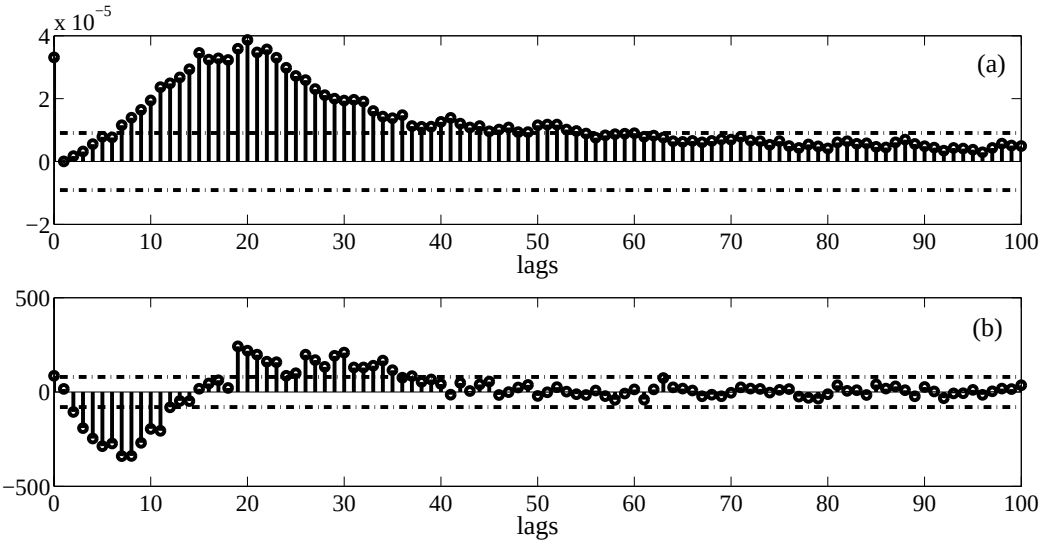

Figure 4.7: (a) Impulse response of the detrended T_m at the die. (b) Impulse response of the detrended filtered P_m at the die.

4.6.4 Spectral Analysis

Spectral estimation is used to describe the distribution of the power contained in a signal based on a finite set of data. Such an analysis describes how the energy (or variance) of a signal or a time series is distributed with frequencies. An estimated power spectrum of T_m and P_m was made using the MATLAB supplied spectral analysis function contained the script file '*spa.m*'. Figure 4.8 shows the spectral density plot of T_m and P_m data. The plot shows that the experiment was performed over a wide range of frequencies. Both T_m and P_m time series data contain a bit more energy in the low frequency region compared to that of the high frequency region. It can be observed that P_m data contains more energy than that of T_m data over the entire range of frequencies.

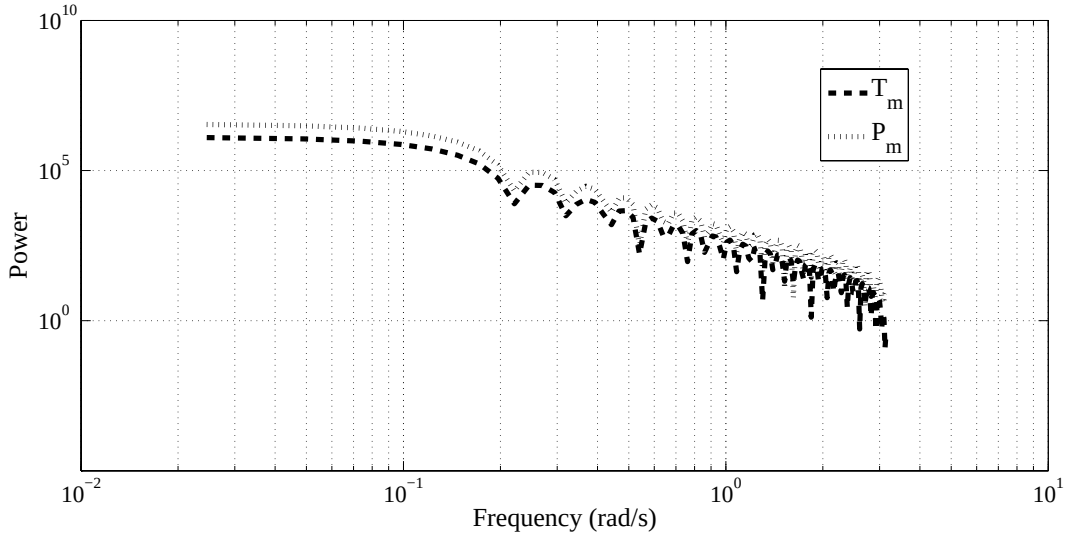

Figure 4.8: Power spectrum plot of T_m (broken line) and P_m (dotted line).

4.6.5 Model Development

The first half of the complete data set was used to estimate the model. The whole dataset was used in validating the obtained model to avoid initialization errors. Different model structures and orders were tried and the final model was selected based on the model selection criteria. The selected models between T_m at the die and N, and P_m at the die and N , are shown in equations 4.13 and 4.14, respectively.

$$\begin{aligned} T'_m(t) &= \frac{-4.372\times10^{-6}(\pm1.3\times10^{-6})q^{-1}+8.409\times10^{-6}(\pm1.4\times10^{-6})q^{-2}}{1-1.85(\pm0.011)q^{-1}+0.853(\pm0.011)q^{-2}}u_1(t) \\ &\quad +\frac{1-0.366(\pm0.02)q^{-1}-0.088(\pm0.02)q^{-2}}{1-1.85(\pm0.011)q^{-1}+0.853(\pm0.011)q^{-2}}e(t) \end{aligned} \tag{4.13}$$

$$P'_m(t) = \frac{-153.2(\pm 12.99)q^{-1} + 155(\pm 13.11)q^{-2}}{1 - 2.59(\pm 0.026)q^{-1} + 2.229(\pm 0.052)q^{-2} - 0.636(\pm 0.025)q^{-3}} u_2(t) + \frac{1 - 1.265(\pm 0.034)q^{-1} - 0.2911(\pm 0.033)q^{-2}}{1 - 2.59(\pm 0.026)q^{-1} + 2.229(\pm 0.052)q^{-2} - 0.636(\pm 0.025)q^{-3}} e(t) \quad (4.14)$$

where T'_m and P'_m are in the deviation forms, i.e., detrended. Values in the parentheses of equations 4.13 and 4.14 show the standard errors of the corresponding parameters. Equation 4.13 shows that the obtained model has an autoregressive moving average with an exogenous input (ARMAX) structure. The order of the model shows that the dynamics of T_m due to changes in N are second order. Both plant and disturbance transfer functions of the developed model have identical denominators. This indicates that screw speed and disturbance affect T_m in the same way.

This phenomenon can also be explained mechanistically. Only HDPE1 was used in the dynamic study. The feed rate was within the practical operating range for this small-scale extruder. Thus, the effect of bulk density as a potential disturbance on the output variables may not be significant. The change in P_m at the die was about ± 10 psi only, which indicates that the effect of die resistance may not be significant. Therefore, it can be assumed that the disturbance comes into play predominantly because of fluctuations due to the rotation of the screw, i.e., screw speed. Thus, it is assumed that the way the screw speed affects the output variables is similar to the way the disturbance affects the output variables. Thus, the physics of the process indicates that T_m should show dynamics similar to N due to changes in the disturbance because the noise affects T_m through the same channel as it affects N . Based on the physics of the extrusion process, the ARMAX structure is quite reasonable.

Equation 4.13 also shows the presence of right-half plane zeros that indicates an inverse response dynamics of T_m with changes in N. This means that an increase in N causes a sudden increase in throughput in the die section. Thus, more polymer melt from upstream, which has relatively lower temperature than that of the melt at the die section, is pushed into the die section and decreases the temperature of the melt in that location. Since the TSE is starve-fed, the throughput returns to its original value after the system recovers from its initial dynamic stage. The shear rate increases with the screw speed; hence, there will be more viscous heat dissipation. So, the temperature of the melt initially decreases for a short duration and then increases. This initial stage of the dynamics has a very short period. Such inverse dynamics were not observed in the time trend data of T_m at the die; however, the estimated grey box model was able to capture this successfully.

The model structure of equation 4.14 is also ARMAX. The obtained model for

P_m is the third order. Again, this model structure indicates that the change in N and disturbance affects the dynamics of P_m in the same way, which is in agreement with the physics of the twin screw extrusion process. Equation 4.14 also shows non-minimum phase zeros, which indicates an inverse response. Such response was indeed observed, as shown in Figure 4.6. A sudden increase in throughput at the die section due to an increase in N increases P_m at the die. Again, due to the starve-fed nature of a TSE, the throughput returns to its original value immediately. Since an increase in screw speed increases the shear rate, viscosity decreases and thus so does P_m.

Figure 4.9 shows the T_m at the die model fit for the infinite prediction horizon and almost 89% of model fit was obtained. There was a small mismatch in the gain; however, the predicted output from the model was still excellent. Comparison between P_m at the die model output and measured data is presented in Figure 4.10. The model fit was almost 59% for the infinite prediction horizon. Clearly, such a moderate model fit is due to the presence of significant noise even in the filtered data. Of course, it is tempting to increase the model fit by using heavily filtered data, but in such a case, the filter dynamics would confound the process dynamics. The steady state part of the data has significant noise and the model tries to fit those data as well. Thus, the model fit is moderate. However, the model predicted output agrees with the measured data satisfactorily, which is important for the design and implementation of a model-based control scheme online.

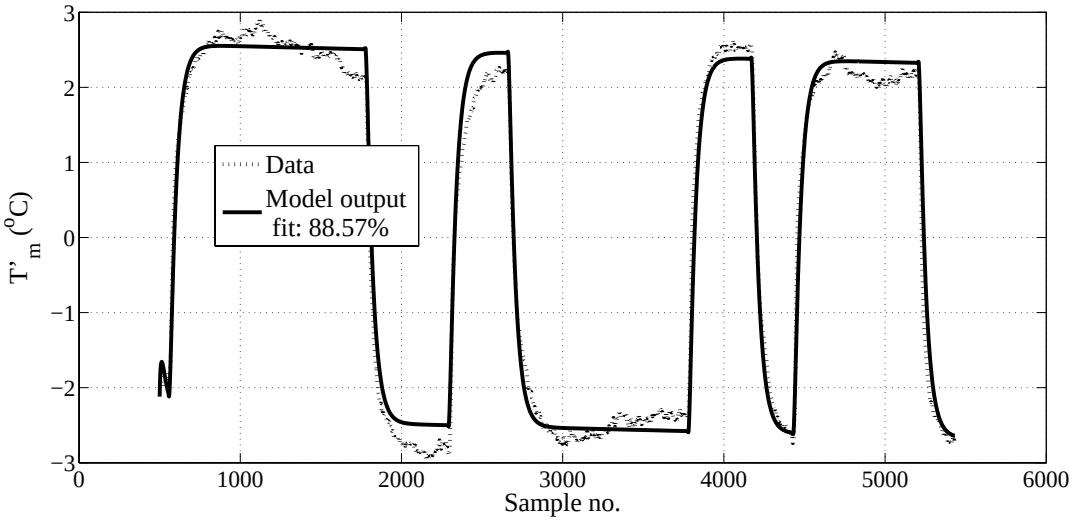

Figure 4.9: Comparison between the simulated melt temperature model output and the experimental data.

Model prediction errors, i.e., residuals, were analyzed to check the performance of the model. Note that if the model captures all the information from the data,

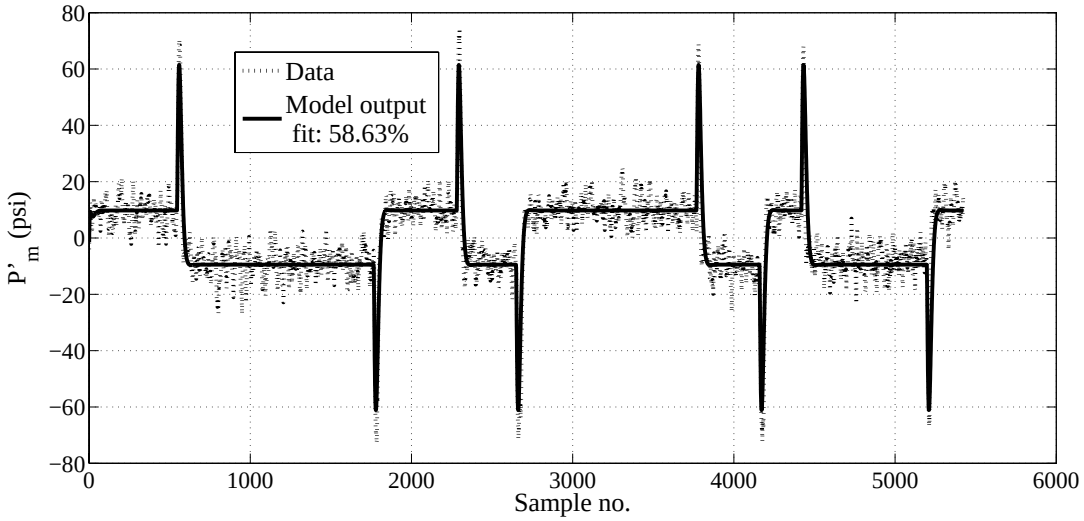

Figure 4.10: Comparison between the simulated melt pressure model output and the experimental data.

the residuals should look like white noise. It is also worthwhile to mention that in autocorrelation analyses, white noise shows nonzero peak at zero lag and zero peaks at other lags. On the other hand, white noise shows no peaks at any lag in cross correlation analyses. The top part of Figure 4.11 shows the autocorrelation between the residuals, and the bottom part of Figure 4.11 shows the cross correlation between the residuals and the input for the model for T_m at the die. Only one peak outside the 99% confidence interval was observed at lag zero, which indicates that the residuals are essentially white noise. In the bottom part of Figure 4.11, no peak was found outside the 99% confidence interval, which again suggests that there is no linear relation between the residuals and the input, i.e. the model extracted almost all the information from the measured data.

Residual analysis for the melt pressure model is presented in Figure 4.12. Autocorrelation (top part of Figure 4.12) of the residuals showed that almost all the peaks at any lag are within the 99% confidence interval except lag zero, i.e., the nature of the residuals was white noise. Cross correlation (bottom part of Figure 4.12) also showed that all the peaks were within the 99% confidence interval, indicating that there is no linear relation between the input data and the residuals. The white noise nature of the residuals suggests that the melt pressure model captured the process dynamics successfully.

4.7 Analysis of the Models

The obtained models were simulated to check their quality and robustness. This is done by checking the step response, the pole zero map, the bode plot, etc. It is

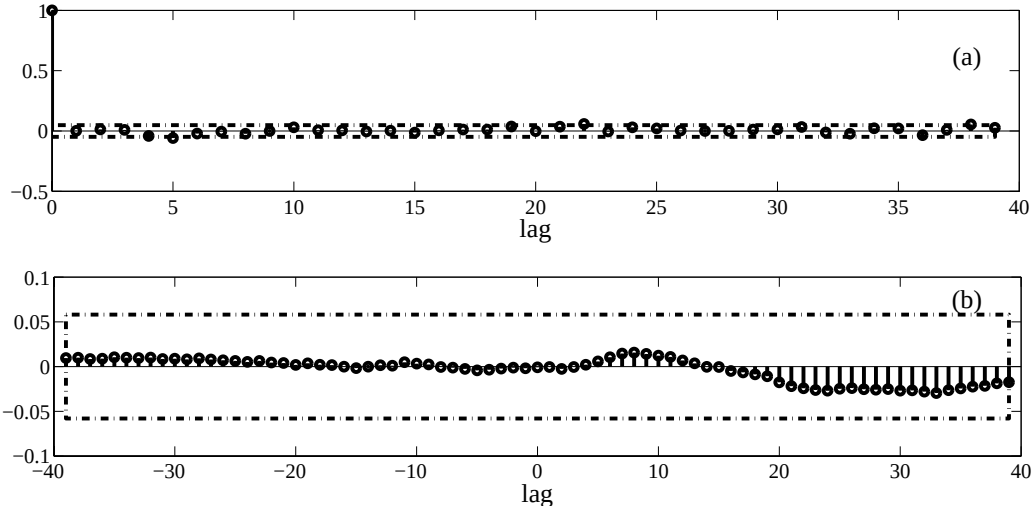

Figure 4.11: (a) Correlation function of residuals from the T_m model output, (b) Cross correlation function between u_1 and residuals from the T_m model output.

imperative to check such criteria to design a model-based control scheme using a model.

4.7.1 Melt Temperature Model

One of the applications of an open loop step test is to check the boundness of a process. Figure 4.13 shows the simulated response in T_m due to a unit step change in u_1. Both data and model predicted outputs come to a steady state value indicating the boundness of the system, i.e., the system is controllable. A slight mismatch between data and model predicted output was observed, which could be due to nonlinearity of the data.

Figure 4.14 shows the pole-zero map for the T_m model. Poles are shown by crosses ($\times$) and zeros are shown by circles ($\circ$). It can be observed that all the poles are inside the unit circle, which indicates that the system's poles are negative in the continuous s-domain. Also, poles inside the unit circle indicate the boundness of the system. Similar behavior was observed in the step response. The poles are not clustered on the unit circle. A concentration of the poles at the circumference of the unit circle indicates a fast sampling rate and a concentration of poles at the origin of the unit circle indicates a slow sampling rate. The poles are not concentrated at either locations; however, one pole is close to the circumference. Thus, the sampling rate for the model development was reasonable. Figure 4.14 also shows one zero outside the unit circle. Such a zero is known as an unstable zero. The obtained model has no pole zero cancelation or redundancy of parameters, which is good in the sense of controller design.

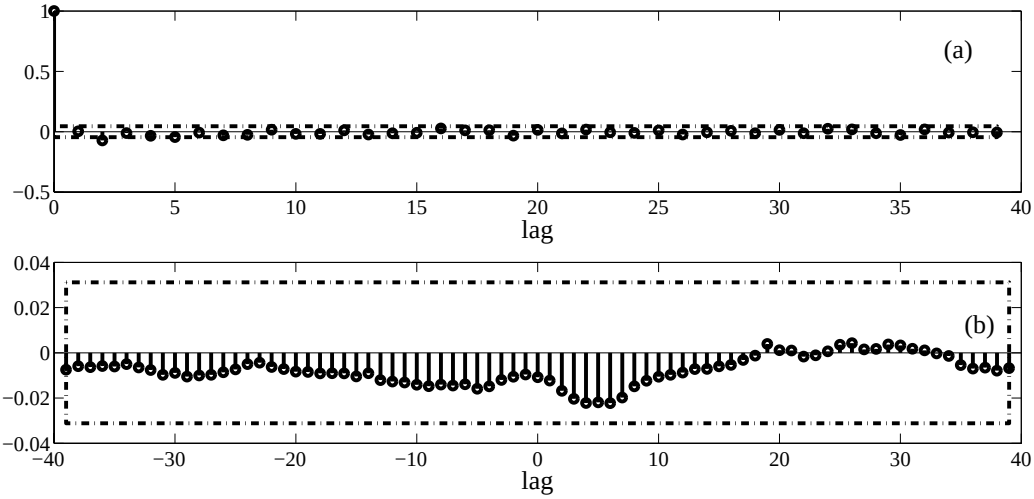

Figure 4.12: (a) Correlation function of residuals from the P_m model output, (b) Cross correlation function between u_2 and residuals from the P_m model output.

4.7.2 Melt Pressure Model

Figure 4.15 shows the step responses of experimental data and P_m model output due to a unit step change in u_2. Both responses come to a steady state which indicates boundness. Responses show a considerable inverse response, which was also observed in the time series P_m data obtained from the excitation in N.

Figure 4.16 shows the pole-zero plot of the P_m model. Poles are shown by crosses ($\times$) and zeros are shown by circles ($\circ$). All the poles are inside the unit circle, which indicates the boundness of the system. Figure 4.16 shows that poles are clustered neither on the circle circumference nor at the origin. Thus, the sampling rate is quite good. One zero is inside the unit circle and another zero is on the unit circle; no unstable zero is observed. Like the T_m model, no pole zero cancelation is observed for the P_m model.

4.8 Summary

A systematic approach was detailed to select controlled variables and to develop grey box models between the selected controlled variables and screw speed to design a control scheme for a plasticating TSE. Controlled variables need to be selected based on both steady state and dynamic considerations. T_m at the die and P_m at the die were finally selected as controlled variables and were used for further study. Pre-designed random binary sequences were successfully used to give persistent excitation in screw speed to yield a good and meaningful data set. The given excitation covered a wide frequency spectrum. In addition, the range of screw speed (120 rpm to 160 rpm) was large and covered a significant operating region.

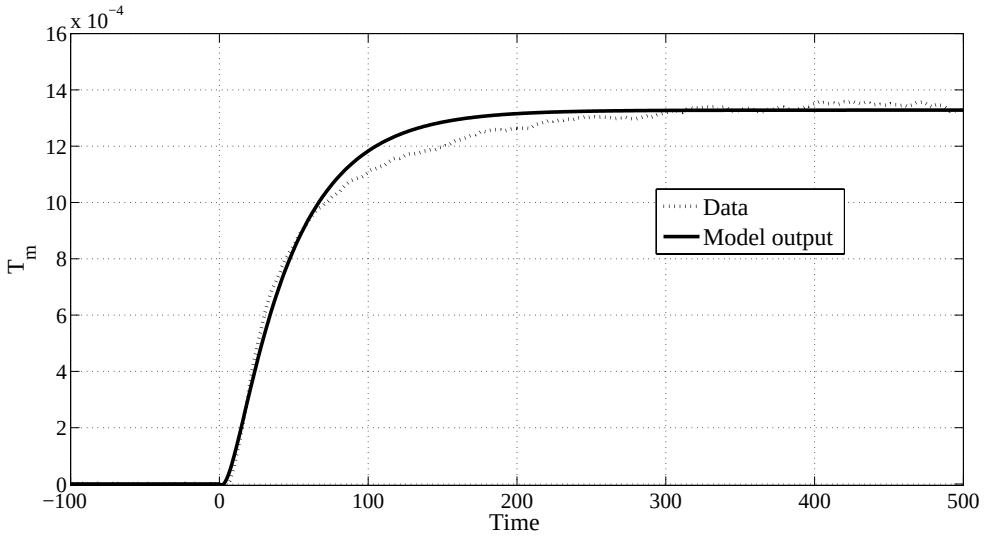

Figure 4.13: Comparison of step responses between experimental data and the T_m model predicted outputs.

The impulse response provided good preliminary estimation of the model structure. However, the time delay was estimated based on the physics of the extrusion process. Time delay of one sample was observed between T_m at the die and N, and P_m at the die and N which was due to discretization. However, the physical insight of the extrusion process suggested that there was indeed no time delay between the selected controlled variables and N in the continuous time domain.

The estimated grey box models with ARMAX structure for T_m at the die and P_m at the die explained the physics of the twin screw extrusion process quite successfully. For example, the inverse response of T_m at the die was captured and explained from the physics of the process. The model fit with experimental data for T_m at the die was almost 89%. Due to the significant noise level, the P_m at the die model showed about 59% fit with measured data. However, the prediction from the P_m at the die model agreed with the measured data quite satisfactorily.

The models' effectiveness in the design of model-based control schemes were checked. Simulated step responses for both models showed boundness of the systems, which indicates the systems were controllable. Similar conclusions were derived from observations pole-zero plots, which showed all poles inside the unit circle in both models.

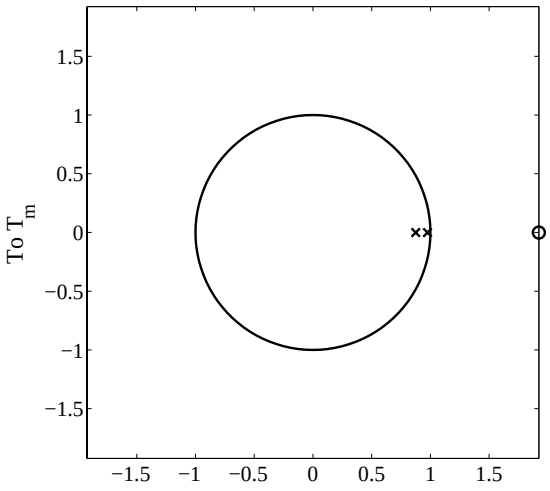

Figure 4.14: Pole-zero map for the T_m model.

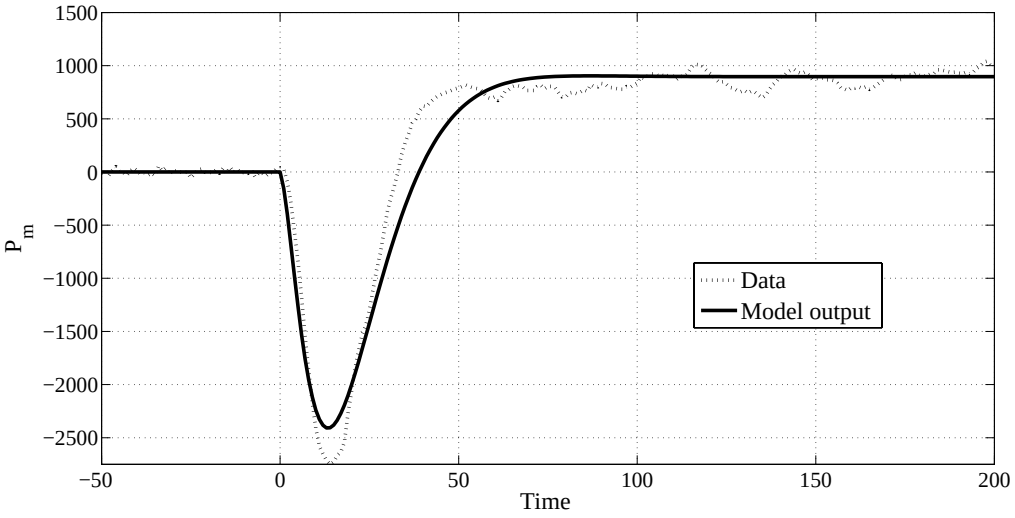

Figure 4.15: Comparison of step responses between experimental data and the P_m model predicted outputs.

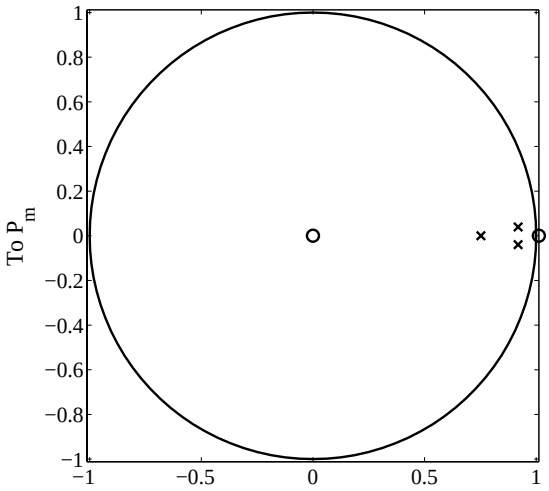

Figure 4.16: Pole-zero map for the P_m model.

Chapter 5

Process Identification Using Feed Rate Excitation

5.1 Introduction

Plasticating extrusion is a multiple interactive process for which interactions between inputs and outputs can be modeled. The total response of the extrusion process is a function of the individual component responses. A TSE has a number of input variables, which are also used as manipulated variables. Studying and modeling the effect of one input or manipulated variable is not adequate to design multiple-input multiple-output control schemes. In most cases, the behavior of a plasticating TSE has been studied by changing screw speed and different types of models were developed relating the behavior of the process variables to screw speed. An increase in screw speed increases throughput instantaneously. Since a TSE is a starved feed machine, the throughput backs to its initial value within a short period of time. Thus, it is also important to study the effect of feed rate on process variables. Very limited research has been performed to study the effect of feed rate on the extrusion process. In a commercial extrusion process, feed rate is usually maximized and controlled separately. However, varying feed rate offers greater flexibility to design and implement a process control scheme and may offer possibilities to optimize product properties. In the case of an extruder at the end of a polymerization process, the feed rate is always based on the reactor output. Thus, it is also important to develop a model relating extrusion process variables and feed rate.

Dynamic responses of process output variables due to the change in the feed rate (F) of a plasticating co-rotating TSE was studied in this work. In this chapter, models of the transient responses between process output variables and feed rate are detailed. Empirical models relating responses of process variables and F were developed using a classical system identification approach.

Portions of this chapter have been accepted for publication in *Poly. Eng. Sci.*

5.2 Dynamic Modeling Technique

5.2.1 Input Excitation

In order to identify or model any process behavior, excitation in the input is very important. Real processes have higher dimension than the models developed for them. To capture as much information from the data as possible, it is imperative to impose persistent excitation on the process (Ljung 2006).

The classical input excitation method for any open loop system is step or impulse type perturbation in the input followed by measurement of the response of one or more process output variables. Step type excitation is frequently done in TSEs used for food processing (Moreira *et al.* 1990, Cayot *et al.* 1995, Akdogan and Rumsey 1996). Such excitation was also used in a plasticating single screw extruder by Chan *et al.* (1986). However, step response tests are often unable to excite the high frequency components; hence, dynamic models developed from these experiments do not predict well the process behavior at the higher frequencies. Because of the complex nature of plasticating extrusion processes, it is important to excite the process over a wide range of frequencies. In some studies, a Gaussian sequence type of excitation in the input was used for plasticating single screw extruders (McAfee and Thompson 2007, McAfee 2007). In another study, pulse type perturbation was used in a plasticating TSE to develop a grey box model (Garge *et al.* 2007).

Another widely used input excitation method for an open loop system is the random binary sequence (RBS). The RBS excitation method is capable of exciting a process over a wide spectrum of frequencies. Use of RBS excitation in plasticating TSE is limited. However, RBS excites the process both above and below the central set-point, which reduces some of the nonlinearity associated with the process.

5.2.2 Model Development

Classical linear system identification techniques are used to develop process model using process input-output data. The generic form of such a model in discrete time domain can be written according to equation 5.1:

$$A(q^{-1})y(k) = \frac{B(q^{-1})}{F(q^{-1})}u(k) + \frac{C(q^{-1})}{D(q^{-1})}\varepsilon(k) \tag{5.1}$$

where *y(k)*, *u(k)*, and $\varepsilon(k)$ are the discrete value of output, input and disturbance, respectively, at the k^{th} sampling instant and q^{-1} is the backshift operator. In equation 5.1, A, F, C and D are monic polynomials, i.e., the leading coefficient of these polynomials is 1. The time delay in units of sampling interval is presented in polynomial B as a number of leading zero-valued coefficients.

In equation 5.1, polynomials A, D, and F describe the present value of output in terms of past values of output. The discrete time model with these polynomials has an autoregressive nature. A model with polynomial B is considered to have external or exogenous components. Models with polynomial C are considered to have moving average behavior. Thus, model structure for a specific process is selected by combining some autoregressive, moving average and exogenous components based on model fit, statistical analysis of the model prediction errors, the parsimony principle, and the final model prediction errors. Details of model selection criteria are described in chapter 4. The model fit is calculated using the following relation:

$$Modelfit = 100 \times [1 - \frac{\sqrt{(}y_{measured} - y_{predicted})^2}{\sqrt{(}y_{measured} - y_{average})^2}] \tag{5.2}$$

5.3 Experimental Section

5.3.1 Extrusion System

The ZSK-25 twin screw extruder, used in this study, is described in previous chapters. Correlation analyses between six process output variables and final product quality variables, melt index and steady shear viscosity at steady state condition were performed and is detailed in chapter 4. Better correlations with product quality variables were obtained for the melt pressure at the die (P_m) and the melt temperature at the die (T_m) compared to other output variables. In addition, the transient behavior of the output variables was studied, and P_m and T_m were found to be suitable control variables.

The high density polyethylene (HDPE) used in this study was generously donated by Nova Chemicals (Calgary, Alberta, Canada). The commercial name of this polymer is SCLAIR 2907. According to the manufacturer, the melt index of HDPE is 4.9 g/10 min. The melting point of this polyethylene is 135^{o}C. A loss-in-weight feeder was used to feed the polyethylene to the TSE. The feed rate was controlled by a KSL/KLCD feed controller. This feed controller is cable of communicating with a PC to store data and send command for new set-points.

5.3.2 Feed Rate Excitation

Feed rate was excited between 4 kg/h and 8 kg/h. Nominal operating conditions for the barrel temperature and screw speed were 210^{o}C and 140 rpm, respectively. To get an estimate of the process time constant, step tests in F were performed in both positive and negative directions from the central set-point. A step of 2 kg/h was imposed in F from 6 kg/h in the positive direction. The process was run at a particular condition for sufficient time to equilibrate the response of the process

variables. After completing the step test in the positive direction, the process was brought back to the original operating conditions. The same magnitude of step was imposed in the negative direction to bring feed rate down to 4 kg/h. The response of P_m was much faster than that of T_m. Thus, a time constant (τ_p) of 16 sec estimated from the response of P_m was used to design the RBS.

A sampling time (t_s) of 1 sec was selected based on $\frac{\tau_p}{20} \leq t_s \leq \frac{\tau_p}{10}$. A value of zero was used for lower bound of input frequency (ω_L) to get a good estimate of the process gain. However, the normalized upper bound of input frequency (ω_U) was calculated based on the relation given in equation 4.9. From the range of input frequencies, a value of 0.06 was selected as an upper bound of input frequency for the experimental design. A total of 150 RBS samples of F were generated between 4 kg/h and 8 kg/h within the bound of input frequencies. Process data were acquired every 0.1 sec (10 Hz).

Figure 5.1(c) shows RBS excitation of the feed rate. Figures 5.1(a) and 5.1(b) show the responses of P_m and T_m, respectively, due to the RBS excitation in F. It was observed that both process output variables increased with an increase in F and decreased with a decrease in F. However, P_m has significant noise. It was necessary to filter the noise prior to further analysis. The change in P_m with a change in F was quite large and showed faster response compared to that of T_m. Thus, if the objective was to control P_m, there would be better resolution and faster set-point tracking. Figure 5.1(b) shows a long-term drift in T_m. Since the drift is very small, it was neglected.

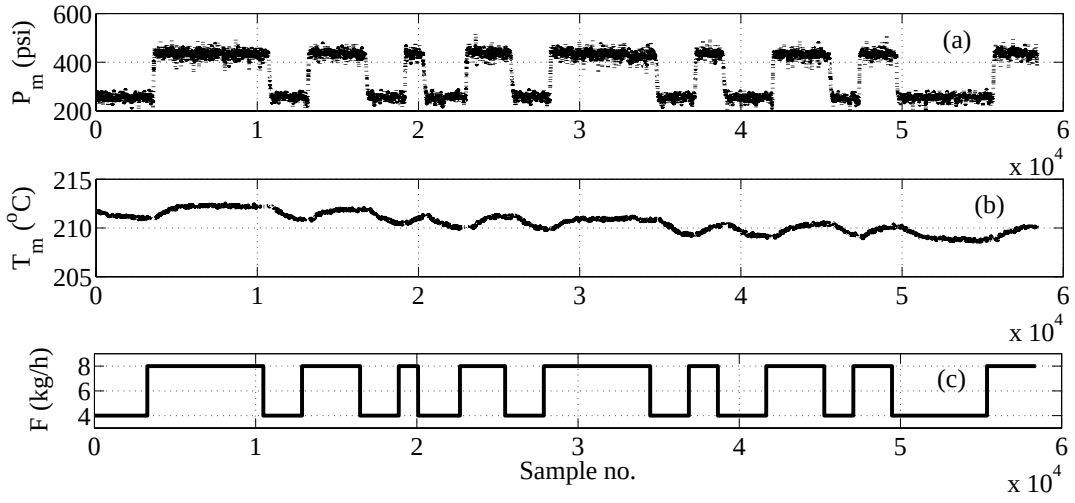

Figure 5.1: (a) Response of the melt pressure at the die. (b) Response of the melt temperature at the die. (c) A random binary sequence type excitation in the feed rate.

To observe the process behavior, the TSE was also excited by stair type step

changes in the feed rate. Figure 5.2(c) shows the stair type excitation in feed rate. Starting from the central set-point of 6 kg/h, a step change in F of 1 kg/h was made and held for sufficient time to let the process come to a new steady state. A complete stair type excitation was imposed by changing F in both positive and negative direction. This excitation was limited within 4 kg/h to 8 kg/h to provide operating conditions similar to the RBS excitation. This comparison allowed us to observe the effects of the type of input excitation on output process variables. Like the RBS excitation procedure, process data were collected every 0.1 sec. Figure 5.2(b) shows the response of the melt temperature at the die. It was observed that T_m did not follow the changes in F, which clearly indicates existence of nonlinearity. However, P_m was found to follow the change quite nicely; however, with a high level of noise (Figure 5.2(a)).

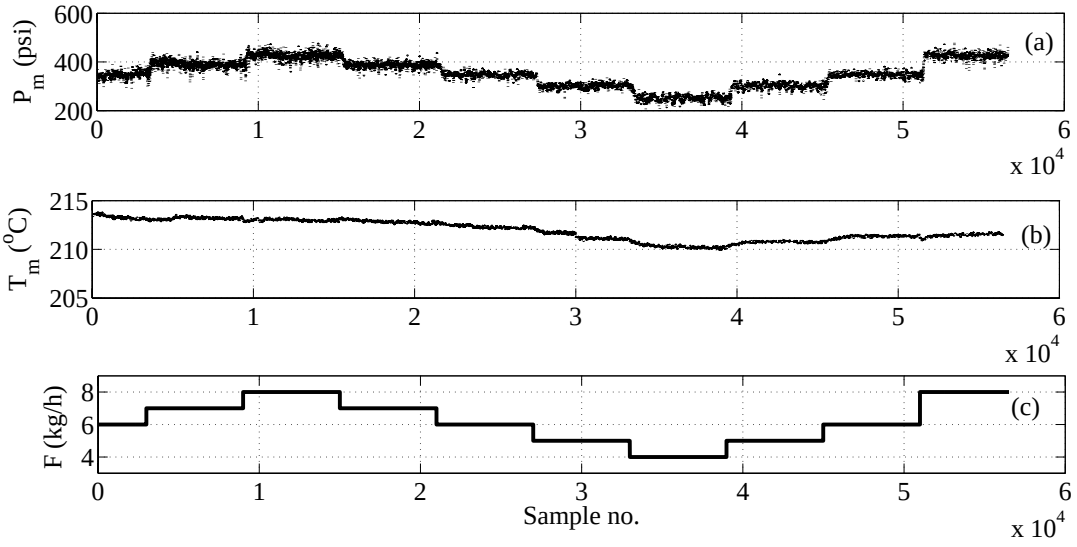

Figure 5.2: (a) Response of melt pressure at die. (b) Response of melt temperature at die. (c) Stair type type excitation in feed rate.

By comparing the responses of T_m to both types of excitation, it can be observed that the RBS type excitation reduced the effect of inherent process nonlinearity compared to that of the stair type excitation. This outcome indicates that the response of a nonlinear extrusion process can be modeled satisfactorily by a linear model using the data obtained from RBS excitation in the input variable. It is common practice to develop a process model that is as simple as possible to design and implement a control scheme in real-time. For example, a first order process can be satisfactorily controlled by using a proportional-integral controller in a closed loop. Thus, the type of excitation is important in identifying the response of a process variable, and RBS was observed to be a very good excitation method for nonlinear processes. Note that although RBS excitation reduced the effect of nonlinearity,

the degree of persistent excitation should not be so high that it enters the nonlinear region from the central set-point. Thus, it is important to design the RBS excitation properly before imposing it on the process.

Since RBS excitation reduced the effect of process nonlinearity within the given operating conditions, a part of these data were used to estimate process models relating P_m and T_m with F. However, the estimated models were validated using the dataset obtained from both types of excitation.

5.4 Results and Discussions

5.4.1 Data Preprocessing

Data preprocessing is one of the most important steps in developing a model with measured data. Measured data might be corrupted with different types of process noise or disturbances resulting from different sources. For example, screw speed introduces high frequency noise and the periodic change in cycling heater power gives low frequency noise in the measured data. Filtering or signal conditioning reduces the effect of noise on the data. There are a number of filtering techniques available in the literature. In this study, an exponentially weighted moving average (EWMA) filter was used to reduce the level of noise and prepare the measured data to develop the process model. As mentioned in chapter 4, such a filter can be represented by equation 5.3.

$$y_f(k) = \alpha y_r(k) + (1 - \alpha) y_f(k - 1) \tag{5.3}$$

where y_r is the raw data (measured), y_f is the filtered data, and α is any value between 0 and 1. As detailed in chapter 4, a value of 0.012 was used as a preliminary estimation of α. Different values of α were used to filter the data and the level of noise in the data was visualized. Finally, a value of 0.01 was selected. Note that data obtained either from RBS or stair type excitation were filtered using EWMA with the stated value of α. The linear trend from both time series data was removed, i.e., data were detrended, to make it stationary. Figures 5.3(a) and (b) show the time trends of filtered and detrended P_m and T_m data obtained from RBS excitation. The advantage of such detrending is that the developed model does not depend on the initial conditions.

Modeling of the low and mid-frequency dynamics of a process is hindered by the use of high frequency data. Thus, it is common practice to downsample data to reduce an overabundance of high frequency data. The time trend of the variables shows that the response of P_m was faster than the response of T_m. Thus, P_m data were downsampled to every 1 sec to reduce the overabundance of data. The complete

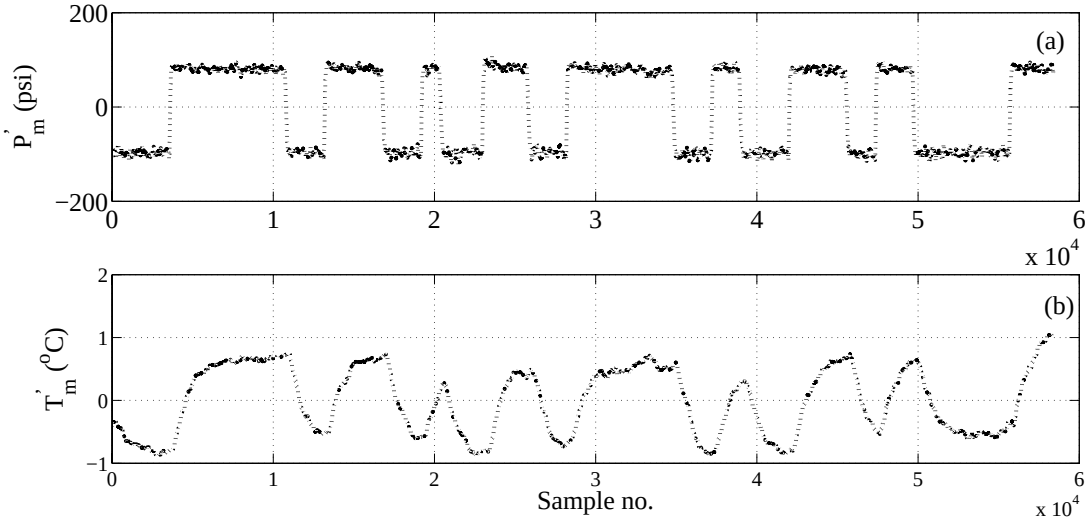

Figure 5.3: (a) Time trend of filtered and detrended melt pressure at the die (filtered with $\alpha = 0.01$). (b) Time trend of filtered and detrended melt temperature at the die (filtered with $\alpha = 0.01$).

response to thermal changes due to a change in F is relatively slower. Thus, T_m data were downsampled to every 2 sec.

5.4.2 Impulse Response

The impulse response between an output variable and an input variable of a process estimates the time delay and the model order. To estimate the time delay and model order, the impulse response was estimated between preprocessed P_m and F, and preprocessed T_m and F, and the results are represented in Figure 5.4. Figure 5.4 (a) shows the estimation between P_m and F. It was observed that the first nonzero appears outside the 99% confidence interval at the 25th lag. As the sampling time is 1 sec, the estimated time delay between P_m and F is 25 sec. The shape of the impulse response coefficients suggests that the model order relating P_m and F is second order. The impulse response estimate between T_m and F is presented in Figure 5.4 (b). The first peak outside the 99% confidence interval appears at the 29th lag, which indicates a possible time delay between F and T_m of 58 sec (since the data were downsampled to 2 sec). Again, the orientation of the coefficients indicates that the model order between T_m and F should be at least second order.

5.4.3 Melt Pressure Model

The first half of the dataset was used to develop the model between P_m and F. However, the complete dataset was used in validating the model to avoid initializa-

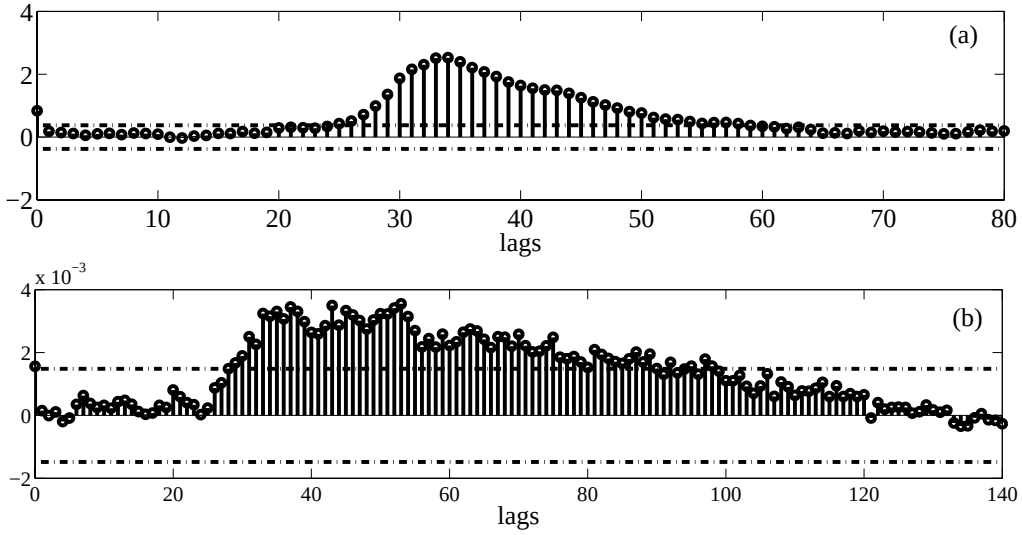

Figure 5.4: (a) Impulse response of P_m. (b) Impulse response of T_m.

tion errors. The model was also validated with the experimental data obtained from stair type excitation. Different model orders and structures were tried, and the final model was selected based on the model selection criteria detailed in section 5.2.2. Equation 5.4 shows the obtained melt pressure model.

$$\begin{aligned} P'_m(t) &= \frac{0.0879(\pm 0.058)q^{-25} + 0.488(\pm 0.065)q^{-26}}{1 - 1.796(\pm 0.009)q^{-1} + 0.809(\pm 0.008)q^{-2}} F'(t) \\ &\quad + \frac{1 - 0.15(\pm 0.009)q^{-1}}{1 - 1.796(\pm 0.009)q^{-1} + 0.809(\pm 0.008)q^{-2}} \varepsilon(t) \end{aligned} \tag{5.4}$$

where P'_m and F are in deviation forms, i.e., detrended, and ε is disturbance. Values in the parentheses of equation 5.4 show the standard error of the corresponding parameters. Equation 5.4 shows that the obtained model has an autoregressive moving average with exogenous input (ARMAX) structure. By comparing with equation 5.1, the orders of polynomials A, B, C, D and F are 0, 2, 1, 2, and 2, respectively. Therefore, the dynamics of P_m due to change in F are second order. Polynomials D and F are identical. Polynomial B contains time delay of 25 samples. The model order gives us an intuitive explanation of the extrusion process. The identical denominator for both process and noise models indicates that the feed rate and disturbances are processed in the same way, which is reasonable. The obtained discrete domain plant model was converted to Laplace domain using a zero-order hold and is shown in equation 5.5. A dynamic model can be explained better in Laplace domain compared to discrete domain.

$$\frac{P'_m(s)}{F'(s)} = \frac{-0.2341s + 0.6405}{s^2 + 0.2116s + 0.01437} e^{-24s} \tag{5.5}$$

It can be observed that the plant model in equation 5.5 contains a right half

plane zero, indicating an inverse response. The value of the parameter is small, which shows that such a response is instantaneous; however, a root cause diagnosis of such a response is imperative. In this study, excitation only in the feed rate was performed while screw speed and barrel temperature were assumed constant. It was observed that screw speed varied within ±2 rpm from the central set-point (140 rpm) in the course of the experiment. For example, when an RBS change in F was made from 4 kg/h to 8 kg/h, screw speed changed from 138 rpm to 142 rpm instantly. Any change in feed rate takes time to affect the melt pressure at the die because of the transportation delay of the material from the feed end to the die end. On the other hand, an increase in screw speed increases shear rate immediately and decreases viscosity; and hence, melt pressure decreases. Whenever more material reaches the die due to an increase in F, melt pressure increases. Thus, an inverse type of response was observed that was intuitively captured by the obtained model. This is an example of useful process dynamics information being captured by the model and being explained using process knowledge.

Figure 5.5 shows a comparison between the experimental data and the model simulated output for an infinite horizon. Almost 93% model fit was obtained with measured data, which indicates that the obtained model captured the dynamics quite satisfactorily. A small mismatch in gain was observed between the simulated value and the experimental value due to the existence of lower level noise in the dataset. However, this model is quite good and is simple enough to use for designing a control scheme.

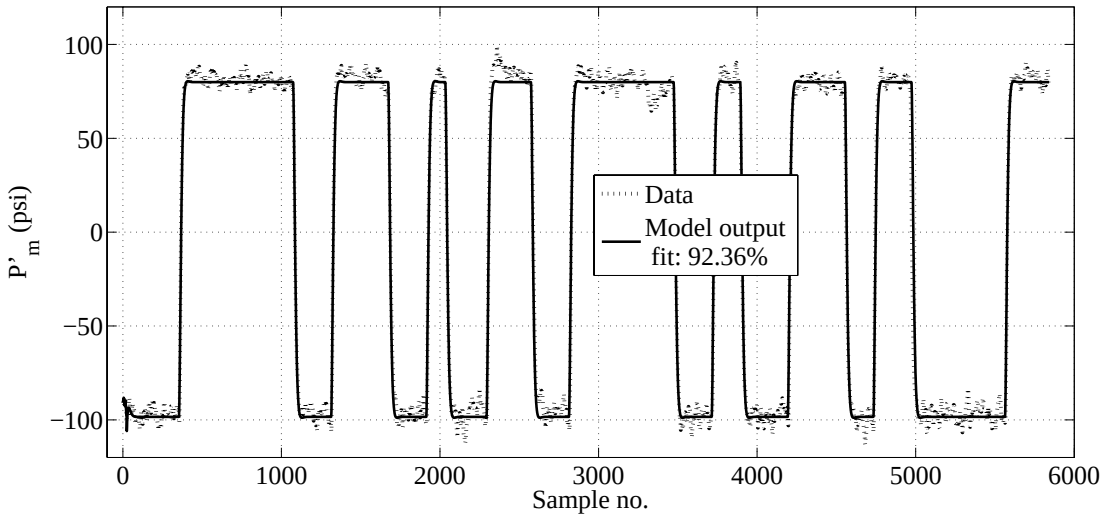

Figure 5.5: Validation of melt pressure model output with RBS excitation data set.

To check the amount of information captured by the model from the measured data, model prediction errors (i.e., residuals) were analyzed. An autocorrelation

function (ACF) among the residuals and a cross-correlation function (CCF), between the input and the residuals, are widely used for such analysis. As mentioned earlier, if the model captures almost all the information from the data, the prediction errors will be white noise type. An ACF of white noise has unit value at lag zero and zero at other lags. A CCF of white noise is zero at all lags. Figure 5.6 shows the ACF and CCF of the P_m model prediction error. The top plot shows that the ACF has a unit value (1) at zero lag and is almost within the 99% confidence interval of other lags. The bottom plot indicates that the CCF at all lags is within the 99% confidence interval. Thus, the prediction errors are essentially white noise.

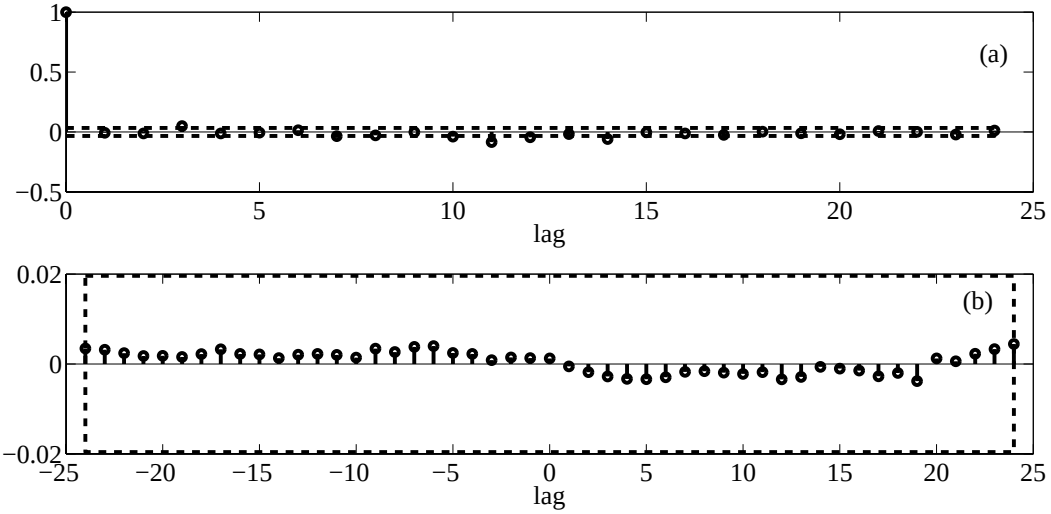

Figure 5.6: Analysis of residuals for the melt pressure model: (a) Correlation function of residuals from output P'_m, (b) Cross correlation function between input F' and residuals from output P'_m.

Figure 5.7 shows the comparison between P_m model simulated outputs with the outputs obtained from stair type excitations in F. Almost 90% model fit was obtained. Such a model fit indicates that the developed model can predict the output satisfactorily. Note that the model was developed using the data obtained from an RBS excitation in F. However, the model gives excellent fit with data obtained from another type of excitation. This is exciting in that it gives us confidence to use the data not only for a range of operating conditions but also for a range of operating protocols.

It was observed that the response of melt pressure due to changes in feed rate was quite fast. However, the impulse response shows the existence of considerable time delay. This time delay was quite large compared to the time constant. In such a case, the dynamic of the process can be ignored and a nonparametric model can be obtained. Thus, the melt pressure model was considered as a delay-gain model

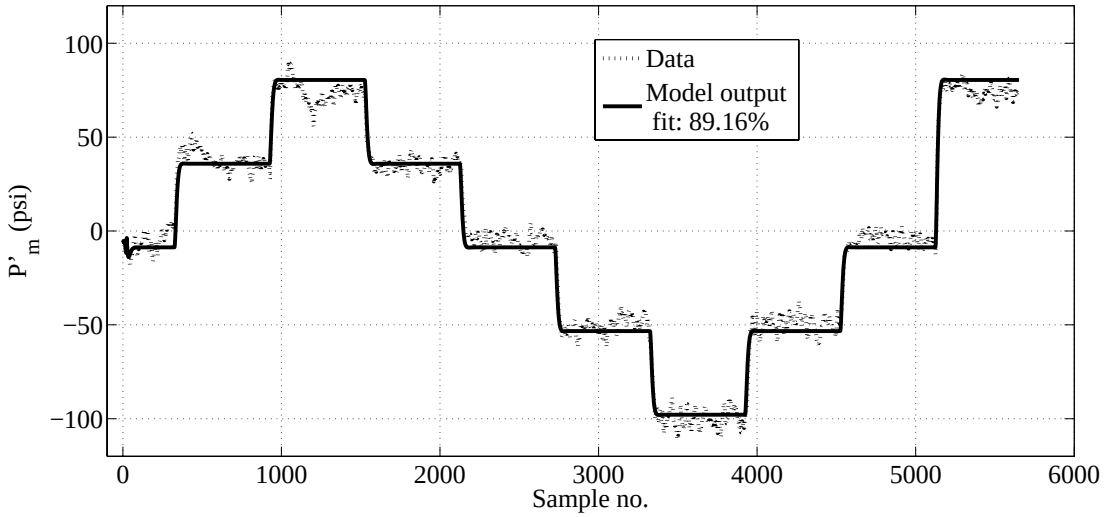

Figure 5.7: Validation of the melt pressure model output with stair type excitation data.

only. Steady state gain (K) is defined as:

$$\begin{aligned} K &= \frac{\Delta(output)}{\Delta(input)} \\ or, K &= \frac{\Delta P_m}{\Delta F} \\ or, \Delta P_m &= K \times \Delta F. \end{aligned} \tag{5.6}$$

The value of the steady state gain is 45, which was obtained from RBS excitation. Figure 5.8 shows the comparison between the delay-gain melt pressure model and the measured data. About 65% model fit was obtained. Such a model fit was achieved while ignoring the process dynamics. However, the delay-gain model simulated output gives a fairly satisfactory prediction. Such a simple model is also very useful for process control.

5.4.4 Melt Temperature Model

Similar to the melt pressure model development, the first half of the melt temperature dataset was used to develop a dynamic model relating T_m and F. The obtained model is presented in equation 5.7:

$$\begin{aligned} T'_m(t) &= \frac{1.37 \times 10^{-3}(\pm 6.6 \times 10^{-4})q^{-29} + 1.63 \times 10^{-3}(\pm 7.1 \times 10^{-4})q^{-30}}{1 - 1.581(\pm 0.037)q^{-1} + 0.588(\pm 0.036)q^{-2}} F'(t) \\ &\quad + \frac{1 - 0.05(\pm 0.04)q^{-1}}{1 - 1.581(\pm 0.037)q^{-1} + 0.588(\pm 0.036)q^{-2}} \varepsilon(t) \end{aligned} \tag{5.7}$$

where T'_m is in deviation form. Values in the parentheses show the standard deviation of the corresponding parameter. Equation 5.7 shows that the obtained model

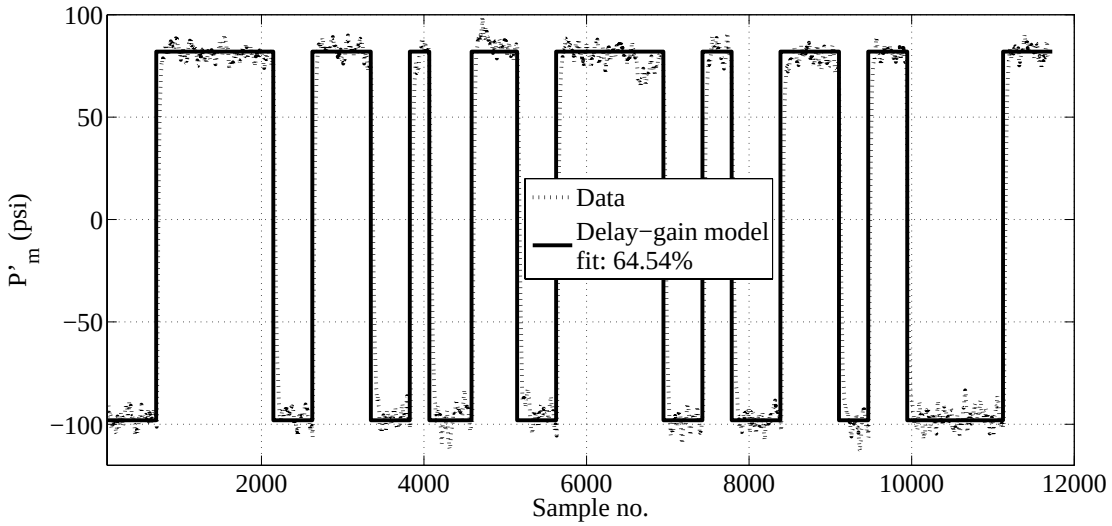

Figure 5.8: Validation of the delay-gain melt pressure model output with data obtained from RBS excitation.

has ARMAX structure with orders of polynomial A, B, C, D, and F of 0, 2, 1, 2, and 2, respectively. Polynomials D and F are similar in the T_m model. Therefore, the dynamics of T_m due to changes in F are second order. Leading zero-valued coefficients in polynomial B indicate the time delay is 29 samples. Like the melt pressure model, the melt temperature model provides us insight and intuition into the twin-screw extrusion process. Identical polynomials for both process and disturbance models indicate that the feed rate and disturbance affect T_m in a similar way.

Figure 5.9 shows the model validation with the whole dataset obtained using RBS excitation. The model was simulated for an infinite prediction horizon. More than 70% model fit was obtained, which is quite good from a control point of view. A very small gain mismatch was observed, which was attributed to the nonlinear nature of melt temperature and the existence of low level noise in the data. However, the simulated output of the model agreed the experimental value well. Figure 5.10 shows the residual analysis of the melt temperature model. Both the ACF and CCF show that the model prediction errors are white noise. So, the developed melt temperature model captures the process dynamics from the data quite successfully.

The melt temperature model was also validated with data obtained from stair type excitation. Figure 5.11 shows a comparison between melt temperature model simulated outputs and stair type excitation data. A noticeable discrepancy is observed between the model outputs and experimental data. Experimental data clearly shows the existence of nonlinearity in the melt temperature. Thus, a linear melt temperature model is not able to give a good fit for data with considerable nonlin-

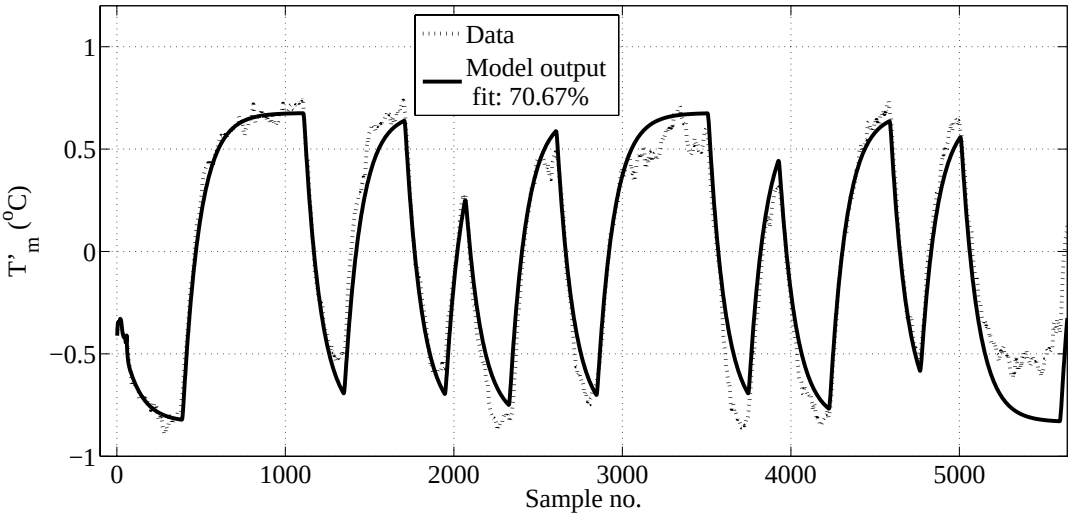

Figure 5.9: Validation of the melt temperature model output with RBS excitation data.

earity. However, the model is good enough to track the trend of the measured data.

5.5 Analysis of Models

The purpose of modeling is to use the obtained models for designing model-based control schemes. Thus, step tests, analyses of poles and zeros, Bode plots, Nyquist diagrams, etc., were performed.

5.5.1 Melt Pressure Model

The parametric P_m model, i.e., equation 5.5, has been used for further analysis. Figure 5.12 shows the responses of experimental data and P_m model predicted output due to unit step changes in feed rate. The P_m model predicted outputs are almost the same as the values of experimental data. It is noticed that the responses are bounded, i.e., the responses attain a new steady state. Thus, P_m is controllable with changes in F.

Figure 5.13 shows the pole-zero map of the P_m model. All the poles are inside the unit circle, which indicates all the poles are in the negative region of the s-domain. A system with negative poles in the s-domain is a bounded system. Thus, the response of P_m is a bounded response with changes in F. The location of the poles in the unit circle indicates the sampling rate is reasonable since the poles are concentrated neither at the origin nor at the circumference. Figure 5.13 also shows no pole-zero cancelation or redundancy of model parameters. One unstable zero can

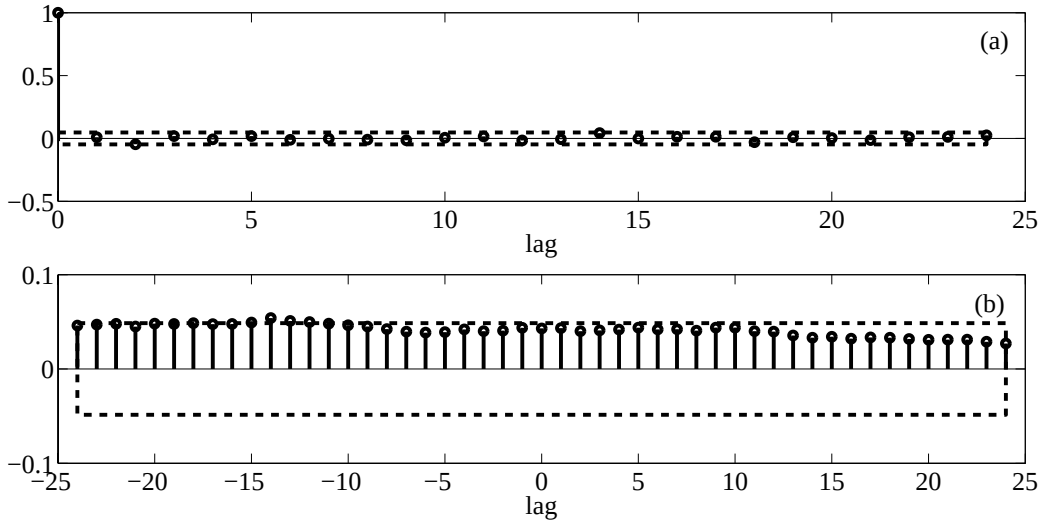

Figure 5.10: Analyses of residuals for the melt temperature model: (a) Correlation function of residuals from output T'_m, (b) Cross correlation function between input F' and residuals from output T'_m.

be observed outside the unit circle in Figure 5.13.

Time domain P_m data were converted to frequency domain data by using MATLAB supplied spectral analysis functions and the command *'spa'*. A Bode plot was generated for this frequency domain data and is represented in Figure 5.14 by a dotted line. A Bode plot for the P_m model is represented in Figure 5.14 by a solid line. Figure 5.14 (a) shows a good match in amplitude between the model and data in the low frequency region. Considerable mismatch is noticed at higher frequencies. This is due to insufficient excitation at higher frequencies. According to the experimental design, the process was excited with a upper limit frequency of 0.06. Usually, chemical processes are not operated in too high frequency regions. An excitation at these frequencies was not considered at the predesigned experimental step. Thus, the obtained P_m model is good enough to use for a model-based control scheme.

Figure 5.14 (b) shows good match in phase shift between the model and data in low frequency and high frequency regions. A mismatch is observed in the intermediate frequency region. However, the model fits well with experimental data up to the frequency range of interest for the designing of control schemes.

Two different RBSs for feed rate were generated with two different input frequency spectra: [0 0.1] and [0 0.006]. The first spectrum has much higher frequency than the frequency (0.06) used for the experimental design. On the other hand, the second spectrum has much lower frequency. The P_m model was simulated using these inputs. Simulated outputs were used to developed two ARMAX models for the melt pressure with the same structure as the P_m model. Nyquist plots of the two newly developed ARMAX models and the P_m model are shown in Figure 5.15.

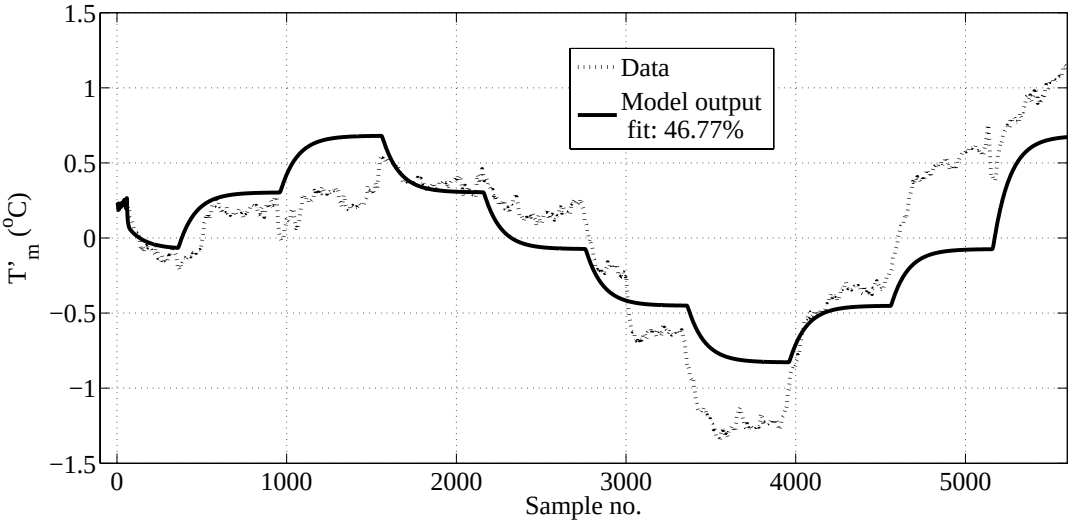

Figure 5.11: Melt temperature model validation with stair type excitation data.

It can be observed that the two models developed from the simulated data with different input spectra and the P_m model overlap in the Nyquist plot. It can be concluded that the P_m model is a robust model and represents the process well even at other input frequencies.

5.5.2 Melt Temperature Model

Step responses of experimental data and T_m model predicted output are presented in Figure 5.16. Both the responses attain a new steady state after unit step changes in F. Thus, T_m is controllable with the changes in F. However, a little mismatch can be observed due to nonlinearity of T_m data. Such mismatch was also observed in Figure 5.9.

Locations of poles and zeros for the T_m model are shown in Figure 5.17. Since all the poles are inside the unit circle, the response of T_m due to changes in F is bounded. Such a bounded response was also noticed in the step test analysis. Figure 5.13 shows that one of the poles is close to the circumference of the unit circle. However, the location of another pole indicates that the sampling rate was quite good. One unstable zero is located outside the unit circle.

Bode plots of the experimental data and T_m are presented in Figure 5.18. The dotted line represents a Bode plot for the experimental data and the solid line represents a Bode plot for the T_m model. Figure 5.18 (a) shows a mismatch in amplitude between model and data. This could be due to the existence of nonlinearity in T_m. A mismatch in amplitude at lower frequencies indicates that the process was not allowed for sufficient time for the T_m to respon completely. Insufficient excitation results in mismatch even at low frequencies.

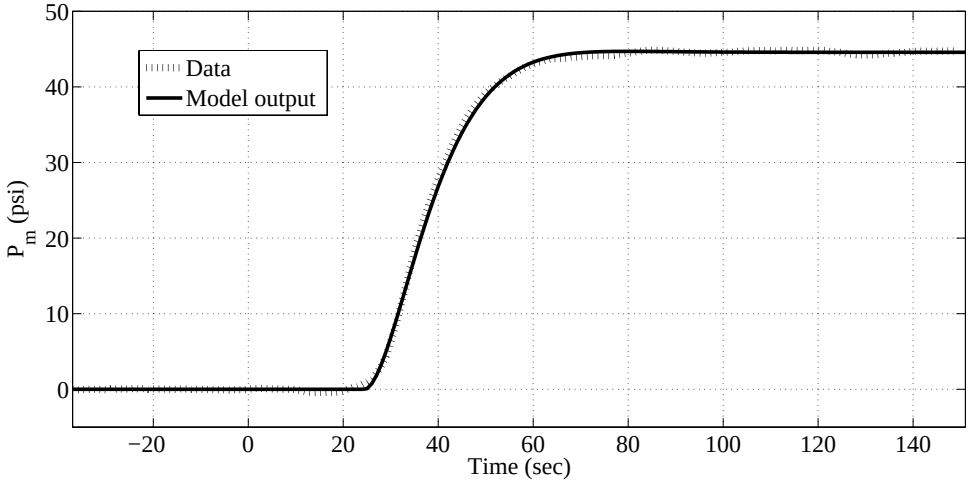

Figure 5.12: Comparison of step responses between experimental data and P_m model predicted outputs.

Figure 5.18 (b) shows that the model followed the phase shift trend with the experimental data at medium to higher frequencies with considerable mismatch. Again, this could be due to the nonlinearity in T_m. However, a good match can be observed at lower frequencies. Thus, the model can be satisfactorily used to design a model-based control scheme.

Like the P_m model, the T_m model was simulated using feed rates at different spectra: [0 0.1] and [0 0.006]. Models with order and structure similar to the T_m model were developed using the simulated outputs. Figure 5.19 shows Nyquist plots of the two models developed from the simulated outputs and the T_m model. Overlapping of all the models in the Nyquist plot indicates that the T_m model is robust.

5.6 Summary

Transient responses of process variables due to changes in feed rate were studied and modeled in this work. Random binary sequence and stair type excitations were used to excite F. Data obtained from RBS excitation were used to develop a model for dynamic behavior.

Random binary sequences gave persistent excitation in the feed rate. Such excitation covered a wide frequency spectrum. Moreover, the operating range of the feed rate was large enough to observe transient effects in process output variables. RBS excitation, compared to that of the stair type excitation, was found to reduce more effectively the effect of process nonlinearity on the responses of process variables. The reduction of process nonlinearity was clearly observed in the data for

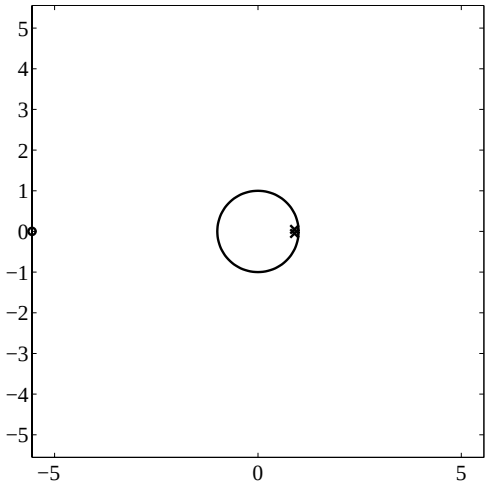

Figure 5.13: A pole-zero map for the P_m model.

melt temperature at the die. Models developed from RBS excitation were also able to predict the output obtained from stair type excitation.

The melt pressure model gave about 93% fit and 90% fit for RBS excitation data and stair type excitation data, respectively. Thus, the developed P_m model captures the process dynamics well. The melt temperature model gave about 71% fit with RBS excitation data. However, only moderate model fit (about 47%) was obtained for stair type excitation data, due mainly to nonlinear effects in the measured data

Developed models for melt pressure and melt temperature have autoregressive moving average with exogenous input structures. Such models intuitively explain the physics of the extrusion process. For example, both plant and disturbance models have similar denominators, which indicates that feed rate and disturbance affect melt pressure and melt temperature in the same way.

Responses in melt pressure due to changes in feed rate are quite fast. Thus, a delay-gain model was proposed and was found to capture the response of melt pressure fairly satisfactorily for control purposes.

A Bode plot showed insufficient excitation in T_m, which resulted in gain mismatch between experimental data and model predicted outputs. A Nyquist plot showed that both P_m and T_m models are sufficiently robust and represent the process at different input frequencies. Such robustness is very useful for process control because a process is high dimensional and a developed model is low dimensional. In addition, there might have uncertainty in the model parameters. Thus, a robust model is imperative for model-based process control.

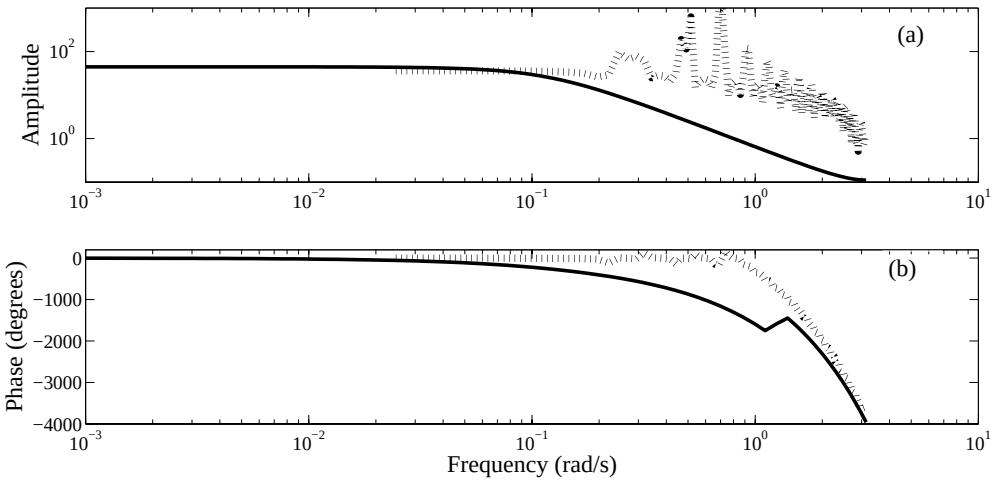

Figure 5.14: Bode diagrams of the P_m model and experimental data: (a) Amplitude vs. frequency, (b) Phase shift vs. frequency.

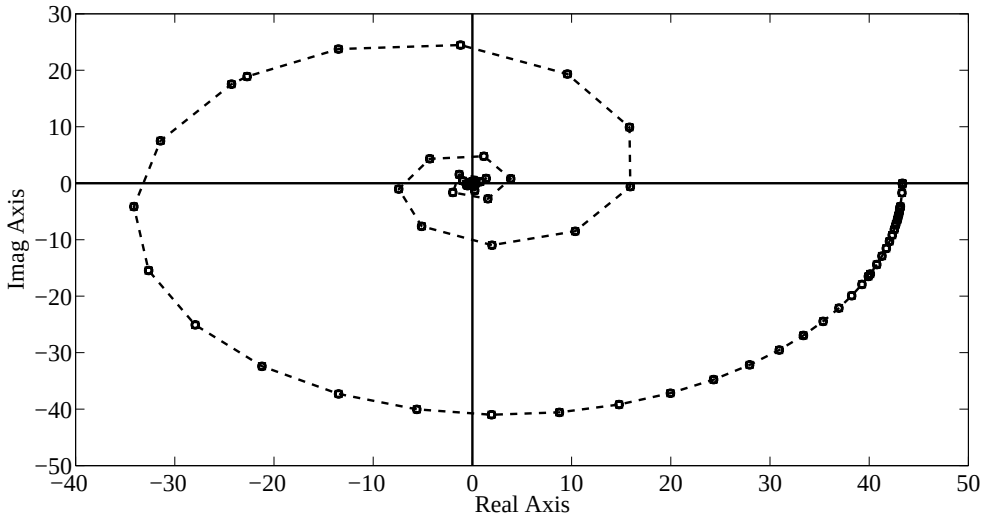

Figure 5.15: Nyquist plots of P_m model (broken line), P_m model with [0 0.1] input frequency spectrum (square) and P_m model with [0 0.006] input frequency spectrum (circle)

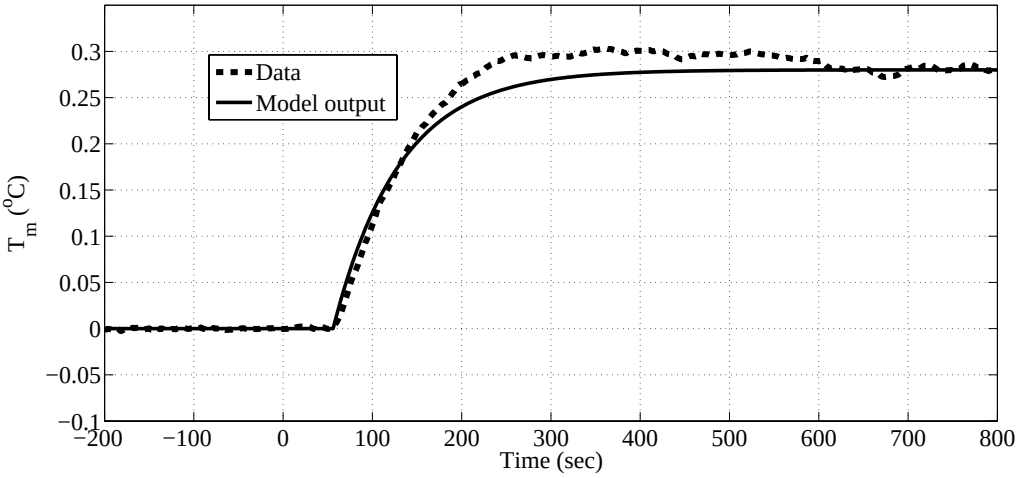

Figure 5.16: Comparison of step responses between experimental data and T_m model predicted outputs.

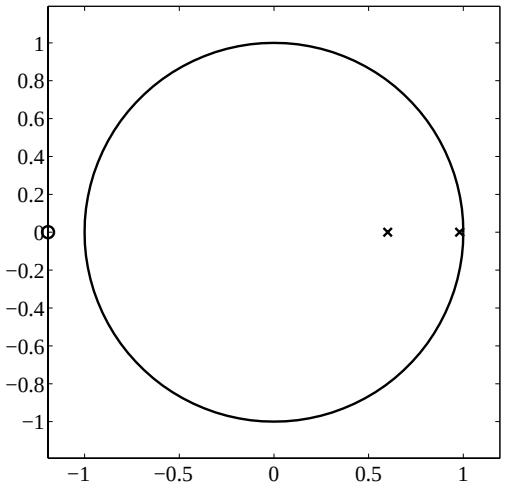

Figure 5.17: A pole-zero map for the T_m model.

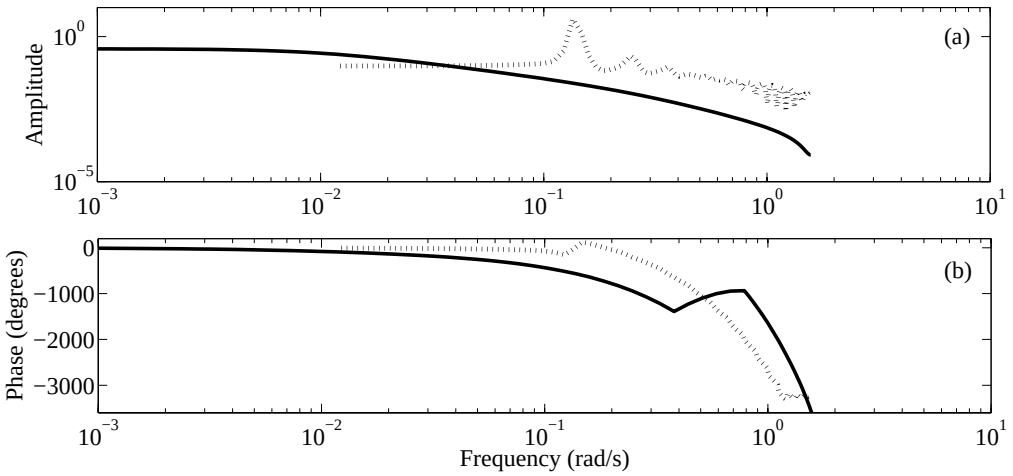

Figure 5.18: Bode diagrams of the T_m model and experimental data: (a) Amplitude vs. frequency, (b) Phase shift vs. frequency.

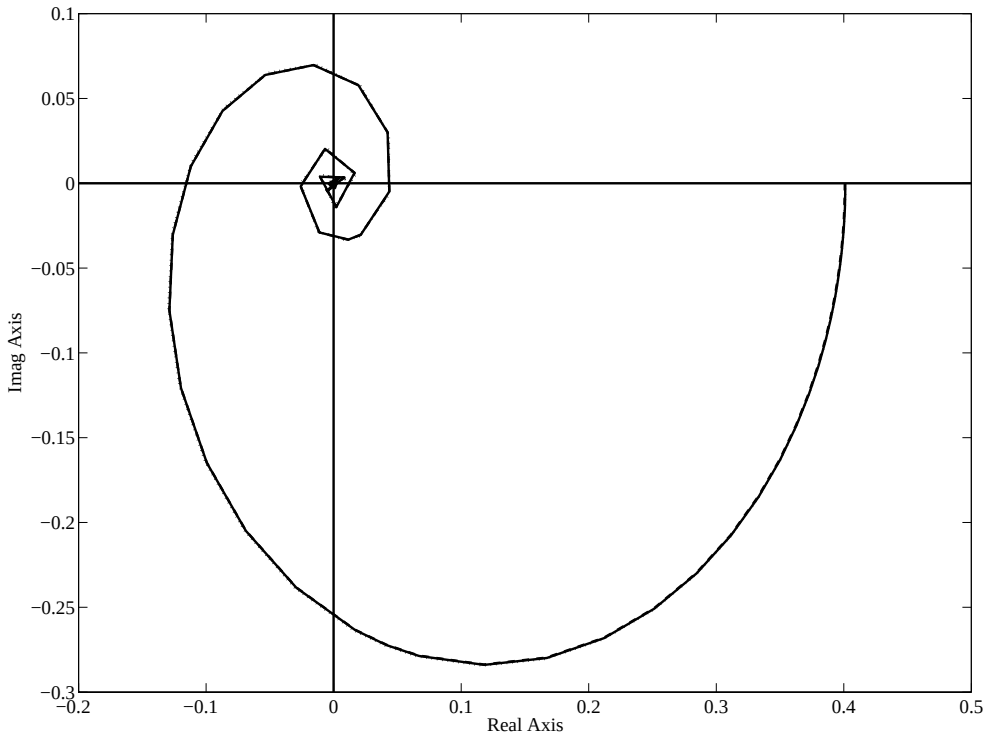

Figure 5.19: Nyquist plots of the T_m model (solid line), the T_m model with [0 0.1] input frequency spectrum (broken line) and the T_m model with [0 0.006] input frequency spectrum (dotted line)

Chapter 6

Model Predictive Controller

6.1 Introduction

It is very important to have a stable extrusion process to establish consistent product quality. Off-specification products can be produced due to any fluctuation in the operating variables. Thus, it is imperative to have an automatic control system. However, control of a twin screw extrusion process is mainly manual (Wang *et al.* 2008). Manual control of a TSE is tedious, slow, and unreliable. Thus, recent interest in controlling TSEs has prompted the investigation of various design methods for automatic extruder control. Success in the development of automatic control systems for extrusion processes is limited because of complex dynamic behavior, multivariable interaction, nonlinear dynamics, time-delay, sensor noise, varying feedstock composition, and other factors. In addition, multiple hardware configurations increases the complexity of automatic control.

Some work has been reported on control of plasticating extrusion processes (Costin *et al.* 1982a, Costin *et al.* 1982b, Kochhar and Parnaby 1977, Previdi *et al.* 2006). Costin *et al.* (1982b) designed a proportional-integral (PI) controller and self-tuning controller for a single screw extruder in which controllers were designed to control melt pressure by manipulating screw speed. Extrusion is a multivariate process; hence, control of a single process variable is not adequate for effective control of the whole process. In another study, Previdi *et al.* (2006) designed and implemented a prototype feedback controller for a plasticating single screw extruder to control volumetric flow through the die, which was achieved by regulating the melt pressure and the melt temperature at the die by manipulating screw speed and barrel temperature. Good set-point tracking and disturbance rejection by the controller were reported. However, no quality variable was considered in the design of the control scheme. Limited work has also been reported on the control of product quality variables, especially viscosity, for plasticating extruders (Broad-

Portions of this chapter have been submitted for review in *Control Engineering Practice*.

head *et al.* 1996, Chiu and Lin 1998, Chiu and Pong 2001). Most of these studies were performed on single screw extrusion processes and the control schemes were designed as single-input single-output systems. Research on control of twin screw food extrusion processes has been performed more extensive than that on twin screw plasticating extruders (Haley and Mulvaney 2000b, Tan and Hofer 1995, Hofer and Tan 1993, Kulshreshtha *et al.* 1991a, Singh and Mulvaney 1994). Thus, there is much scope for research on control of plasticating TSEs.

Design and implementation of a multiple-input multiple-output (MIMO) model predictive control (MPC) scheme for a plasticating twin screw extruder is detailed in this chapter. A MIMO MPC computed the trajectories of manipulated variables to optimize the future behavior of a plant (Richalet *et al.* 1978). The objective of this work was to develop a real-time MPC system for a plasticating TSE. This work was a part of a project to achieve advanced control of a plasticating twin screw extruder; it included setup for process data access, modeling of the extrusion process, system development for process automation, design and implementation of an advanced control scheme in real-time. The MPC was designed to control melt temperature (T_m) at the die and melt pressure (P_m) at the die by manipulating screw speed and feed rate. Essentially, the designed MPC controlled a 2X2 system.

6.2 Model Predictive Controller

Model predictive control (MPC) is an advanced control technique for difficult multi-variable control problems. An MPC scheme refers to a class of algorithms that compute a sequence of manipulated variable adjustments in order to optimize the future behavior of a process. MPC was originally developed to meet the specialized control needs of power plants and petroleum refineries (Qin and Badgwell 2003). With the improvement in modern computers, MPC technology has been successfully used in a wide variety of industries including chemical, petrochemicals, automotive, food processing, aerospace, metallurgy, and pulp and paper.

A reasonably accurate dynamic model of a process is a prerequisite for MPC. The model and current measurements can be used to predict future values of the outputs. Appropriate changes in input variables can be calculated based on both predictions and measurements. Essentially, changes in individual input variables are coordinated after considering the input-output relationships represented by the process model. Model predictive control has a number of important advantages over other methods:

- A process model captures dynamic and static interactions between manipulated, controlled, and disturbance variables.

- Constraints on manipulated and controlled variables are taken care of in a systematic manner.
- Control calculations are optimized.
- Model predictions can provide early warnings of potential problems.

6.2.1 Basic Concepts of MPC

The basic concepts of model predictive control are presented in Figure 6.1. MPC calculates a sequence of control moves so that the predicted response moves to the set-point in an optimal manner. The manipulated input (u), actual output (y), and predicted output ($\hat{y}$) are shown in Figure 6.1. At the current sampling instant k, the MPC scheme calculates a set of M values of the input $u(k+i-1), i = 1, 2, .., M$. The set consists of current input $u(k)$ and $(M-1)$ future inputs. After M control moves, the input is held constant. The inputs are calculated so that a set of P predicted outputs $\hat{y}(k+i), i = 1, 2, ..., P$ reaches the set-point in an optimal manner. The control moves are calculated based on optimizing an objective function. The number of predictions P is referred to as the prediction horizon and the number of control moves M is called the control horizon.

Although a sequence of M control moves is calculated at each sampling instant, only the first one or two moves is implemented. Then a new sequence of moves is calculated at the next sampling instant, after a new measurement is available. This procedure is called the receding horizon approach and the approach is repeated at each sampling instant.

6.2.2 Fundamentals of an MPC

The basic elements are same for any MPC algorithm. Different options can be chosen for each one of these elements resulting in different algorithms. These basic elements are:

- prediction model,
- objective function, and
- algorithms to obtain the control law.

Process and Disturbance Models

A prerequisite of MPC is a model. The process model typically represents the input-output relationship of a process. The disturbance model is often used to represent disturbance, or is used simply to approximate model-plant mismatch.

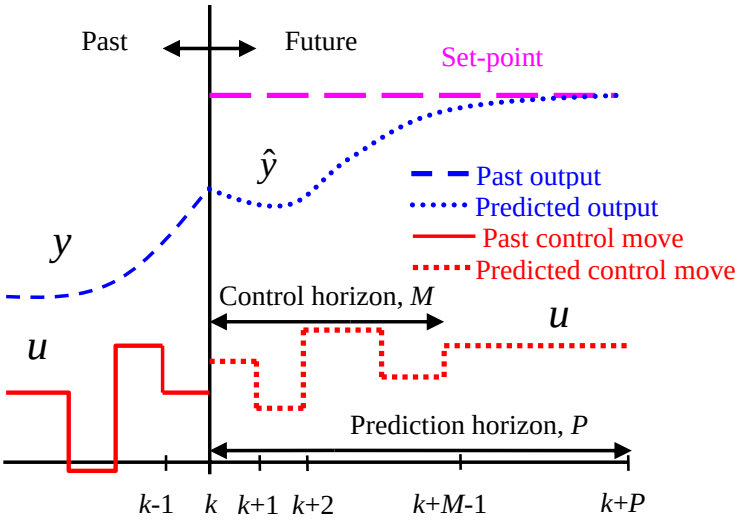

Figure 6.1: Basic concepts of MPC.

Predictions

Models are not used directly in an MPC scheme. Predictors are designed first, according to the models, and then control laws are designed according to the predictions. In the prediction step, future outputs are predicted based on past inputs and outputs. MPC determines future inputs in order to drive the process to a desired target. Thus, future inputs are critical components of the predictors. In MPC, the process does not follow the set-point at one specific point. It follows a trajectory of the set-point instead. Thus, prediction is not simply one step ahead, but multiple steps ahead of the process.

Objective Function

Different MPC algorithms propose different objective or cost functions for obtaining the control law. The issues considered to design the objective functions can be summarized as:

- The future output should follow a reference trajectory over the horizon of

interest.

- The necessary control action should be included in the objective function.

Typically, the objective function penalizes squared input changes and output deviations from the set-point and includes separate output and input weight matrices. Equation 6.1 shows the objective function, which needs to be minimized to calculate a sequence of moves for manipulated variables. The general expression for such an objective function for a single-input single-output (SISO) system is:

$$J = \sum_{j=N_1}^{N_2} (r_{t+j} - \hat{y}_{t+j})' Q_j (r_{t+j} - \hat{y}_{t+j}) + \sum_{j=1}^{M} [\triangle u_{t+j-1}]' R_j [\triangle u_{t+j-1}] \tag{6.1}$$

where r_t is the reference trajectory, y_t is the output, u_t is the input, M is the control horizon, Q_j is the weighting matrix reflecting the relative importance of y and R_j is the weighting matrix penalizing the relative big changes in u.

Prediction starts at N_1, and N_2 is the maximum prediction horizon. $N_2 - N_1 + 1$ determines a prediction window in which it is desirable for the predicted output to follow the set-point. A large value of N_1 implies that it is not important if there are errors in the first few instants up to N_1. However, a large value of $N_2 - N_1 + 1$ implies that the output errors extend over a long time horizon.

Reference Trajectory

The reference trajectory is a series of set-points. It is a sequence of future desired targets. The desired target may not be the same as the actual output due to performance limitations of control systems such as hard constraints on the actuator, time delay of the process, model-plant mismatch, etc. The ultimate goal of actual process output is to reflect the desired process. Most objective functions use a reference trajectory that does not necessarily follow the real reference, but is a smooth approximation of the current values of output y_t toward a known reference.

Constraints

Every process has constraints. Many process outputs are subject to constraints for economic or safety reasons. For example, higher screw speed may be desirable for better mixing of different polymers in a twin screw extruder, but high screw speed causes an increase in polymer melt temperature, which may degrade the quality of the polymer blend. Thus, in almost all practical model predictive controls, constraints in the amplitude, in the slew rate of the control signal, and in the output

are considered. Equation 6.2 shows such constraints.

$$\begin{aligned} u_{min} \leq u_t \leq u_{max} \qquad & \forall t \\ \Delta u_{min} \leq \Delta u_t \leq \Delta u_{max} \qquad & \forall t \\ y_{min} \leq \hat{y}_{t+j} \leq y_{max} \qquad & N_1 \leq j \leq N_2, \forall t \end{aligned} \tag{6.2}$$

where u_{min} is minimum value of the input, u_{max} is the maximum value of the input, Δu_{min} is the minimum rate of change of the input, Δu_{max} is the maximum rate of change of the input, y_{min} is the minimum value of the output, and y_{max} is the maximum value of the output.

Control Law

Control actions Δu_{t+j} are calculated by minimizing the objective function. By taking derivatives of J with respect to Δu_t, Δu_{t+1}, ..., Δu_{t+M-1}, and equating the derivatives to zero, an analytical solution can be obtained. This is a typical least square problem. However, analytical solutions are not possible if there are constraints on u_t, Δu_t, or $\hat{y}_{t+j}$. In that case, numerical optimization is necessary. All computation is completed within the sampling interval.

In a nutshell, the design of model predictive control involves specification of prediction models, objective functions, and optimization to obtain control laws.

6.2.3 Controllability Test

Before designing a control scheme, the controllability of a system is checked by computing the rank of a controllability matrix. Consider a linear time-invariant system which has n states and p inputs in a continuous time domain. Such a system can be represented in a state-space model according to equation 6.3.

$$\dot{\mathbf{x}} = \mathbf{A}\mathbf{x} + \mathbf{B}\mathbf{u} \tag{6.3}$$

where $\mathbf{A}$ has dimension $n \times n$ and $\mathbf{B}$ has dimension $n \times p$. For such a linear system the controllability matrix can be obtained according to equation 6.4:

$$\mathbf{Co} = \begin{bmatrix} \mathbf{B} & \mathbf{AB} & \mathbf{A}^2\mathbf{B} & \cdots & \mathbf{A}^{n-1}\mathbf{B} \end{bmatrix} \tag{6.4}$$

For a system to be controllable, the number of states of the system must be equal to the rank of the controllability matrix, i.e., $n = \text{rank}(\mathbf{Co})$.

6.3 Experimental section

This work was performed on a ZSK-25 TSE manufactured by Coperion and described in chapter 1. An extrusion process usually has three input variables: screw

speed, feed rate, and barrel temperature. These input variables can be used as manipulated variables as well. The heating and cooling dynamics of the barrel temperature are rarely identical, and the barrel temperature is dynamically slow compared to screw speed and feed rate. Thus, screw speed and feed rate were selected as potential manipulated variables. The extrusion process was reduced to a two-input and two-output process based on the steady state and the dynamic analysis performed by Iqbal *et al.* (2010a).

6.4 Process models

Inherently, twin screw extrusion is a multiple-input multiple-output (MIMO) process. Controlled variables, manipulated variables, and disturbances are selected prior to designing a control scheme for a process. Variables for a twin screw extruder are detailed in chapter 4. Two process output variables, T_m and P_m, were selected as controlled variables based on a correlation with product quality attributes. Two input variables, screw speed (N) and feed rate (F), were used as manipulated variables. Figure 6.2 shows the open loop block diagram for a ZSK-25 TSE with a reduced number of process variables.

Figure 6.2: Open loop block diagram for a ZSK-25 TSE.

Screw speed was excited using a predesigned random binary sequence (RBS) excitation to develop models relating T_m and P_m with N. Grey box models were developed using a new approach introduced in chapter 4. The obtained models relating T_m and P_m with N were nonlinear. Equation 4.13 shows the relation between T_m and N and equation 4.14 shows the relation between P_m and N in discrete time domain. Equations 6.5 and 6.6 were converted to Laplace domain using zero order hold (ZOH), that is, they depict the grey box models in s-domain:

$$g_{11}(s) = \frac{T_m}{u_1} = \frac{-6.972 \times 10^{-6} s + 4.367 \times 10^{-6}}{s^2 + 0.1586 s + 0.003288} \tag{6.5}$$

$$g(s) = \frac{P_m}{u_2} = \frac{-89.23 s^2 - 191.3 s + 2.259}{s^3 + 0.4518 s^2 + 0.05643 s + 0.002522} \tag{6.6}$$

where, $u_1 = N^{1.8}$ and $u_2 = N^{-0.2}$.

The feed rate was excited using a predesigned RBS excitation. Details of the modeling is explained in chapter 5. Developed models relating T_m and P_m with F

are represented in equations 5.7 and 5.4, respectively, in the discrete time domain. These models were converted to a continuous s-domain using a ZOH. T_m and P_m s-domain models are described by equations 6.7 and 6.7, respectively.

$$g_{12}(s) = \frac{T_m}{F} = \frac{-1.7 \times 10^{-4}s + 9.7 \times 10^{-4}}{s^2 + 0.265s + 0.002571}e^{-56s} \tag{6.7}$$

$$g_{22}(s) = \frac{P_m}{F} = \frac{-0.2341s + 0.6405}{s^2 + 0.2116s + 0.01437}e^{-24s} \tag{6.8}$$

Equations 6.5 and 6.6 show T_m and P_m have linear relation with u_1 and u_2, respectively. However, both u_1 and u_2 have nonlinear relations with screw speed with different powers. Such relationships appeared because of the application of first principles knowledge in the modeling. However, dealing with different nonlinearities evaluating from a single variable is not a trivial in a control scheme. A nonlinear MPC can be designed for such a process. However, real-time applications of nonlinear MPCs are limited in industries.

RBS excitation of N and the corresponding response of P_m are presented in Figure 6.3. Screw speed was excited between 120 rpm and 160 rpm in that experiment. Operating conditions were: 210^{o}C barrel temperature, 6 kg/h feed rate, high density polyethylene feed. Details of this experiment are described in chapter 4. The value of P_m varied within $\pm$10 psi with significant noise. Instantaneous peaks with a significant magnitude were observed with changes in N. If these peaks are not considered, then the effect of changes in N on P_m can be neglected and it can be assumed that the transfer function model between P_m and N is zero, i.e., $g(s) = 0$. In this case, the continuous-time model for the extruder can be presented by equation 6.9.

$$\mathbf{y} = \mathbf{G}\mathbf{u} \tag{6.9}$$

where $\mathbf{y} = \begin{bmatrix} T_m \\ P_m \end{bmatrix}$, $\mathbf{G} = \begin{bmatrix} g_{11} & g_{12} \\ 0 & g_{22} \end{bmatrix}$ and $\mathbf{u} = \begin{bmatrix} u_1 \\ F \end{bmatrix}$.

It is worth mentioning that relative gain array (RGA) analysis is an another measure of interactions between input and output variables for a multiple-input multiple-output process. However, this analysis measures interactions at steady state conditions only. In addition to that RGA analysis for this TSE is not trivial since the models have different nonlinearities with the same input variables, screw speed. Thus, it is important to consider dynamic interactions, which can be observed from dynamic behaviors between input and output variables.

The transfer function model in equation 6.9 was converted to discrete time state-space model (Equation 6.10) using the MATLAB command "[A,B,C,D]=ssdata(c2d(G,t_s))," where t_s is the sampling time. A t_s of 1 sec was used in this work. The obtained

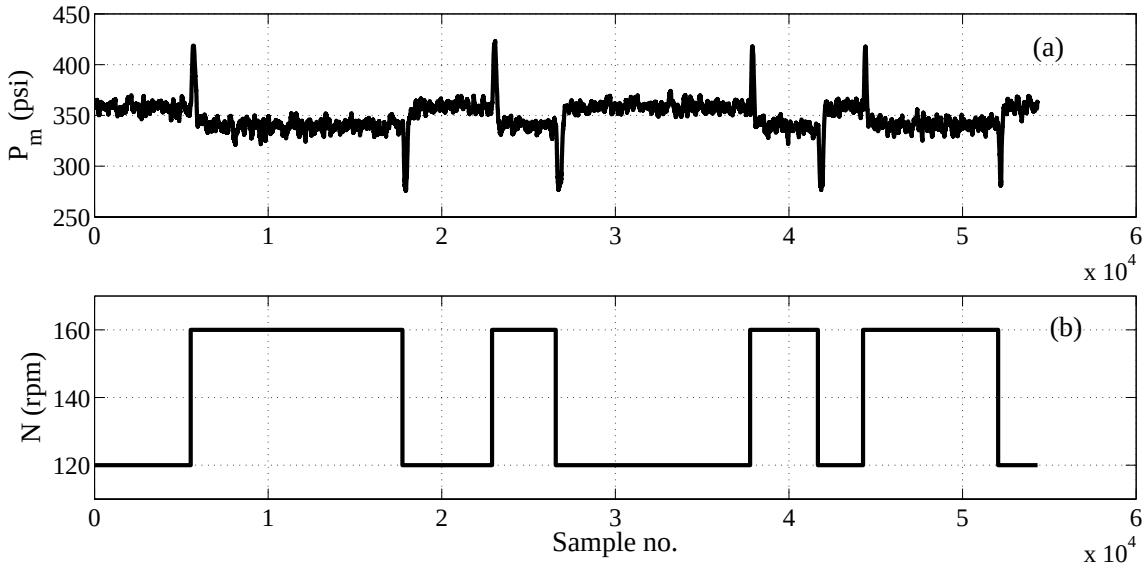

Figure 6.3: (a) Response of melt pressure due to RBS excitation of screw speed, (b) RBS excitation in screw speed.

discrete state-space model is represented by equation 6.10.

$$\begin{aligned} \mathbf{x_{k+1}} &= \mathbf{A x_k} + \mathbf{B u_k} \\ \mathbf{y_k} &= \mathbf{C x_k} \end{aligned} \tag{6.10}$$

where $\mathbf{A} = \begin{bmatrix} 1.8503 & -0.8533 & 0 & 0 & 0 & 0 \\ 1 & 0 & 0 & 0 & 0 & 0 \\ 0 & 0 & 1.7649 & -0.7672 & 0 & 0 \\ 0 & 0 & 1 & 0 & 0 & 0 \\ 0 & 0 & 0 & 0 & 1.7964 & -0.8093 \\ 0 & 0 & 1 & 0 & 1 & 0 \end{bmatrix}$

$\mathbf{B} = \begin{bmatrix} 0.0039 & 0 \\ 0 & 0 \\ 0 & 0.0313 \\ 0 & 0 \\ 0 & 1 \\ 0 & 0 \end{bmatrix}$

$\mathbf{C} = \begin{bmatrix} -0.0011 & 0.0022 & 0.0094 & 0.0178 & 0 & 0 \\ 0 & 0 & 0 & 0 & 0.088 & 0.4886 \end{bmatrix}$

Equation 6.10 was used as the basis for the design of discrete time model predictive controller. The obtained discrete state space model had a total of 6 states. Since these are identified models, it is hard to explain the states physically. However, the state space model shows that the melt temperature is a linear combination of first 4 states and the melt pressure is a linear combination of last two states. The controllability matrix for this system was obtained using equation 6.4 as follows:

$$\mathbf{Co} = \begin{bmatrix} \mathbf{B} & \mathbf{AB} & \mathbf{A^2B} & \mathbf{A^3B} & \mathbf{A^4B} & \mathbf{A^5B} \end{bmatrix} \tag{6.11}$$

A rank of 6 was calculated for the controllability matrix of this system. Since, the rank of the controllability matrix is equal to the number of states of the process, the system was controllable.

6.5 Designed Control Scheme

The objective of the MPC scheme was to design a multiple-input multiple-output (MIMO) system. Equation 6.12 shows the objective function that needed to be minimized to a calculate sequence of moves for manipulated variables:

$$\mathbf{J} = \sum_{j=1}^{P}(\parallel \mathbf{r_{t+j}} - \mathbf{y_{t+j}} \parallel_Q^2 + \sum_{j=1}^{M}(\parallel \triangle \mathbf{u_{t+j-1}} \parallel_R^2)) \tag{6.12}$$

where P is the prediction horizon, M is the control horizon, $\mathbf{r}$ is the reference variable or set-point, $\mathbf{Q}$ is the weighting matrix for $\mathbf{y}$, and $\mathbf{R}$ is the weighting matrix for $\mathbf{u}$. The output weighting matrix $\mathbf{Q}$ was selected according to the relative importance of the output variables. In a similar way, $\mathbf{R}$ allowed the manipulated variables to be weighted according to their relative importance. Both $\mathbf{Q}$ and $\mathbf{R}$ were chosen to be diagonal matrices. The norm terms in equation 6.12 were defined as:

$$\parallel \mathbf{r} - \mathbf{y} \parallel_Q^2 = (\mathbf{r} - \mathbf{y})'\mathbf{Q}(\mathbf{r} - \mathbf{y}) \tag{6.13}$$

The extrusion system explained in state-space form by equation 6.10 has two inputs and two outputs. An MPC scheme was designed for this extruder to control T_m and P_m by manipulating N and F. A description of MPC tuning parameters follows:

Prediction horizon, P: It is recommended that the prediction horizon be larger than the time delay. Equations 6.7 and 6.8 show time delays of 24 sec and 56 sec, respectively. Thus, a prediction horizon of 70 sec was chosen in designing the MPC.

Control horizon, M: MPC predicts control action for up to 70 sec after the first action is implemented. Thus, a control horizon of 1 was selected for the MPC.

Weighting matrices: Weighting matrices $\mathbf{Q}$ and $\mathbf{R}$ were chosen for the MPC. The objective of this MPC is to control the temperature and pressure of the polymer melt. Temperature has more effect than the pressure on the properties of the polymer melt; hence, temperature was given more weight than pressure. A change in screw speed affect outputs faster than a change in feed rate. Thus, less weight was given to N than F. Equation 6.14 shows $\mathbf{Q}$ and $\mathbf{R}$ weighting matrices. Note that the weight for screw speed in $\mathbf{R}$ is actually not for N, it is for u_1. However, u_1 was converted to N to get the actual screw speed since $N = (u_1)^{1/1.8}$.

$$\mathbf{Q} = \begin{bmatrix} 3 & 0 \\ 0 & 1 \end{bmatrix}$$
$$\mathbf{R} = \begin{bmatrix} 0.01 & 0 \\ 0 & 0.1 \end{bmatrix} \tag{6.14}$$

MPC algorithm: The model predictive control algorithm was written in MATLAB (version 7.5) using the *Model Predictive Control Toolbox*. The followings steps were used to execute the algorithm and to calculate the control moves:

- Step 1: Nominal values of the output variables ($\mathbf{y}_{ss}$=$[\bar{T}_m \ \bar{P}_m]'$) and manipulated variables ($\mathbf{u}_{ss}$=$[\bar{N} \ \bar{F}]'$) were selected.
- Step 2: The MPC objective function, the initial states of the process, and the tuning parameters were defined.
- Step 3: The reference trajectory $\mathbf{r}$ was selected.
- Step 4: The process output variables were measured and noise was removed using an exponentially weighted moving average (EWMA) filter.
- Step 5: The output variables were converted to deviation form, i.e., $\mathbf{y}$=$[(T_m$-$\bar{T}_m)$, $(P_m$-$\bar{P}_m)]'$.
- Step 6: The move for manipulated variables in deviation form ($\mathbf{u}$) was computed using the MATLAB command *'mpcmove'* based on $\mathbf{y}$, $\mathbf{r}$, and the MPC objective function.
- Step 7: The actual manipulated variables were calculated for implementation, i.e., $\mathbf{u}_a$=$\mathbf{u}$+$\mathbf{u}_{ss}$
- Step 8: The states were updated using the state-space equation to calculate the next move and execute steps 4 to 8.

This algorithm was executed in LabVIEW matlab script online. Signals corresponding to algorithm outputs (screw speed and feed rate) were sent from LabVIEW to the corresponding terminals.

6.6 Real-time Experiments

The designed MPC was tested by conducting several closed loop experiments in real-time. The objective of these experiments was to evaluate the controller performance in terms of disturbance rejection and set-point tracking. The robustness of the controller was also examined.

All experiments were conducted using similar nominal values. A feed rate of 6 kg/h, a screw speed of 140 rpm, and a barrel temperature of 210^{o}C were used as the nominal operating conditions. A high density polyethylene (SCLAIR 2907) provided by Nova Chemicals was used as a processing material. This material has a melt index of 4.9 g/10 min and a melting point of 135^{o}C. Nominal values of 211^{o}C for T_m and 350 psi for P_m were used. After making a change in the process under closed loop control, experiments were conducted for sufficient time to allow the process to come to a new steady state. Since only one high density polyethylene was used for real-time experiments, no product quality, e.g., melt index, analysis was done.

In designing the MPC, the operating range of the screw speed was constrained between 110 rpm and 170 rpm with a rate of change of 5 rpm/sec. The feed rate was constrained to operate between 2 kg/h and 10 kg/h with a rate of change of 0.1 kg/h. The process was operated for sufficient time ($\cong$ 20 minutes) to bring all the variables to their nominal values. Then, model predictive control action was activated for closed loop operation. It was observed that the melt temperature decreased slowly due to heat loss from the extruder. This decrease was ignored when developing models relating melt temperature to screw speed and feed rate. Thus, the nominal value for T_m was considered pseudo-steady state. Data were collected every 1 sec.

Responses of controlled or output variables T_m and P_m are presented in Figures 6.4(a) and 6.4(b), respectively. The dotted lines represent experimental values and the solid lines show the set-points. Both the controlled variables stayed at their set-points; however, the P_m response was noisy. The MPC algorithm calculated values of screw speed and feed rate for the closed loop operation of the extruder. Changes in screw speed and feed rate and outputs of the MPC algorithm are shown in Figures 6.4(c) and 6.4(d), respectively. The dotted lines show measured value and the solid lines represent outputs from MPC algorithm. The obtained responses indicate that the transfer from open loop to closed loop processes was bumpless.

Figure 6.4(c) shows that N increased over the course of experiment. To overcome the drift in T_m, MPC increased screw speed and kept T_m at its set-point. Thus, Figure 6.4(c) showed a small increasing trend in screw speed. A slight difference was observed between the actual screw speed and the screw speed calculated with the MPC algorithm. This could be due to the one-way communication between the PC and the motor drive. Figure 3.5 shows that the algorithm output was sent from computer to the motor drive only, no feedback was observed from the motor drive to the PC. Thus, no corrective action was taken to compensate for this difference. This difference was very small ($\cong$ 1 rpm) compared to the actual value of the screw speed. Figure 6.4(d) shows that the response of F was almost at the nominal value and did not vary significantly.

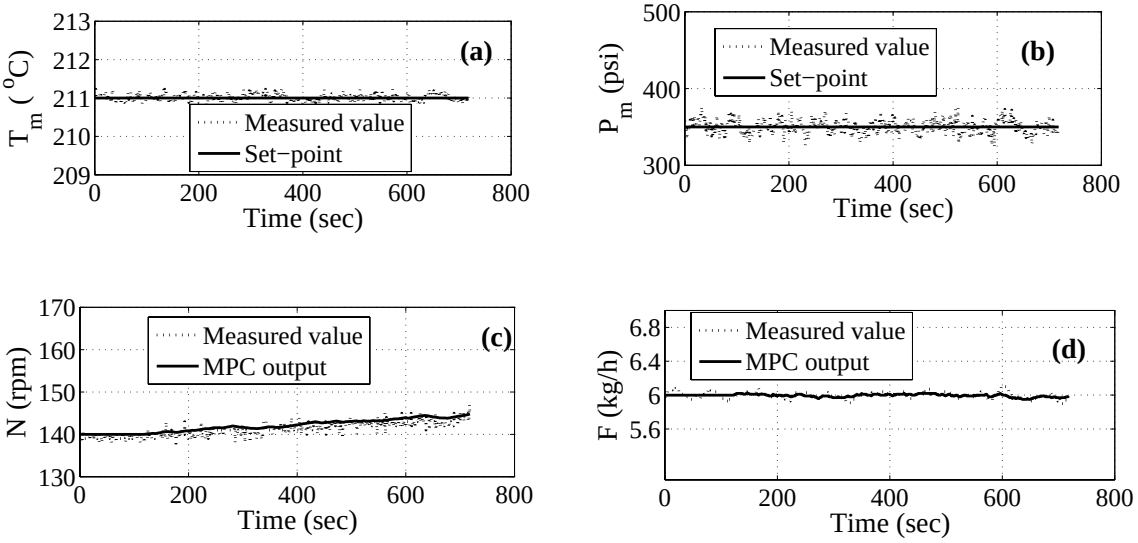

Figure 6.4: Responses of variables in closed loop operation: (a) Melt temperature, (b) Melt pressure, (c) Screw speed, (d) Feed rate.

6.6.1 Disturbance Rejection

The robustness of the controller was tested by imposing an external disturbance in the extrusion process. A handful of polypropylene (PP) with a melt index of 30 g/10 min was fed to the extruder along with the HDPE processing material. The addition of PP to the HDPE changed the bulk density of the feed material and the total feed rate in the extruder. PP was fed to the extruder 5 min after activating the MPC. The controlled and manipulated variables were $\mathbf{y}=[0\ 0]'$ and $\mathbf{u}=[0\ 0]'$, respectively, in deviation form. Again, the reference variables were $\mathbf{r}=[0\ 0]'$. Initial conditions of the estimated state variables were assumed to be $\hat{\mathbf{x}}(0)=[0\ 0\ 0\ 0\ 0\ 0]'$. Figure 6.5 shows the responses of the controlled variables and changes in the manipulated variables due to the external disturbance.

Figure 6.5(a) shows that the melt temperature decreased and Figure 6.5(b) shows that the melt pressure increased due to the disturbance. However, the MPC brought both the controlled variables to their set-points. Figures 6.5(c) and (d) show that an increase in N and a decrease in F, respectively, overcome the effects of the disturbance. However, the increase in N was observed to continue after the effect of the disturbance had been mitigated. This was because of the slow drift in T_m. The feed rate was observed to return almost to its nominal value after recovering from the effect of the disturbance.

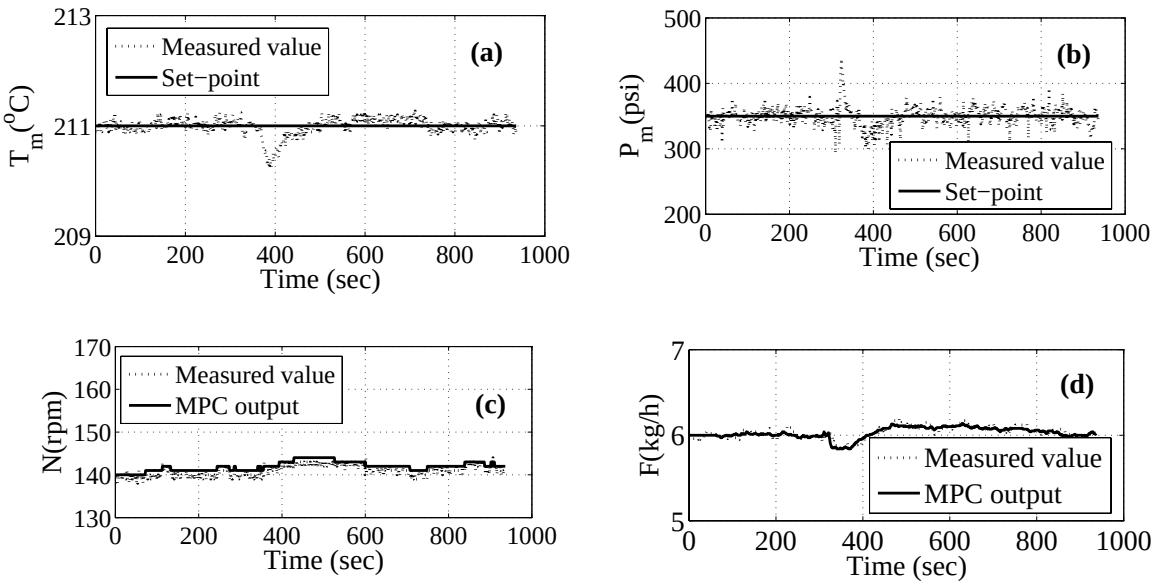

Figure 6.5: Response of variables due to an external disturbance: (a) Melt temperature, (b) Melt pressure, (c) Screw speed, (d) Feed rate.

6.6.2 Servo Control

The performance of the model predictive controller was also studied by examining its ability to automatically adjust the process outputs to new set-points. Two experiments were performed for this study.

Set-point Change in Melt Temperature

A positive step change in T_m was imposed to observe the set-point tracking ability of the MPC. Melt temperature was increased from 211^{o}C to 212^{o}C after 2 min of closed loop operation. The melt pressure was maintained at its nominal value. In deviation form, the controlled and manipulated variables were $\mathbf{y}$=[0 0]$'$ and $\mathbf{u}$=[0 0]$'$, respectively. For the unit step change in T_m, the reference variables became $\mathbf{r}$=[1 0]$'$. Similar initial conditions for estimated state variables were considered. Figure 6.6 shows the responses of controlled variables and changes in manipulated variables.

Figure 6.6(a) shows that the new T_m set-point was automatically adjusted by the MPC within a few minutes of the disturbance. The response of T_m was a bit slow that can be overcome by doing some fine tuning. Besides, control action can be made faster by relaxing constraints imposed on manipulated variables. The change in response of P_m due to the step change in T_m was hard to observe because of the noise in P_m . However, it seems that there was no considerable change in P_m. Figure 6.6(d) shows that the feed rate decreased but eventually returned to its

nominal value. Figure 6.6(c) shows a considerable change in the screw speed than in the feed rate. In fact, the step change in T_m produced more change in the screw speed than in the feed rate.

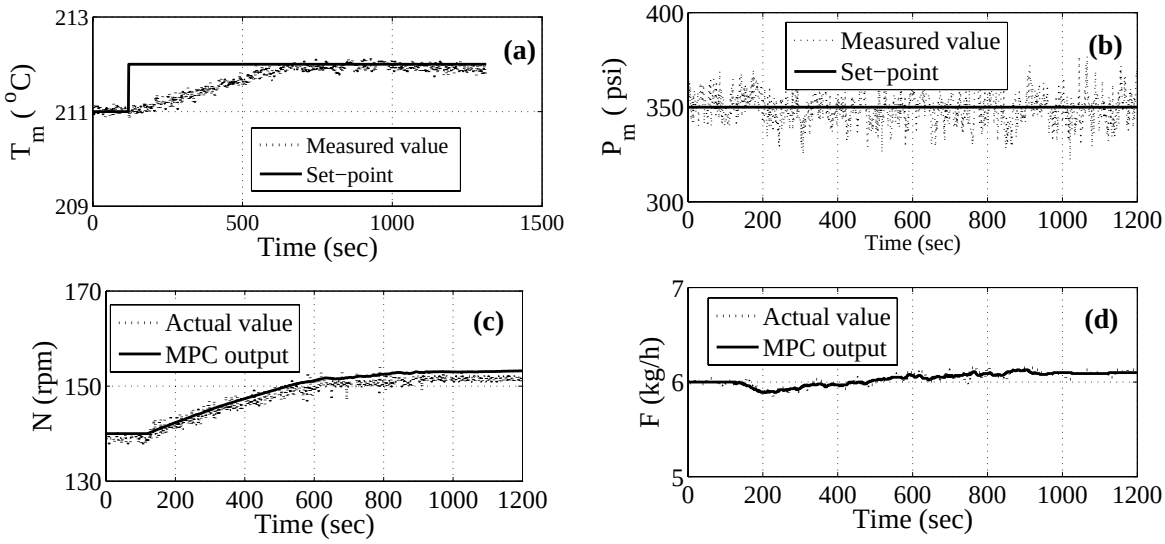

Figure 6.6: Responses of variables due to a step change in melt temperature: (a) Melt temperature, (b) Melt pressure, (c) Screw speed, (d) Feed rate.

This study indicated that a change in N had almost no effect on P_m in the closed loop operation. Thus, the assumption made in the designing of the MPC, the effect of changes in N on P_m can be ignored, was a reasonable assumption.

Set-point Change in Melt Pressure

The set-point tracking ability of the MPC was examined by imposing a step change in P_m. Because P_m had significant noise, a step of 20 psi was imposed to ensure the step change in P_m was higher than the noise, so the response in P_m could be observed. In this case, the melt pressure increased from its nominal value of 350 psi to 370 psi. The controlled variables and manipulated variables in deviation form were $\mathbf{y}=[0\ 0]'$ and $\mathbf{u}=[0\ 0]'$, respectively. The reference variables became $\mathbf{r}=[0\ 20]'$ because of the 20 psi step change in P_m. Similar initial conditions for estimated state variables were used. Figure 6.7 shows the responses of controlled variables and changes in manipulated variables.

Automatic adjustment of P_m to the new set-point by the MPC action can be observed in Figure 6.6(b). Figure 6.6(a) shows no change in T_m owing to the step change in P_m. Figure 6.6(c) shows a slight increase in N because of the slow drift in T_m. A sudden change in F was observed as shown in Figure 6.6(d). However, this change was within the physical limit.

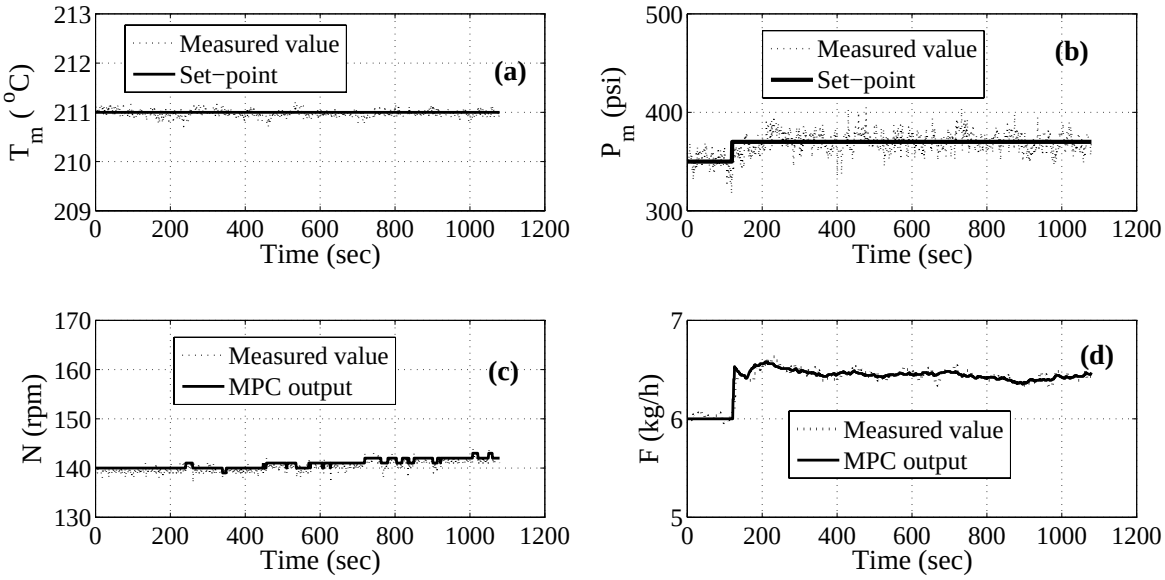

Figure 6.7: Responses of variables due to a step change in melt pressure: (a) Melt temperature, (b) Melt pressure, (c) Screw speed, (d) Feed rate.

All experiments performed in real-time indicated that the designed model predictive controller successfully controlled T_m and P_m by manipulating N and F. The MPC algorithm changed the manipulated variables within the physical limits to overcome any process upset. Bumpless transfer from the manual mode to the auto mode was implemented using the MPC scheme.

6.7 Summary

In this work, a model predictive controller was designed for a plasticating twin screw extruder. Melt temperature at the die and melt pressure at the die were controlled using this controller by manipulating screw speed and feed rate. In this case, four transfer functions were obtained from a laboratory scale twin screw extruder and were converted to a state-space model to perform the model predictive control algorithm. Performance and robustness of the MPC scheme were examined by conducting real-time experiments. Experimental outcomes showed that real-time regulation and set-point tracking performance by the designed control scheme were achieved. The MPC was found to be robust to an external disturbance. Since the objective was to design and implement an advanced controlller for the TSE, no classical controller, e.g., PI or PID was studied in real time.

Chapter 7

Multimodel Approaches for Modeling and Control

7.1 Introduction

The control of processes for a wide range of operating conditions has attracted a great deal of attention from the process control community in recent years (Ozkan *et al.* 2000). Fixed and specific linear controllers are generally not adequate for such applications, especially for chemical processes that have nonlinear behavior. A controller with varying structure and/or parameters is needed to meet the control demands at multiple operating points. A basic approach for controlling multiple regimes in complex systems is based on a multiple-model approach. In this approach, a nonlinear system is represented as a combination of multiple linear models. A number of techniques have been proposed in the literature to approximate a nonlinear system using multiple-linear models. However, the approaches differ mainly in the choice of model weights.

The extrusion process is a nonlinear process (Haley and Mulvaney 2000b, McAfee and McNally 2006). It is most likely that controllers designed for one operating range might not work in the other operating conditions. Thus, there is huge scope to apply multimodel approaches to extrusion processes. In this chapter, the multimodel approach has been used to design nonlinear control schemes to control a twin screw extruder over a wide range of operating conditions. Nonlinear behavior in the melt temperature (T_m) due to changes in the screw speed (N) was detailed in chapter 4 and a nonlinear grey box model was developed. A model predictive controller was designed using this nonlinear model and successfully implemented in real-time in chapter 6. The capture of this nonlinear behavior of T_m due to changes in N using multimodel approach is described in this chapter. Also, design and simulation of a nonlinear proportional-integral controller (n-PI) and a nonlinear model predictive controller (n-MPC) are detailed in this chapter.

7.2 Operating Regime Approaches

Any model or controller has a limited range of operating conditions in which it is sufficiently accurate to serve its purpose. This range may be restricted for several reasons, for example, linearization of a nonlinear process, modeling assumptions, or experimental conditions. Such a model or controller is known as a local model or controller. However, the ultimate goal is a global model or controller.

The operating modeling approach is based on the decomposition of a system's full range of operation into a number of possibly overlapping operating regimes as depicted in Figure 7.1. A simple local model or controller is used in an operating regime. These local models or controllers are combined to obtain a global model or controller. It is not always easy to find a natural sequence in which these tasks should be approached. Several iterations of the same tasks are usually needed before a satisfactory model or controller is found.

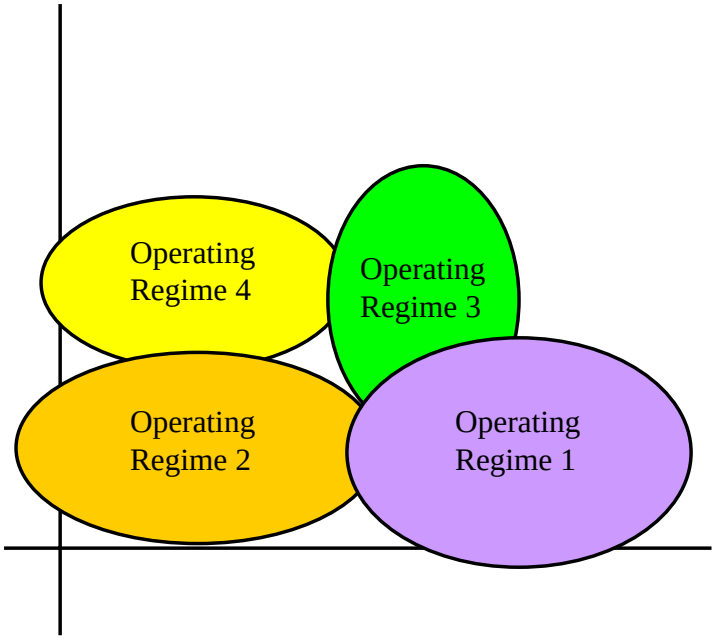

Figure 7.1: Operating range of a complex process decomposed into a number of operating regimes.

7.2.1 Combining Local Models or Controllers

An operating regime approach consists of a family of local models or controllers and a scheduler. The simplest form of scheduling is hard switching between models or controllers, but control action is not smooth with this method. In some cases, sudden changes between operating regimes may not be convenient. For example, if a system's operating regimes are characterized by different behaviors or mechanisms, these behaviors or mechanisms will change with a change in operating regimes; most physical systems have this property. In such cases, the operating regimes can be described as overlapping sets and a smooth scheduler can be implemented between regimes.

Fuzzy sets and fuzzy logic can be applied to describe the soft boundaries between operating regimes. Fuzzy sets are characterized by gradual membership and are a natural way of describing an operating regime. The basic concepts of fuzzy logic state the natural ways of making inference. The resulting inference mechanism can be applied to form an interpolation that gives more or less weight to the local models or controllers in different operating regimes, depending on the operating points (Takagi and Sugeno 1985).

For example, local PID controller outputs or the local PID controller parameters can be interpolated (Kuipers and strm 1994). The controller structure has to be assumed homogeneous to interpolate controller parameters. At each sampling instant, the scheduler will assign a weight to each controller and the weighted sum of the outputs will be applied as an input to the system for interpolation of local controller outputs.

7.2.2 Fuzzy Logic

Consider a nonlinear system represented by the following differential equations:

$$\dot{x} = \bar{f}[x, u, d], \tag{7.1}$$

$$y = \bar{g}[x, u, d]. \tag{7.2}$$

Equation 7.1 describes a dynamic system and equation 7.2 describes the relationships between outputs and states. Linearization or identification of this system at different central points yield a number of local models. The Takagi and Sugeno (T-S) fuzzy approach can be used to obtain a weight for each local model or controller (Takagi and Sugeno 1985). The T-S fuzzy dynamic model is a piecewise interpolation of local linear models through a membership function. This dynamic model is described by IF-THEN rules which represent local linear input-output relations of the nonlinear system.

If the nonlinear system is linearized around M number of central points, the transfer function models obtained at each operating point $(\bar{u}_i, \bar{y}_i)$ can be represented as $G_i(z) = \frac{\Delta y_i(z)}{\Delta u_i(z)}$, where $\Delta y_i(z)$ are output variables in deviation form, $\Delta u_i(z)$ are input variables in deviation form and i = 1 $\cdots$ M.

The global output of the fuzzy dynamic model can be obtained according to equation 7.3:

$$y_m(k) = \sum_{i=1}^{M} h_i[z(k)][\Delta y_i + \bar{y}_i] \tag{7.3}$$

where $h_i[z(k)]$ is a relative grade of membership function of i^{th} regime and is defined as

$$h_i[z(k)] = \frac{\mu_i[z(k)]}{\mu(k)} \tag{7.4}$$

In equation 7.4, $\mu_i[z(k)]$ is a grade of membership function of i^{th} regime $\mu(k) = \sum_{i=1}^{N} \mu_i[z(k)]$.

It should be noted that the relative grade of membership should be $h_i[z(k)] \in [0, 1]$ and $\sum_{i=1}^{N} h_i[z(k)] = 1$.

7.3 Experimental Procedure

A ZSK-25 twin screw extruder was used in this study. Previous studies showed that polymer melt temperature had a nonlinear relationship with the input variables. For example, melt temperature at the die showed a nonlinear relationship with screw speed. Thus, a multimodel approach was used to model T_m due to changes in N. An operating range of 120 rpm to 140 rpm was used in developing the grey box model between T_m and N in chapter 4. A much higher screw speed is used in industry. The ZSK-25 can operate up to 1200 rpm according to the manufacturer; that is considerably higher than the speed used in this work. We did not operate the ZSK-25 at such high speeds for a number of reasons. For example, barrel temperature at zone 4 fluctuated if the extruder operated at 200 rpm, with a feed rate of 6 kg/h and a barrel temperature of 210^{o}C for all zones. This temperature fluctuation was due to poor temperature control at that zone. The barrel temperature at each zone was controlled by a local PID controller.

High density polyethylene (SCLAIR 2907) was used as a processing polymer in this study. The operating conditions for feed rate and barrel temperature were 6kg/h and 210^{o}C, respectively. The range of screw speed covered in this study was 100 rpm to 160 rpm. The overall operating range was divided into three regimes with 20 rpm intervals. Thus, regime 1 covered 100 rpm to 120 rpm, regime 2 covered

120 rpm to 140 rpm, and regime 3 covered 140 rpm to 160 rpm. The central points of regime 1, regime 2, and regime 3 are 110 rpm, 130 rpm, and 150 rpm, respectively.

Step tests were performed both in positive and negative directions for each regime starting from the central point of the corresponding regime. A sampling time of 2 sec was selected to design a random binary sequence (RBS) in screw speed for all the regimes. The extruder was excited using the predesigned RBS in screw speed for each operating regime. Data were collected every 2 sec in all runs.

Figure 7.2, Figure 7.3, and Figure 7.4 show time plots of melt temperature and designed RBS screw speeds for regime 1, regime 2, and regime 3, respectively. The time trend of T_m in each regime shows that T_m increased with an increase in N and T_m decreased with a decrease in N. A slow drift in T_m was observed in all regimes. Such a trend can be neglected to make the time series stationary. This decreasing trend was compensated by the controller in a closed loop operation, as described in chapter 6. Time plots showed no considerable noise in the data.

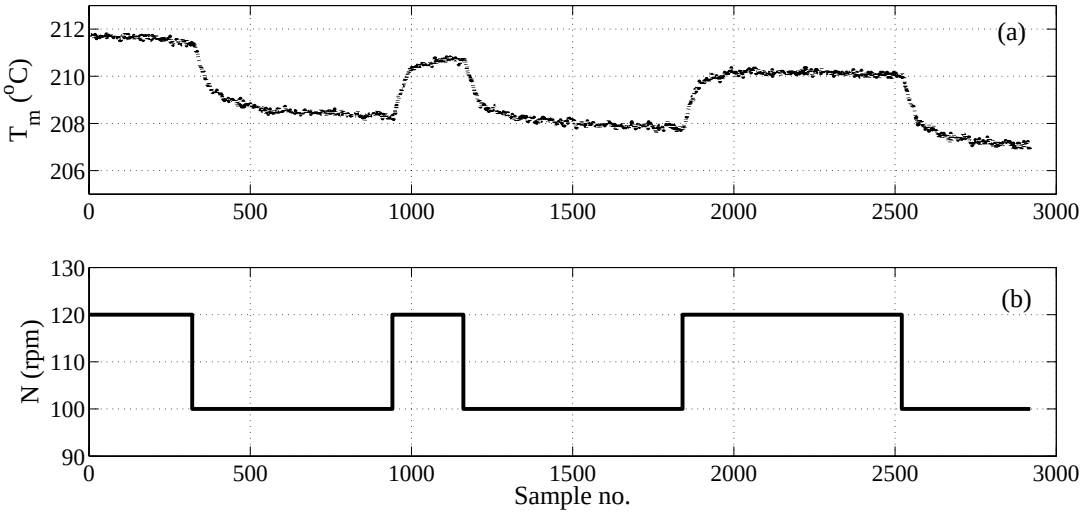

Figure 7.2: Regime 1: (a) Response of melt temperature to changes in N, (b) RBS in N.

Figure 7.5 shows the impulse response estimates for all the three regimes. It can be observed that some of the coefficients fall outside the 99% confidence interval at the lower value of lags. Such an orientation indicates existence of time delay in the process. However, this peak appears outside the confidence interval mainly because of the noise. Such a phenomenon was explained mechanistically using process knowledge in chapter 4. In fact, there were no time delays in T_m due to changes in N for this extruder.

The orientation of the impulse response coefficients for each regime indicates that the model order should be first order.

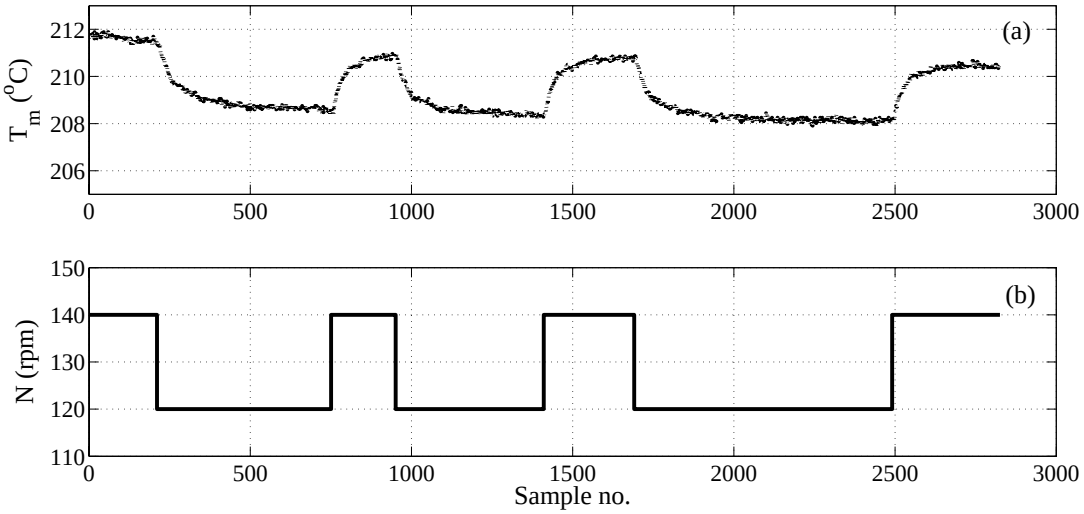

Figure 7.3: Regime 2: (a) Response of melt temperature to changes in N, (b) RBS in N.

7.4 Model Development

7.4.1 Local Models

A model for each operating regime was developed using system identification, a technique detailed in chapter 4. The complete response of T_m due to changes in N was observed to be slow. Thus, data were downsampled to every 4 sec. Such downsampling eliminates the clustering of poles at the circumference of the unit circle in the discrete z-domain.

The first half of the dataset was used to develop the model and the whole dataset was used to validate the obtained model. Different model structure and order were tried to obtain a process model based on the criteria used in chapters 4 and 5. Finally, a first order autoregressive moving average with exogenous input (ARMAX) structure was selected for each regime. Equation 7.5 shows the generic form of the model. Local model parameters are presented in Table 7.1.

$$T'_m(t) = \frac{\gamma q^{-1}}{1+\beta q^{-1}} N'(t) + \frac{1+\delta q^{-1}}{1+\beta q^{-1}} e(t) \tag{7.5}$$

where T'_m and $N'(t)$ melt temperature and screw speed, respectively, in deviation form, and $e(t)$ is noise. β, γ, and δ are model parameters. Values and standard errors of these parameters are provided in Table 7.1.

Figure 7.6 shows a comparison between model predicted output and experimental data for regime 1. It can be observed that the model predicted outputs and the experimental data almost overlap. Nearly 90% model fit was obtained that is the obtained model predicts T_m quite well in regime 1.

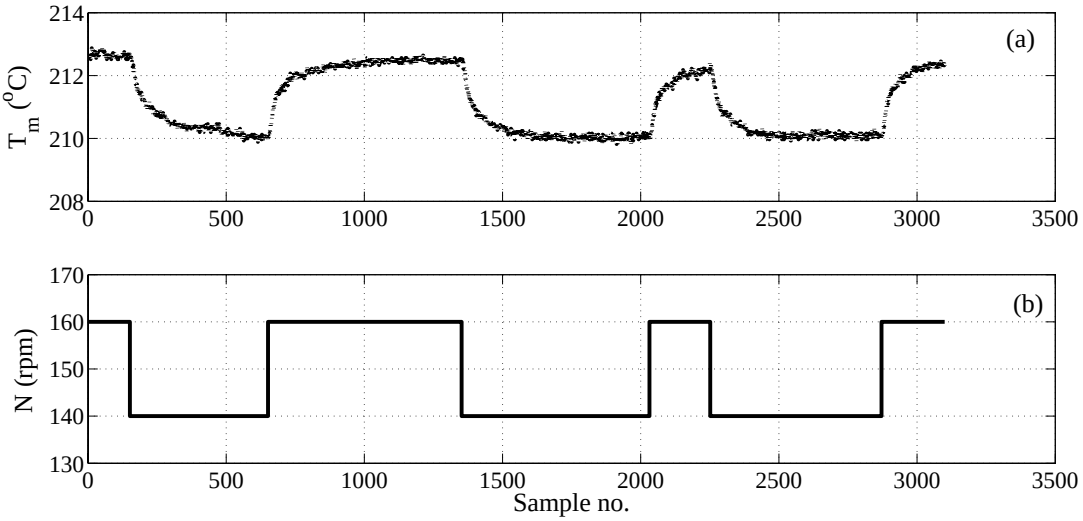

Figure 7.4: Regime 3: (a) Response of melt temperature to changes in N, (b) RBS in N.

Table 7.1: Local model parameters.

Operating regime	β	γ	δ
Regime 1: 100 to 120 rpm	-0.9204 ± 0.004	0.01077 ± 0.0005	-0.4906 ± 0.0046
Regime 2: 120 to 140 rpm	-0.9179 ± 0.004	0.01054 ± 0.0005	-0.5535 ± 0.0047
Regime 3: 140 to 160 rpm	-0.9309 ± 0.005	0.00793 ± 0.0005	-0.4241 ± 0.0049

A comparison between model predicted output and experimental data for regime 2 is shown in Figure 7.7. A model fit of almost 88% was obtained. So, the developed ARMAX model was good enough to capture the dynamics of T_m within the operating conditions of this regime.

Experimental data and model predicted output were also compared for regime 3, as shown in Figure 7.8. The developed T_m model gives about 86% fit with the experimental data. Such a model fit is also good.

Comparison between model predicted outputs and the experimental data were made for an infinite prediction horizon for each local model. Comparison in all the local model fits showed that model fit decreased when screw speed increased. This was mainly due to the nonlinearity in T_m and was not considered significant. Note that the operating range for screw speed covered in this study is not as wide as the range used in industry. In case of a significantly wide range of operating conditions, this nonlinearity might affect model fit considerably.

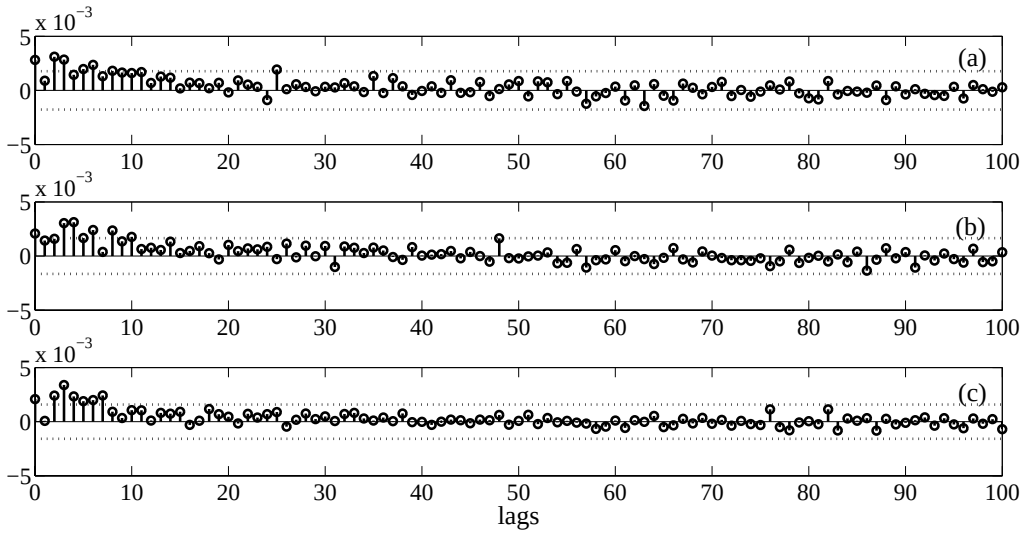

Figure 7.5: (a) Impulse response estimate for regime 1, (b) Impulse response estimate for regime 2, (c) Impulse response estimate for regime 3.

Table 7.2 shows the central operating conditions of output and input variables, gain (K), and time constant (τ_p) of each local model. No significant change in gain among local models was observed. Also, changes in time constant among models was not significant. However, these changes could be significantly higher for systems with a wider range of operating conditions.

Table 7.2: Operating conditions, gains, and time constants of identified models.

Operating regime	**Central points**	**Gain (K_i)**	**Process time constant ($\tau_{p,i}$)**
Regime 1	$N = 110$ rpm, $T_m = 209^o$C	0.135	51
Regime 2	$N = 130$ rpm, $T_m = 209.5^o$C	0.128	46
Regime 3	$N = 150$ rpm, $T_m = 211^o$C	0.114	55

7.4.2 Global Model

A dynamic global model was developed by combining the local models to cover the overall operating range of screw speed. The global dynamic model was developed using fuzzy logic. Multiple local linear input-output models were weighted using a fuzzy membership function. Screw speed was selected as a premise or scheduling variable to partition the operating space. The domain of each operating regime was characterized by a fuzzy set of membership functions to express smooth transitions between adjacent regimes. Triangular shape was selected for the fuzzy membership function as shown in Figure 7.9.

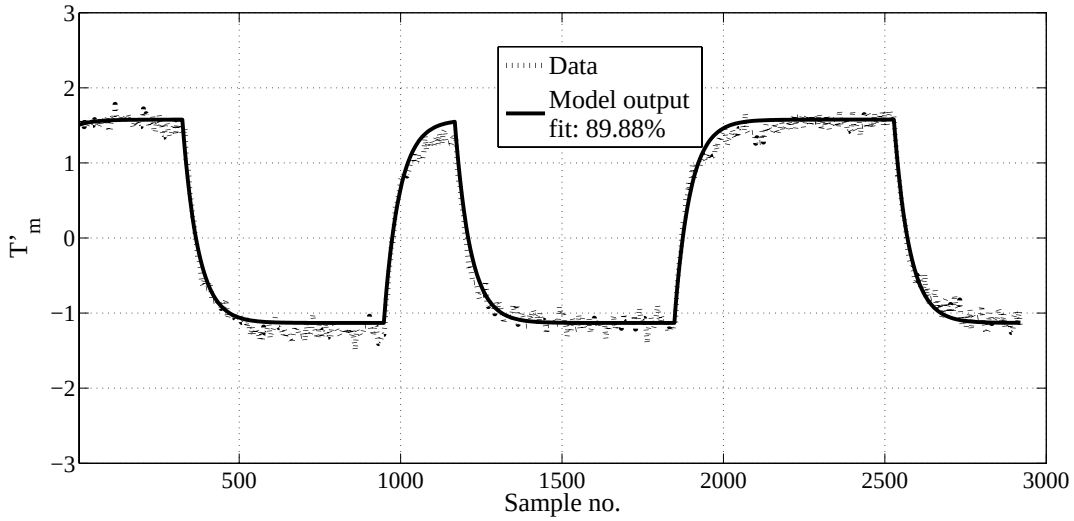

Figure 7.6: Comparison of experimental data and melt temperature model output for regime 1.

In this work, the operating space was divided on a single parameter, screw speed, and three local linear models (M = 3) have been developed. Figure 7.10 shows the simulated open loop responses of T_m global model due to the changes in screw speed.

7.5 Nonlinear Controller

In multimodel approach, local controllers are designed for each regime that combine the control laws over the range of operating conditions. In this work, a nonlinear proportional-internal (n-PI) controller and a nonlinear model predictive controller (n-MPC) were designed to control the process over the entire operating range of the study. Closed loop performances of the controllers were evaluated and compared.

7.5.1 n-PI Controller

Local PI controllers were designed on the basis of local linear models. Global PI controller outputs were developed by combining local PI controller actions. A discrete PI controller is represented by equation 7.6 in the discrete time domain.

$$\Delta u_i(k) = K_c[e(k) - e(k-1)] + \frac{K_c t_s}{\tau_I} e(k) \tag{7.6}$$

where K_c and τ_I are proportional gain and integral time constant, respectively, of a PI controller and t_s is sampling time. Like the global model, fuzzy logic was used to combine the local linear PI controller outputs to obtain the global controller outputs. The following rules were applied to determine global controller output $u(k)$:

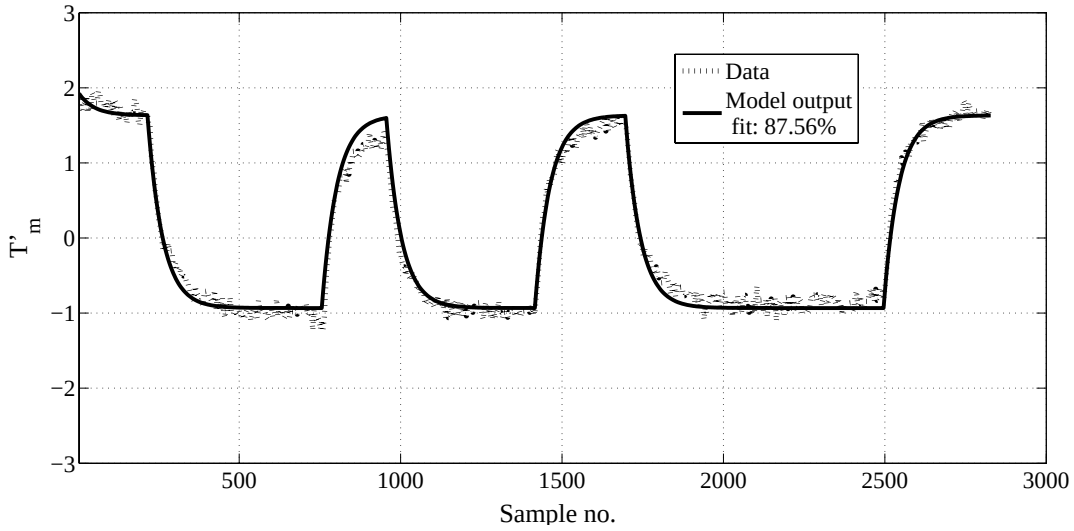

Figure 7.7: Comparison of experimental data and melt temperature model output for regime 2.

If $z_1(k)$ is $M_{i,j}$ and $\cdots$ $z_g(k)$ is $M_{i,g}$ then

$$\Delta u_i(k) = K_{c,i}[e(k) - e(k-1)] + \frac{K_{c,i}t_s}{\tau_{I,i}}e(k) \tag{7.7}$$

where, $K_{c,i}$ and $\tau_{I,i}$ are proportional gain and integral time constant, respectively of i^{th} PI controller. The global controller output is calculated by fusion of all linear PI controller outputs with membership functions as follows:

$$\begin{aligned} \Delta u(k) &= \sum_{i=1}^{N} h_i[z(k)]\Delta u_i(k) \\ u(k) &= \sum_{i=1}^{M} h_i[z(k)]\Delta u_i(k) + u(k-1) \end{aligned} \tag{7.8}$$

Three local PI controllers were designed based on local models. Tuning parameters for each PI controller were determined using direct synthesis method. Closed loop time constant for a local PI controller chosen as 2/3 of the process time constant. Table 7.3 shows the tuning parameters for the local controllers.

Table 7.3: PI controller parameters

Operating regime	**Proportional gain** ($K_{c,i}$)	**Integral time constant** ($\tau_{I,i}$)
Regime 1	11.08	48.24
Regime 2	11.68	46.68
Regime 3	13.06	55.86

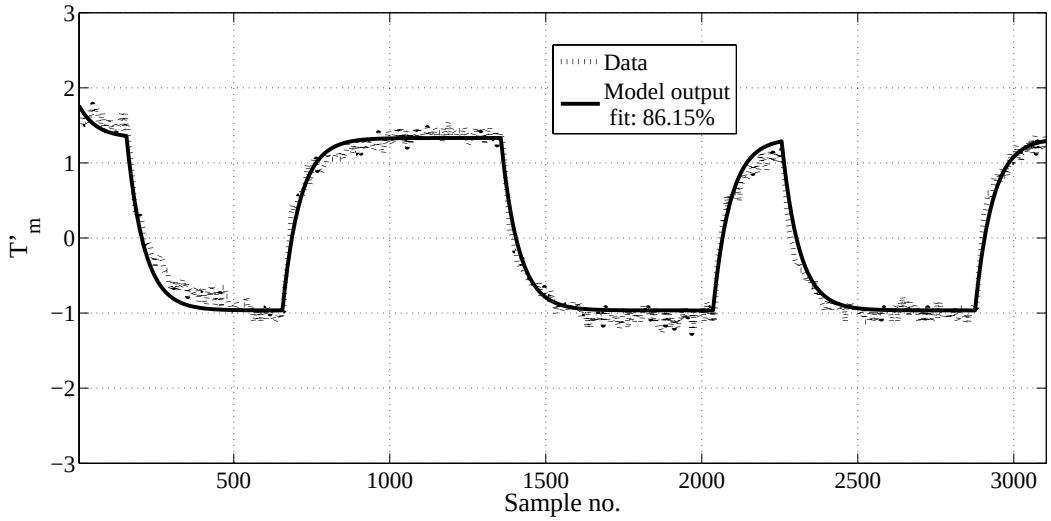

Figure 7.8: Comparison of experimental data and melt temperature model output for regime 3.

7.5.2 Closed Loop Response of n-PI Controller

The closed loop performance of the global (n-PI) controller was evaluated by simulating the set-point tracking ability of the controller as shown in Figure 7.11. It can be observed that the set-point tracking is quite good using the n-PI controller over the entire operating range. Figure 7.11(a) shows that the controller brought T_m to its new set-point quite well. However, considerable inverse response was observed for some set-point changes due to the changes in operating regime. The open loop response showed no inverse response in the entire operating range but drastic changes were observed in closed loop response. Such a drastic change in T_m suggests the use of a membership function that is smoother than the triangular membership function.

Figure 7.11 (b) shows the changes in the manipulated variables screw speed. Reasonable changes in N were observed, but considerable proportional kicks were observed in some cases to compensate the inverse responses in T_m.

7.5.3 n-MPC

Global MPC (n-MPC) output was obtained by fusing local MPC outputs. Local MPCs were designed using the local models. The philosophy of an MPC was explained in chapter 6. Global MPC outputs were obtained by fusing the local MPC outputs with fuzzy membership function.

Local MPCs were designed using state space approach. This approach was detailed in chapter 6. Local models were converted to discrete state-space models

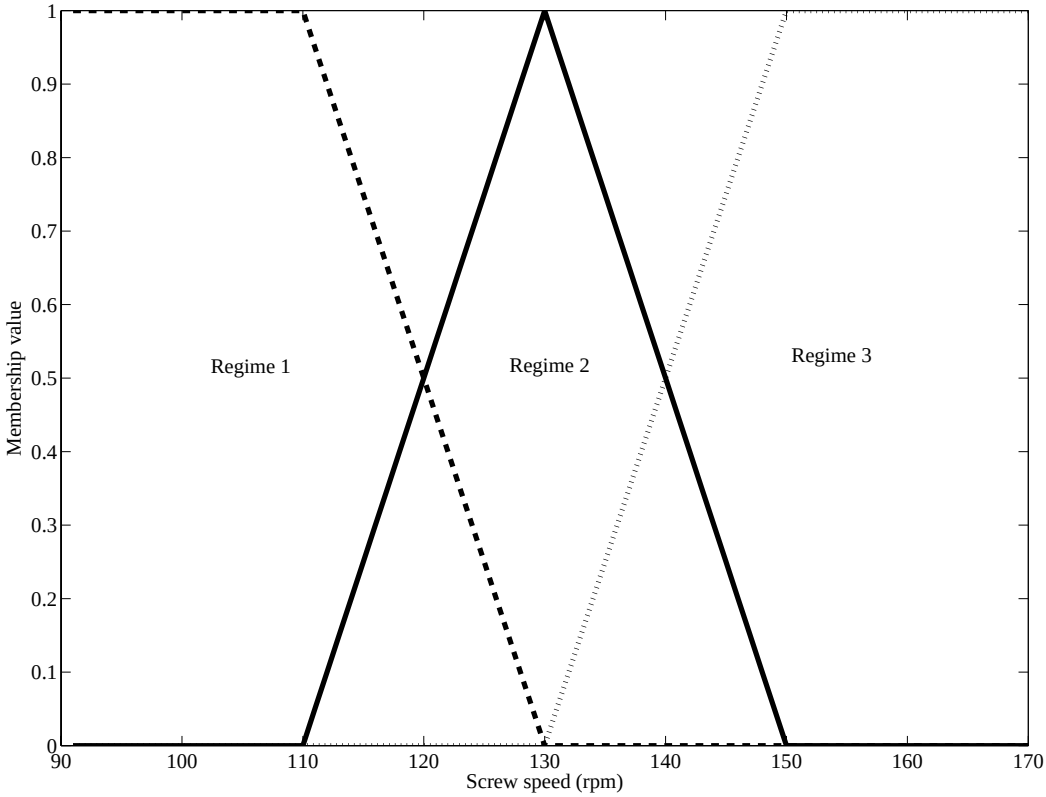

Figure 7.9: Fuzzy membership function of N.

according to equation 7.9:

$$\begin{aligned} x_{k+1} &= Ax_k + Bu_k \\ y_k &= Cx_k \end{aligned} \tag{7.9}$$

where A, B, and C are state-space parameters of a local model. Table 7.4 shows the state-space model parameters of the local models. It can be observed that the poles of the local models fall in the negative side of s-domain indicated bounded response of T_m due to changes in N. So, the process was controllable.

Table 7.4: State space parameters of local models.

Operating regime	A_i	B_i	C_i
Regime 1	0.9204	0.1250	0.0862
Regime 2	0.9179	0.1250	0.0843
Regime 3	0.9309	0.1250	0.0635

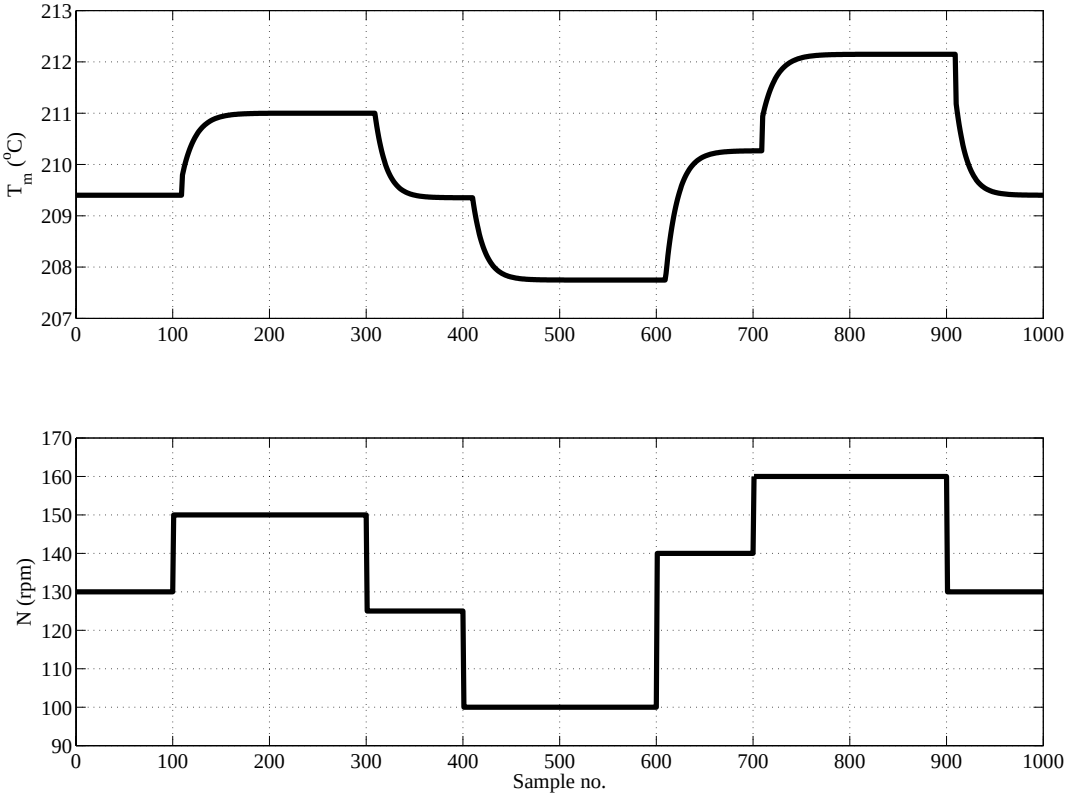

Figure 7.10: Open loop response of the global T_m model.

7.5.4 Closed Loop Response of n-MPC

The closed performance of n-MPC was evaluated by simulating the set-point tracking ability of the controller. A sampling time of 4 sec was used for this simulation. Following tuning parameters were used for local MPCs:

- prediction horizon = 10 samples,
- control horizon = 1 samples,
- weight in $N = 0.01$,
- weight in rate of change of $N = 1$,
- weight in $T_m = 1$.

The set-point tracking performance of n-MPC is shown in Figure 7.12(a). n-MPC showed excellent set-point tracking performance. No drastic change was observed in T_m over the range of operating conditions. Bumpless transitions from one operating regime to another regime were observed. Changes in N are presented in Figure

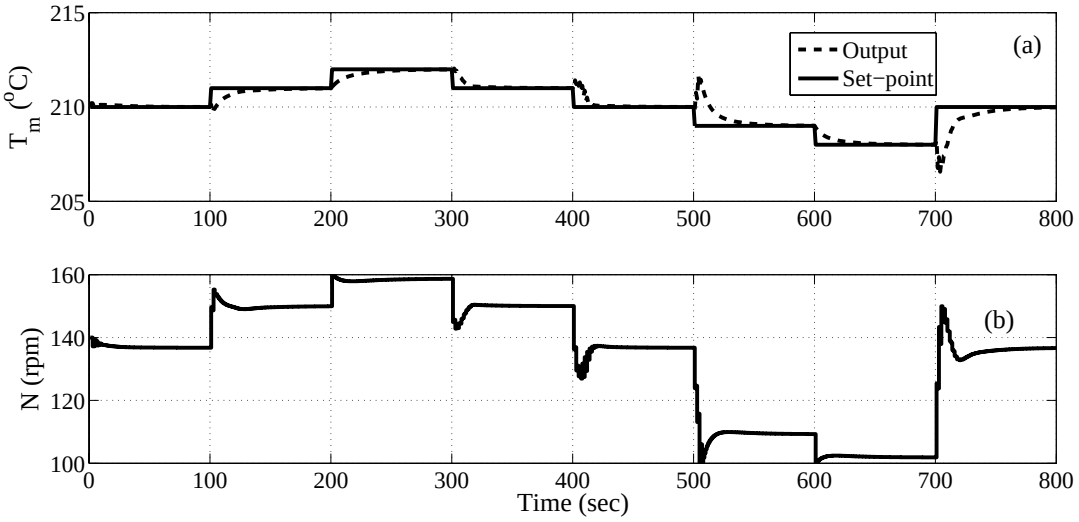

Figure 7.11: (a) Set-point tracking of n-PI controller, (b) Changes in manipulated variable N with time.

7.12(b). Smooth changes in screw speed were also observed. Slower changes in N were observed in closed loop response indicated no aggressive control action was performed by N.

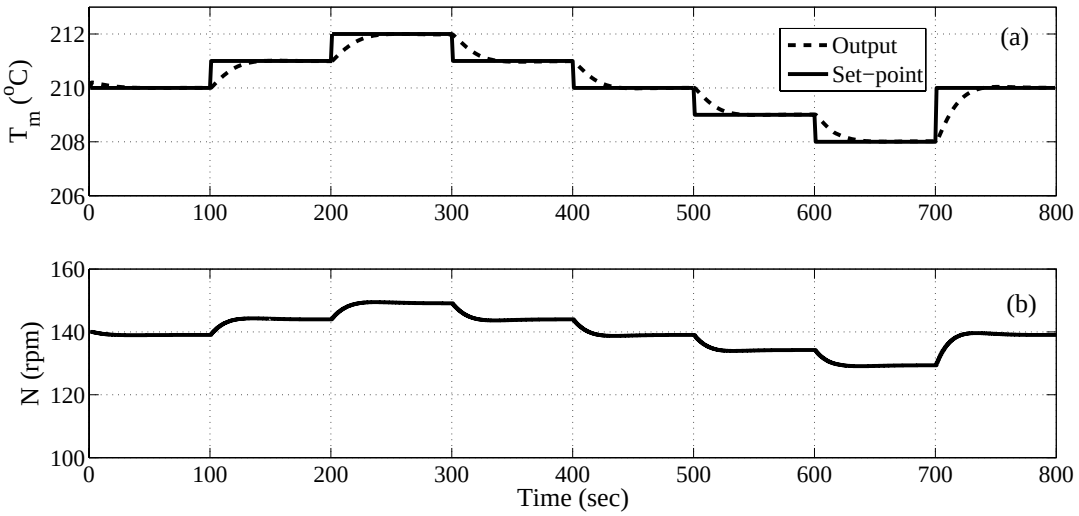

Figure 7.12: (a) Set-point tracking of the n-MPC, (b) Changes in manipulated variable N with time.

Fusion of local MPC outputs using triangular membership function was a good approach to design the n-MPC. n-MPC showed better set-point tracking performance compared to that of n-PI controller. Smoother transition from one operating regime to another operating regime was observed by n-MPC compared to n-PI controller. n-MPC showed less aggressive control action than that of n-PI controller.

7.6 Summary

A multimodel approach was used to develop a global model between melt temperature and screw speed. The global model represented the relationship between T_m and N over a screw speed range of 100 rpm to 160 rpm. The overall range was divided into three regimes and three local first order ARMAX models were developed using system identification approach. The global model was developed by combining the three local models using fuzzy logic. Triangular membership functions were used to weight the local models for fusion. Simulated results over a wide range of screw speeds showed excellent model prediction. No drastic changes in output were observed, i.e., transfer from one regime to another regime was bumpless.

A nonlinear PI controller was designed using the multimodel approach. This n-PI controller was used to control T_m by manipulating N. Closed loop response showed good set-point tracking by this controller, but drastic changes were observed in some cases due to the transition from one regime to another regime.

The multimodel approach was also used to design nonlinear model predictive controller. The n-MPC showed good set-point tracking ability with smooth transition from one regime to another regime. n-MPC showed less aggressive control action.

Chapter 8

Concluding Remarks and Future Work

8.1 Summary

The development of advanced controller for twin screw extrusion processes is inspired by industrial applications and involves research in many chemical engineering fields. This thesis describes the creation and implementation of an advanced control scheme for a plasticating twin screw extruder (TSE) including data acquisition setup, model development, controller design, and implementation of the controller in real-time. The advanced control scheme was designed for a laboratory scale ZSK-25 co-rotating intermeshing TSE used for polymer processing. Two high density polyethylenes with different melt indices were used as processing materials.

An in-depth review of modeling and control of a twin screw extrusion process was done and a number of process control challenges were identified including multiple-input multiple-output, process nonlinearity, time delay, interaction between process variables, and real-time measurement of product qualities. To the author's knowledge no other work has been reported regarding real-time implementation of advanced control schemes for a plasticating TSE.

An infrastructure for data gathering was developed and an upgrade of the extruder automation was done. Such structures are imperative for the modeling, validation, control, and monitoring of extruders in real-time. Data acquisition was performed using RSlinx as an OPC server and LabVIEW as an OPC client. Process automation allows control of the motor drive and feed rate by sending commands to the system from a PC.

The manipulated variables, screw speed and feed rate, were selected based on the process knowledge. Controlled variables were selected based on a steady-state correlation analysis and dynamic considerations. The correlation analyses were performed between process output variables and the product quality variables melt index and viscosity. Based on these selection criteria, melt temperature (T_m) and

melt pressure (P_m) at the die location were finally selected as controlled variables.

A new approach to develop two dynamic grey box models relating T_m and P_m with screw speed was presented utilizing first principles knowledge and empirical data. A predesigned random binary sequence (RBS) screw speed was used to excite the extrusion process. Nonlinearity in T_m data and considerable noise in P_m data were observed. Both the obtained models had autoregressive moving average with exogenous input (ARMAX) structure. The second order T_m model and the third order P_m model explained the physics of the extrusion process successfully. An excellent fit was obtained between the T_m grey box model predicted output and experimental data. The fit obtained between P_m grey box model predicted output and experimental data was only moderate due to the presence of considerable noise in the pressure data.

The extruder was excited using a predesigned RBS in feed rate to develop models relating T_m and P_m with feed rate using system identification technique. The developed P_m model was second order with ARMAX structure. An excellent model fit was found between P_m model predicted outputs and experimental data. This model was validated with another dataset obtained from stair type excitation in feed rate and almost 93% model fit was obtained. Since the response of P_m to changes in feed rate was fast, a non parametric delay-gain model was developed for P_m and good fit with experimental data was observed. A second order ARMAX model was also obtained for T_m. Validation tests showed good fit with the data obtained from a RBS excitation. However, due to the nonlinearity the T_m model gave only moderate fit with the data obtained from stair type excitation.

A multiple-input multiple-output model predictive control (MPC) scheme was designed for a ZSK-25 extruder. Analysis of the extruder showed two inputs: screw speed and feed rate, and two outputs: melt temperature and melt pressure at the die. The inputs could also be used as manipulated variables. Thus, a two-input and two-output MPC was designed. As changes in P_m with changes in screw speed were small, the transfer function between these two variables was neglected in designing the MPC scheme. No effect of this assumption was observed in real-time experiments. The performance and robustness of the MPC were studied in real-time by testing its ability to reject disturbances and track set-points; excellent performance was observed.

The response of T_m to excitation in screw speed and feed rate showed nonlinearity. Therefore, a multimodel approach was used to investigate the relationship between T_m and screw speed over a wide operating range. The operation was divided into three regimes based on screw speed, and first order ARMAX models were developed for each regime. Fuzzy logic and a triangular membership function were used to combine the local models. Simulated results showed good response of

T_m over the entire range of screw speed. A nonlinear proportional-integral (n-PI) controller and a nonlinear model predictive controller (n-MPC) were designed using this approach. Simulated results showed good set-points tracking capability of the nonlinear controllers.

8.2 Major Contributions

This research contributes in the following ways:

- A ZSK-25 twin screw extruder was designed and modified to mount new pressure and temperature sensors. A data acquisition set-up was established to gather process data from the extruder PLC and a feed controller. The extruder was automated to enable control from a PC.
- A new approach was used to select controlled and manipulated variables for a TSE. Such an approach considers both the product quality attributes and the dynamic analysis.
- A detailed and practical methodology was proposed for developing dynamic grey box models relating melt pressure and melt temperature to screw speed for a plasticating TSE.
- Random binary sequence type excitation was experimentally shown to be a good method of excitation for a nonlinear process such as twin screw extrusion.
- A novel model predictive control scheme was designed and implemented in real-time. Performance and robustness of the controller were evaluated by checking its ability to reject disturbances and track set-points.
- A multimodel approach was used to develop a global model for melt temperature to cover a wide operating range. Use of such an approach in a TSE is a novel idea. A nonlinear proportional-integral controller and a nonlinear model predictive controller were also developed using the same approach to control T_m in a wide range of operating conditions.

8.3 Recommendations for Future Works

Additional work is needed in many areas of polymer development. Several ideas for future studies are summarized below.

8.3.1 Inferential Model Development

In this study, correlation between product quality variables and process output variables was one of the criteria used to select controlled variables for closed loop operation. However, set-points from the controlled variables rather than the set-points from the product quality variables were used in the closed loop control. The ultimate objective of an extrusion process is to control the final product quality variables. If the final product quality variable to be controlled is the melt index, the melt index should be the set-point. Thus, inferential models relating on-line measured variables, for example T_m or P_m, with final product quality are imperative. If inferential models or soft sensors determine the values of variables measured on-line for set-points of product quality variables, the control schemes will keep the on-line measured variables at model-determined values. Much work is needed to develop sensors that can allow control of product quality variables in real-time.

8.3.2 Barrel Temperature Excitation

An open loop diagram of a TSE (see Figure 2.1) shows that the barrel temperature is one of the input variables. From a control point of view, it is known that the barrel temperature has a significant effect on the quality of the final product and the energy efficiency of the process (McAfee and McNally 2006). For example, viscosity is strongly related with temperature.

The barrel temperature of a ZSK-25 TSE is controlled zone-wise. Each zone has a local PID controller to keep the barrel temperature at a set-point. However, in dynamic analyses these local controllers could not maintain barrel temperature set-points properly. Thus, barrel temperature has not been used as a manipulated variable in this study. It would be interesting to see how process variables respond to RBS excitation of barrel temperature and models could be developed that express this relationship.

8.3.3 Control of Polymer Blends

In this study an advanced control scheme was designed to control T_m and P_m. Only one high density polyethylene was used as a processing material in the dynamic analysis. One important use of a TSE is to blend different polymers. Considerable future work needs to be done to control the quality of polymer blends.

Experiments in this research employed polymers in pellet form. In practice, different polymer forms may be used, e.g., polymer powder (Anderson 1994). A standard screw configuration was used for the ZSK-25 TSE; however, a number of screw configurations are possible. Testing of closed loop control with different screw configurations and different forms of processing materials could advance the field.

8.3.4 Implementation of Multimodel Approach

Multimodel approaches are used to cover a wide range of nonlinear operations for instance, to model and control a twin screw extruder. To our knowledge this approach has not been used in plasticating TSEs, which are used over a wide operating range in industry. Thus a multimodel approach could be applied to control TSEs.

A multimodel based operating regime was used in this study and a global model relating melt pressure and screw speed was developed. A global proportional controller was also developed using this approach. Simulated results showed good model prediction and closed loop control. However, the controller has not been implemented in real-time. Implementation of such a controller in real-time and over a wide operating range is highly recommended for future work.

8.3.5 Commercial Evaluation

Companies suffer substantial economic losses when off-specification materials are produced, because industrial extruders are usually very large and are used over a wide operating range. Polymers with different grades are produced extensively and frequently in industries. During transition from one grade to another grade, a significant amount of off-specification materials are produced. Fluctuations in die pressure causes fluctuations in melt viscosity which may induce viscoelastic instability in the polymer product. In industry, small variations in final product properties can result in many off-specification materials. Thus, proper control of the extrusion process is extremely important in plastic processing industries. Modeling of dynamic behavior and developing a control scheme using the model would manipulate the extrusion process in such a way that grade transition could be completed in minimal time.

In this work, a complete methodology for closed loop control of a plasticating twin screw extruder with an advanced control scheme was developed for a laboratory-scale extruder. The same methodology could be used in commercial extruders. This methodology explores the design of dynamic models for plasticating extruders and proposes an advanced control scheme to reduce grade transition time. More work using a commercial extruder is needed to evaluate the proposed methodology.

Bibliography

Akdogan, H. and T. R. Rumsey (1996). Dynamic resposnse of a twin-screw lab-size extruder to changes in operating variables. *Food Science and Technology* **29**(8), 691–701.

Anderson, P. G. (1994). *Mixing Practice in Co-rotating Twin-screw Extruders*. Hanser Publishers, New York.

Bai, S. L., G. T. Wang, J. M. Hiver and C. G'Sell (2004). Microstructures and mechanical properties of polypropylene/polyamide 6/polyethylene-octene elastomer blends. *Polymer* **45**, 3063–3071.

Barrès, C., B. Vergnes and J. Tayeb (1991). An improved thermal model for the solid conveying section of a twin-screw extrusion cooker. *Journal of Food Engineering* **15**(3), 167–185.

Bawiskar, S. and J. L. White (1997). A composte model for solid conveying, melting pressure and fill factor profiles in modular co-rotating twin screw extruders. *International Polymer Processing* **12**(4), 331–340.

Bawiskar, S. and J. L. White (1998). Melting model for modular self wiping co-rotating twin screw extruders. *Polymer Engineering and Science* **38**(5), 727–740.

Booy, M. L. (1978). Geometry of fully wiped twin-screw equipment. *Polymer Engineering and Science* **18**(12), 973–984.

Booy, M. L. (1980). Isothermal flow of viscous liquids in co rotating twin screw devices. *Polymer Engineering and Science* **20**(18), 1220–1228.

Booy, M. L. (1981). The influence of non-newtonian flow on effective viscosity and channel eficiency in screw pumps. *Polymer Engineering and Science* **21**(9), 93–99.

Box, G. E. P., G. M. Jenkins and G. C. Reinsel (1994). *Time Series Analysis, Forecasting and Control*. Prentice Hall, New Jersey.

Broadhead, T. O., W. I. Patterson and J. M. Delay (1996). Closed loop viscosity control of reactive extrusion with an in-line rheometer. *Polymer Engineering and Science* **36,**(23), 2840–2851.

Carneiro, O. S., A. Poulesquen, J. A. Covas and B. Vergnes (2002). Visualization and analysis of the flow along the kneading block of a twin-screw extruder. *International Polymer Processing* **17**(4), 301–308.

Carneiro, O. S., J. A. Covas and B. Vergnes (2000). Experimental and theoritical study of twin screw-extrusion of polypropylene. *Journal of Applied Polymer Science* **78**, 1419–1430.

Cayot, N., D. Bounie and H. Baussart (1995). Dynamic modelling of a twin screw food extruder: Analysis of dynamic behaviour through process variables. *Polymer Engineering and Science* **25**, 245–260.

Chan, D., R. W. Nelson and L. J. Lee (1986). Dynamic behaviour of a single screw plasticating extruder part ii: Dynamic modeling. *Polymer Engineering and Science* **26**(2), 152–161.

Chen, H., U. Sundararaj and K. Nandakumar (2004). Investigation of the melting mechanism in a twin-screw extruder using a pulse method and online measurement. *Industrial Engineering and Chemistry Research* **43**, 6822–6831.

Chen, Z. L., P.-Y. Chao and S.-H. Chiu (2003). Proposal of an empirical viscosity model for quality control in the polymer extrusion process. *Polymer Testing* **22**(5), 601–607.

Chiu, S. (1997). Developing commercial applications of intelligent control. *Control Systems Magazine, IEEE* **17**(2), 94–100.

Chiu, S. and C. Lin (1998). Applying constant minimum variance control theory on in-line viscosity control in the extrusion molding process. *Journal of Polymer Research* **5**(3), 171–175.

Chiu, S. and S. Pong (1999). In-line viscosity fuzzy control in an extrusion process with a fuzzy gain scheduled pid controller. *Journal of Applied Polymer Science* **74**(3), 541–555.

Chiu, S. and S. Pong (2001). In-line viscosity fuzzy control. *Journal of Applied Polymer Science* **79**(7), 1249–1255.

Choulak, S., F. Couenne, Y. L. Gorrec, C. Jallut, P. Cassagnau and A. Michel (2004). Generic dynamic model for simulation and control of reactive extrusion. *Industrial Engineering and Chemistry Research* **43**, 7373–7382.

Costin, M. H., P. A. Taylor and J. D. Wright (1982a). A critical review of dynamic modeling and control of plasticating extruders. *Polymer Engineering and Science* **22**(7), 393–401.

Costin, M. H., P. A. Taylor and J. D. Wright (1982b). On the dynamics and control of a plasticating extruder. *Polymer Engineering and Science* **22**(17), 1095–1106.

De Loor, A., P. Cassagnau, A. Michel, L. Delmare and B. Vergnes (1996). Reactive blending in a twin screw extruder. *International Polymer Processing* **11**(2), 139–146.

Della Valle, G., J. Tayeb and J. P. Melcion (1987). Relationship of extrusion variables with pressure and temperature during twin screw extrusion cooking of starch. *Polymer Engineering and Science* **36**(12), 1685–1693.

Della Valle, G., J. Tayeb and J. P. Melcion (1993). Computer simulation of starchy products transformation by twin-screw extrusion. *Polymer Engineering and Science*.

Delmare, L. and B. Vergnes (1996). Computation of the morphological changes of a polymer blend along a twin-screw extruder. *Polymer Engineering and Science*.

Denson, C. D. and B. K. Hwang (1980). The influence of axial pressure gradient on flow rate for newtonian liquids in a self wiping, co-rotating twin screw extruder. *Polymer Engineering and Science* **20**(14), 965–971.

Eerikinen, T., Y.-H. Zhu and P. Linko (1994). Neural networks in extrusion process identification and control. *Food Control* **5**(2), 111 – 119.

Elsey, Justin, Jrg Riepenhausen, Ben McKay, Geoffrey W. Barton and Mark Willis (1997). Modeling and control of a food extrusion process. *Computers & Chemical Engineering* **21**(Supplement 1), S361 – S366.

Fara, D. A., M. R. Kamal and W. I. Patterson (1980). Evaluation of simple dynamic models and controllers for hydraulic and nozzle pressure in injection molding. *Polymer Engineering and Science* **25**(11), 714–723.

Fisher, E. G. (1976). *Extrusion of Plastics*. John Wiley & Sons.

Fortelny, I. D., D. Hiavata and J. Mikesova (2003). Effect of mixing conditions on the morphology and properties of polystyrene/polyethylene blends compatabilized with styrene-butadiene block copolymers. *Journal of Polymer Science* **41**, 609–622.

Garge, S. C., M. D. Wetzel and B. A. Ogunnaike (2007). Quantification of the melting process in a co-rotating twin-screw extruder: A hybrid modeling approach. *Polymer Engineering and Science* **22**(7), 393–401.

Gawthrop, P. J. and L. Wang (2004). Data compression for estimation of the physical parameters of stable and unstable linear systems. *Control, Automation and Tobotics Vision Conference-2* pp. 889–893.

Gawthrop, P. J. and L. Wang (2005). Data compression for estimation of the physical parameters of stable and unstable linear systems. *Automatica* **41**(8), 1313–1321.

Gimenez, J., M. Boudris, P. Cassagnau and A. Michel (2001). Bulk polymerisation of ε-caprolactone in a twin screw extruder, a step toward the process control. *International Polymer Processing* **11**(1), 20–27.

Haley, T. A. and S. J. Mulvaney (2000a). On-line system identification and control design of an extrusion cooking process: Part i: System identification. *Food Control* **11**(2), 103–120.

Haley, T. A. and S. J. Mulvaney (2000b). On-line system identification and control design of an extrusion cooking process: Part ii: Model predictive and inferential control design. *Food Control* **11**(2), 121–129.

Hassan, G. A. and J. Parnaby (1981). Model reference optimal steay-state adaptive computer control of plastics extrusion processes.. *Polymer Engineering and Science* **21**(5), 276–284.

Hofer, J. M. and J. Tan (1993). Extrudate temperature control with disturbance prediction. *Food Control* **4**(1), 17–24.

Hong, M. H. and J. L. White (1998). Fluid mechanics of intermeshing counter-rotating twin screw extruders. *International Polymer Processing* **13**(4), 342–346.

Huang, W. Y., J. W. Shen and X. M. Chen (2003). Effect of compisition on phase morphology and mechanical properties of pp/pa66 in situ composites vis extrusion-drawing-injection method. *Journal of Material Science* **38**, 541–547.

Hussein, I. A., M. H. Iqbal and H. I. A. Wahhab (2005). Influence of mw of ldpe and va content of eva on the rheology of polymer modified asphalt. *Rheologica Acta* **45**, 92–104.

Imagawa, A. and T. C. Qui (1995). Structure-property relationship of polymer blends with co-continuous structures prepared by photo-cross-linking. *Macromolecules* **28**(24), 8388–8394.

Iqbal, M. H., S. L. Shah and U. Sundararaj (2007). Identification and control of plasticating twin screw extruder. *Presented in the 57th Canadian Society for Chemical Engineers*.

Iqbal, M. H., S. L. Shah and U. Sundararaj (2008). Grey box modeling and control of a plasticating twin screw extruder. *Presented in the 58th Canadian Society for Chemical Engineers*.

Iqbal, M. H., U. Sundararaj and S. L. Shah (2010a). New approah to develop dynamic grey box model for a plasticating twin-screw extruder. *Industrial Engineering and Chemistry Research* **49**, 648–657.

Janssen, L. P. B. M. (1977). *Twin Screw Extrusion*. Elsevier Scientific Pub. Co.

Kalyon, D., V. Tan, and M. R. Kamal (1980). The dynamics of parison development in blow molding. *Polymer Engineering and Science* **20**(12), 773–777.

Kamal, M. R., W. I. Patterson, D. A. Fara and A. Haber (1984). A study in injection molding dynamics. *Polymer Engineering and Science* **24**(9), 686–691.

Kamal, M. R., W. I. Patterson, N. Conley, D. A. Fara and G. Lohfink (1987). Dynamics and control of pressure in the injection molding of thermoplastics. *Polymer Engineering and Science* **27**(18), 1403–1410.

Kim, E. K. and J. L. White (2000a). Isothermal transient startup of a starved flow modular co-rotating twin screw extruder. *Polymer Engineering and Science* **40**(3), 543–553.

Kim, E. K. and J. L. White (2000b). Non-isothermal transient startup of a starved flow modular co-rotating twin screw extruder. *International Polymer Processing* **15**(3), 233–241.

Kim, E. K. and J. L. White (2001). Superposed hydrodynamic disturbances from feeders in a starved flow modular intermeshing co-rotating twin screw extruder. *Polymer Engineering and Science* **41**(2), 232–239.

Kim, E. K. and J. L. White (2002). Transient compositional effects from feeders in a starved flow modular co-rotating twin screw extruder. *Polymer Engineering and Science* **42**(11), 2084–2093.

Kiparissides, C. (1996). Polymerization reactor modelling: A review of recent development and future direction. *Chemical Engineering Science* **51**(10), 1637–1659.

Kochhar, A. K. and J. Parnaby (1977). Dynamical modelling and control of plastics extrusion processes. *Automatica* **13**(2), 177 – 183.

Kuipers, Benjamin and Karl strm (1994). The composition and validation of heterogeneous control laws. *Automatica* **30**(2), 233 – 249.

Kulshreshtha, M. K. and C. A. Zaror (1992). An unsteady state model for twin screw extruders. *Transaction of the Institution of Chemical Engineers* **70**(Part C), 21–28.

Kulshreshtha, M. K., C. A. Zaror and D. J. Jukes (1991a). Automatic control of food extrusion: problems and perspectives. *Food Control* **2**(2), 80–86.

Kulshreshtha, M. K., C. A. Zaror and D. J. Jukes (1995). Simulating the performance of food extruders using the model based set point adjustment. *Food Control* **6**(3), 135–141.

Kulshreshtha, M. K., C. A. Zaror, D. J. Jukes and D. I. Pyle (1991b). A generalized steady state model for twin screw extruders. *Transaction of the Institution of Chemical Engineers* **69**(Part C), 189–199.

Lee, B. L. (1992). Electrically conductive polymer composites and blends. *Poly. Engg. Sci.* **32**(1), 36–42.

Lee, J. C., T. Ikehara and T. Nishi (1998). Morphology and electrical properties of carbon black-filled poly(ϵ-caprolactone)/poly(vinyl butyral) blends. *Journal of Applied Polymer Science* **63**, 193–199.

Levy, S. and J. F. Carley (1989). *Plastics Extrusion Technology Handbook*. Industrial Press Inc.

Li, C. H. (2001). Modelling extrusion cooking. *Mathematical and Computer Modelling* **33**(6-7), 553–563.

Linko, S. and P. Linko (1998). Developments in monitoring and control of food processes. *Transaction of the Institution of Chemical Engineers* **76**(Part C), 127–137.

Linko, Susan, J. Luopa and Y. H. Zhu (1997). Neural networks as 'software sensors' in enzyme production. *Journal of Biotechnology* **52**(3), 257 – 266.

Ljung, L. (2006). *System Identification*. PTR Prentice Hall Information and System Sciences Series.

Lu, Q., S.J. Mulvaney, F. Hsieh and H.E. Huff (1993). Model and strategies for computer control of a twin-screw extruder. *Food Control* **4**(1), 25 – 33.

Luo, J. J. and I. M. Daniel (2003). Characterization and modeling of mechanical behavior of polymer/clay nanocomposites. *Composites Science and Technology* **63**, 1607–1616.

McAfee, M. (2007). Enhancing process insight in polymer extrusion by grey box modelling. *Transactions of the Institute of Measurement and Control* **29**(5), 467–488.

McAfee, M. and G. McNally (2006). Real-time measdurement of melt viscosity in single-screw extrusion. *Transactions of the Institute of Measurement and Control* **28**(5), 481–497.

McAfee, M. and S. Thompson (2007). A novel approach to dynamic modelling of polymer extrusion for improved process control. *Proceedings of International Mechanical Engineering, Part I, Journal of Systems and Control* **221**, 617–628.

McAfee, M., L. Cadwell, S. Thompson and G. McNally (2003). Design of a soft sensor for polymer extrusion. *SPE-ANTEC* pp. 207–212.

McAuley, K. B., J. F. MacGregor and A. E. Hamielec (1990). A kinetic model for industrial gas phase ethylene copolymerization. *AIChE Journal* **36**(6), 837–850.

Mohamed, Ibrahim O. and Robert Y. Ofoli (1990). Prediction of temperature profiles in twin screw extruders. *Journal of Food Engineering* **12**(2), 145 – 164.

Moreira, R. G., A. K. Srivastava and J. B. Gerrish (1990). Feedforward control model for a twin-screw food extruder. *Food Control* **1**(13), 179–184.

Nabar, Y. and R. Narayan (2006). Analysis of the dynamic behavior of a starch foam extrusion process. *Journal of Applied Polymer Science* **101**(6), 3983–3995.

Ozkan, Leyla, Mayuresh V. Kothare and Christos Georgakis (2000). Model predictive control of nonlinear systems using piecewise linear models. *Computers & Chemical Engineering* **24**(2-7), 793–799.

Pesneau, I., A. A. Kadi and M. Bousmina (2002). From polymer blends to in situ polymer/polymer composites: Morphology control and mechanical properties. *Polymer Engineering and Science* **42**(10), 1990–2004.

Potente, H., J. Ansahl and B. Klarholtz (1994). Design of tightly intermeshing co-rotating twin screw extruders. *International Polymer Processing* **9**(1), 11–25.

Potente, H., K. Krestschemer and T. Pohl (2004). Physico-mathematical model for the description of the temperature development and the power consumption in co-rotating twin screw extruder. *International Polymer Processing* **19**(1), 3–12.

Potente, H., M. Bastian, J. Flecke and D. Schramm (2001a). Melting of polymer blends in co-rotating twin screw extruders. part iii: Experimental verification. *International Polymer Processing* **16**(2), 143–150.

Potente, H., M. Bastian, J. Flecke and D. Schramm (2001b). Melting of polymer blends in co-rotating twin screw extruders. part ii: Theoretical derivation. *International Polymer Processing* **16**(2), 131–142.

Potente, H., U. Melisch and K. P. Palluch (1996). A physico-mathematical model for solids conveying in co-rotating twin screw extruders. *International Polymer Processing* **11**(1), 29–41.

Poulesquen, A. and B. Vergnes (2004a). A study of residence time distribution in co-rotating twin-screw extruders. part i: Theoritical modeling. *Polymer Engineering and Science* **43**(12), 1841–1848.

Poulesquen, A., B. Vergnes, P. Cassagnau and A. Michel (2004b). A study of residence time distribution in co-rotating twin-screw extruders. part ii: Experimental validation. *Polymer Engineering and Science* **43**(12), 1849–1862.

Poulesquen, A., B. Vergnes, P. Cassagnau, J. Gimenez and A. Michel (2004). Polymerisation of ε-caprolactone in a twin screw extruder. *International Polymer Processing* **16**(1), 31–38.

Premphet, K. and W. Paecharoenchai (2002). Polypropylene/metallocene ethylene-octene copolymer blends with a bimodal particle size distribution: Mehcanical properties and their controlling factors. *Journal of Applied Polymer Science* **85**, 2412–2418.

Previdi, F. and M. Lovera (2003). Identification of a class of non-linear parametrically varying models. *J. Adaptive Control and Signal Process* **17**(1), 33–50.

Previdi, Fabio, Sergio M. Savaresi and Angiolino Panarotto (2006). Design of a feedback control system for real-time control of flow in a single-screw extruder. *Control Engineering Practice* **14**(9), 1111 – 1121.

Qin, S. Joe and Thomas A. Badgwell (2003). A survey of industrial model predictive control technology. *Control Engineering Practice* **11**(7), 733 – 764.

Rauwendaal, C. (2004). *SPC-Statistical Process Control in Injection Molding and Extrusion*. Hanser Pubnlishers, Munich.

Richalet, J., A. Rault, J. L. Testud and J. Papon (1978). Model predictive heuristic control : Applications to industrial processes. *Automatica* **14**(5), 413 – 428.

Rios, A. C., P. J. Gramann and T. A. Osswald (1998). Comparative study of mixing in co-rotating twin screw extruders using computer simulation. *Advances in Polymer Technology* **17**(2), 103–117.

Rodriguez, F. (1996). *Principles of Polymer Systems*. Taylor and Francis.

Scali, C., M. Morretta and D. Semino (1997). Control of the quality of polymer products in continuous reactors: Comparison of performance of state estimators with and without updating of parameters. *Journal of Process Control* **7**(5), 357–369.

Schonauer, S. and R. G. Moreira (1995). Modeling and simulation of product quality attributes of a twin-screw extrusion process for control development. *Food Processing Automation IV: Proceedings of the FPAC IV Conference, 3-5 November* pp. 348–357.

Seborg, D. E., T. F. Edgar and D. A. Mellichamp (2004). *Process Dynamics and Control*. John Wiley & Sons.

Sharmin, R., U. Sundararaj, S. Shah and Y.J. Sun L. V. Griend (2006). Inferential sensors for estimation of polymer quality paramterts: Industrial application of a pls-based soft sensor for a ldpe plant. *Chemical Engineering Science* **61**, 6372–6384.

Shumway, R. H. and D. S. Stoffer (2005). *Time Series Analysis and Its Applications: With R Examples*. Springer, New York.

Singh, B. and S. J. Mulvaney (1994). Modelling and process control of twin-screw cooking food extruder. *Polymer Engineering and Science* **23**, 403–428.

Sohn, J. I., S. T. Lim, S. H. Park, H. J. Choi and M. S. John (2003). Effect of a reactive-type flame retardant on rheological and mechanical properties of pc/abs blends. *Journal of Material Science* **39**, 1485–1491.

Szydlowski, W. and J. L. White (1987). An improved theory of metering in an lntermeshing corotating twin-screw extruder. *Advances in Polymer Technology* **7**(2), 177–183.

Szydlowski, W. and J. L. White (1988). A non-newtonian model of flow in a kneading disc region of a modular intermeshing corotating twin screw extruder. *Journal of Non-Newtonian Fluid Mechanics* **28**, 29–46.

Szydlowski, W., R. Brzoskowski and J. L. White (1987). Modelling flow in an intermeshing co-rotating twin screw extruder: Flow in kneading discs. *International Polymer Processing* **1**(4), 207–214.

Tadmor, Z. and C. G. Gogos (1979). *Principles of Polymer Processing*. John Wiley & Sons.

Tadmor, Z. and I. Klein (1970). *Engineering Principles of Plasticating Extrusion*. Van Nostrand Reinhold Company.

Tadmor, Z., S. D. Lipshitz and R. Lavie (1974a). Dynamic model of a plasticating extruder. *Polymer Engineering and Science* **14**(1), 112–119.

Takagi, T. and M. Sugeno (1985). Fuzzy identification of systems and its applications to modeling and control. *IEEE Transactions on Systems Man and Cybernetics* **15**, 116–132.

Tan, J. and J. M. Hofer (1995). Self-tuning predictive control of processing temperature for food extrusion. *Journal of Process Control* **5**(3), 183–189.

Tan, L. P., A. Lotfi, E. Lai and J. B. Hull (2004). Self computing application in dynamic model identification of polymer extrusion process. *Applied Soft Computing* **2**, 345–355.

Tayeb, J., B. Vergnes and G. D. Valle (1988*a*). A basic model for a twin-screw extruder. *Journal of Food Science* **53**(4), 1047–1056.

Tayeb, J., B. Vergnes and G. D. Valle (1988*b*). Theoritical computation of the isothermal flow through the reverse screw element of a twn screw extrusion cooker. *Journal of Food Science* **53**(2), 616–624.

te Braake, H. A. B., H. J. L. van Can and H. B. Verbruggen (1998). Semi-mechanistic modeling of chemical processes with neural networks. *Engineering Applications of Artificial Intelligence* **11**(4), 507 – 515.

Thongruang, W., R. J. Spontak and C. M. Balik (2002). Bridged double percolation in conductive polymer composites: an electrical conductivity, morphology and mechanical property study. *Polymer* **43**, 3717–3725.

Utracki, L. A. (1990). *Polymer Alloys and Blends: Thermodynamics and Rheology*. Hanser Publishers.

Vergnes, B. and F. Berzin (2004). Modelling of flow and chemistry in twin screw extruders. *Plastics, Rubbers and Composites* **33**(9/10), 409–415.

Vergnes, B., C. Barrès and J. Tayeb (1992). Computation of residence time and energy distribution in the reverse screw element of a twin-screw cooker-extruder. *Polymer Engineering and Science* **16**(3), 1781–1792.

Vergnes, B., G. D. Valle and A. Delamare (1998). A global computer software for polymer flows in corotating twin screw extruder. *Polymer Engineering and Science* **38**(11), 1781–1792.

Vergnes, B., G. Souveton, M. L. Delacour and A. Ainser (2001). Experimental and theoritical study of polymer melting in a co-rotating twin screw extruder. *International Polymer Processing* **16**(4), 351–362.

Wagner, M. G. and G. A. Montague (1994). Modeling and control of a wire coating process. *IEE International Conference on Control* **1**(389), 374–378.

Wang, L. (2001c). Continuous time model predictive control design using orthonormal functions. *International Journal of Control* **74**(16), 1588–1600.

Wang, L. (2004a). Discrete model predictive controller design using laguerre functions. *Journal of Process Control* **14**(2), 131–142.

Wang, L. and J. Tan (2000). Dual-target predictive control and application in food extrusion. *Control Engineering Practice* **8**(9), 1055–1062.

Wang, L. and P. Gawthrop (2001b). On the estimation of continuous time transfer functions. *International Journal of Control* **74**(9), 889–904.

Wang, L. and P.C. Young (2006). An improved structure for model predictive control using non-minimal state space realisation. *Journal of Process Control* **16**(4), 355–371.

Wang, L. and W. R. Cluett (1996). Use of press residuals on dynamic system identification. *Automatica* **32**(5), 781–784.

Wang, L. and W. R. Cluett (1997). Frequency-sampling filters: An improved model structure for step-response identification. *Automatica* **33**(5), 939–944.

Wang, L., C. Chessari and E. Karpiel (2001a). Inferential control of product quality attributes-application to food cooking extrusion process. *Journal of Process Control* **11**(6), 621–636.

Wang, L., P. Gawthrop, C. Chessari, T. Podsiadly and A. Giles (2004b). Indirect approach to continuous time system identification. *Journal of Process Control* **14**(6), 603–615.

Wang, L., S. Smith and C. Chessari (2008). Continuous-time model predictive control of food extruder. *Control Engineering Practice* **16**(10), 1173 – 1183.

Wang, Y. and J. L. White (1989). Non-newtonian flow modelling in the screw regions of an intermeshing corotating twin screw extruder. *Journal of Non-Newtonian Fluid Mechanics* **32**, 19–38.

Wang, Y., J. L. White and W. Szydlowski (1989). Flow in a modular intermeshing co-rotating twin screw extruder. *International Polymer Processing* **4**, 262–267.

Wellstead, P. E., W. P. Heath and A. P. Kjaer (1998). Identification and control of web processes: polymer film extrusion. *Control Engineering Practice* **6**(3), 321 – 331.

White, J. L. and W. Szydlowski (1987). Composite models of modular lntermeshing corotating and tangential counter-rotating twin screw extruders. *Advances in Polymer Technology* **7**(4), 419–426.

White, J. L. and Z. Chen (1994). Simulation of non-isothermal flow in modular co-rotating twin screw extrusion. *Polymer Engineering and Science* **34**(3), 229–237.

White, J. L., W. Szydlowski, K. Min and M. Kim (1987). Twin screw extruders: Development of technology and analysis of flow. *Advances in Polymer Technology* **7**(3), 295–332.

Willis, M. J., G. A. Montague, C. Di Massimo, M. T. Tham and A. J. Morris (1992). Artificial neural networks in process estimation and control. *Automatica* **28**(6), 1181 – 1187.

Yacu, W. A. (1985). Modeling a twin screw co-rotating extruder. *Journal of Food Process Engineering* **8**, 1–21.

Yang, B. and L. J. Lee (1988). Process control of profile extrusion using thermal method. part i: Mathematical modeling and system analysis. *Polymer Engineering and Science* **28**(11), 697–707.

Yeo, J. H., C. H. Lee, C. S. Park, K. J. Lee, J. D. Nam and S. W. Kim (2001). Rheological, morphological, mechanical and barrier properties of pp/evoh blends. *Advances in Polymer Technology* **20**(3), 191–201.

Zhang, J., E. B. Martin, A. J. Morris and C. Kiparissides (1997). Inferential estimation of polymer quality using stacked neural networks. *Computers & Chemical Engineering* **21**, 1025–1030.

Zhang, Q. H. and D. J. Chen (2004). Percolation threshold and morphology of composites of conducting carbon balck/polypropylene/eva. *Journal of Material Science* **39**, 1751–1757.